UiT
THE ARCTIC UNIVERSITY OF NORWAY

Faculty of Science and Technology
Department of Geology

# North Atlantic–Norwegian Sea exchanges during the past 135,000 years: Evidence from foraminiferal $\Delta^{14}C$, $\delta^{11}B$, $\delta^{18}O$, $\delta^{13}C$, Mg/Ca and Cd/Ca

—

**Mohamed Mahmoud Ezat Ahmed Mohamed**

*A dissertation for the degree of Philosophiae Doctor – May 2015*

UNIVERSITY OF TROMSØ

Department of Geology, Faculty of Science and Technology, UiT the Arctic University of Norway

# North Atlantic–Norwegian Sea exchanges during the past 135,000 years: Evidence from foraminiferal $\Delta^{14}C$, $\delta^{11}B$, $\delta^{18}O$, $\delta^{13}C$, Mg/Ca, and Cd/Ca

**Mohamed Mahmoud Ezat Ahmed Mohamed**

**A dissertation for the degree of Philosophiae Doctor**

**Tromsø, Norway, May 2015**

**Acknowledgements**

I have travelled around the world during my PhD study, met with many people whose knowledge and generous help has added much to my work and studies. On May 13th of 2011, I crossed north of the Mediterranean Sea for the first time in my life in a journey directly to the north of the Arctic Circle. In Tromsø airport, Tine Rasmussen, my supervisor, was the first person to meet. Since then, I'm receiving tireless guidance and support from Tine in every possible aspect of my PhD work. I find no words to thank you, Tine, nor to even list in how many occasions you got my back. I'm deeply grateful for all your great supervision, support, patience and giving me the freedom to do whatever it takes to grow and get my job done the best way. I'm greatly indebted to my co-supervisor, Jeroen Groeneveld, for his sincere supervision, encouragement, brilliant support in the lab (and answering the countless numbers of emails I have been sending!). My sincere appreciation and gratefulness to Bärbel Hönisch for her expert advice and amazing mentoring throughout my stay at Lamont. Tine, Jeroen and Bärbel, the completion of this project could not have been possible without your continuous support; it is a great blessing to work with you all.

I would like to thank my co-authors in the second manuscript, Jesper Olsen for conducting the AMS analysis for the enormous number of samples and Luke Skinner for the helpful and inspiring discussions during meetings in Italy and Switzerland. I would like to express my deepest gratitude to Tine's group (names are listed in alphabetically order): Kamila Sztybor, Kasia Zamelczyk, Simon Jessen, Steffen Aagaard Sørensen, Patrycja Jernas and Ulrike Hoff. It has been a great experience and so much pleasure and fun to be part of this group. Deep thanks also for many for enjoyable nonscientific discussions and advice. Steffen, I know you are not really a member in Tine's group, but you are very connected in many ways and also to make some gender balance. Special and sincere thanks to Matthias Forwick and Jan Sverre Laberg for their magnificent help. I would like to thank the paleo-crew, Katrine Husum, Giuliana Panieri, Kari Skirbekk, Chiara Consolaro, Diane Groot, Juho Junttila, Henrik Rasmussen, Sarah Berben, Noortje Dijkstra and Andrea Schneider. My sincere appreciation and thanks to the lab 'ladies': Trine Dahl, Edel Ellingsen and Ingvild Hald for the great help and the amazing working environment. Trine, many thanks also for help with packing my samples before my many trips.

I would like to express my deepest appreciation for Nina Ruprecht, Kat Esswein, Peter DeMenocal, Jesse Farmer, Leo Pena and Kat Allen for their invaluable support in the lab and discussions during my stay in Lamont. I'm very grateful to Arnold Gordon, Bärbel Hönisch, Bob Anderson, Jerry McManus and Wally Broecker for giving me the opportunity to attend invaluable and enjoyable classes during my stay at Lamont. Many thanks go to Jerry McManus, Howie Spero and Anna Silyakova for fruitful discussions. Also sincere appreciation goes to Nils Martin for his help in teaching some lab exercises; Jurgen Mienert for offering his help to speed up the processing of my visa to the U.S.; and Stefan Buenz for taking good care of my PhD application. Many thanks go to Nikoline Rasmussen, Yulia Sen, Vårin Eilertsen for help with some foram pickings and sample sieving.

Great thanks to Inger Solheim, Annbjørg Johansen, Margrethe Linguist, Ann Kirsti Pettersen, Tine Hågensen, Christina With and Kai Mortensen for tireless help with endless administrative stuff. Special thanks to Inger for her great efforts facilitating my visa issuance. Deep thanks to Maja Sojtaric for her amazing jobs in writing public essays about my work. I'm very grateful to Steiner Iversen, Bjørg Runar Olsen and the captains and crews of R/V Helmer Hanssen for assistance, patience and guidance during the cruise trips I have enjoyed throughout my PhD. Also many thanks for Tove Nielsen and Antoon Kuijpers for their help during cruise trips. My sincere thanks to Jan Petter Holm for great help with maps and posters. Thanks go to the marvelous IT staff: Rold Andersen and Bjørn Ivar Evje. I would like to thank Ragna Breines and the former organizers of ResClim for organizing such wonderful meetings and courses.

My deepest thanks for my old office mates Sunil Vadakkepuliyambatta, Alexandros Tasiana, Aleksei Portnov, Andrew Smith; and my new office mates Kamila Sztybor, Calvin Shackleton, Emmelie Åstrom, Mariana Esteves, Giacomo Osti. Aleksei, deep thanks for helping me find my samples once I was abroad. I would like to thank Eythor Gudlaugsson so much for many fruitful chats and lunch/dinner breaks. Sunny Singhraha, great thanks and appreciation for suggesting fantastic Indian movies. Special thanks to Monica Winsborrow, Lina Alexadropoulou, Alexandros Tasianas, Sandra Chopard, Giuliana Panieri, Emilia Piasecka, Andreas Schneider for the very nice company during the last ResClim meeting. I would like to thank Ines Vogt for sharing her office with me while I was visiting MARUM. I would like to thank all friends and colleagues at the Geology institute and at CAGE.

My home friends Khaled Elyameny, Yousef Mohassab, Ahmed Omer, Ahmed Sayed, Ahmed Hamad, Mahmoud Sayed, Mohamed Shenway, Abdrehaman Mohamed, Yasser Feleih, Rabie Ali, Mohamed Mabrouk, Mohamed Ebaid, thanks so much for being at my side whenever I needed you, regardless of the far distances. I would like to express my deepest thanks to all my friends, colleagues and teachers in my *alma mater*, Beni-Suef University in Egypt. Naming all of you would require several pages. For those who helped me overcome my bad moments after my divorce and encouraged me to find a PhD scholarship abroad, to start a fresh life and pass on. Thank you all, you prescription has worked and in addition, I may get a PhD (bonus!). I would like also to thank my Masters' supervisors: Gouda Abdelwawad, Shaaban Saber, Ibrahim Abdelgaid, Essam Abdrehaman, and Mohamed El-Sayed.

***My parents***, you have been showering me with your overwhelming kindness and love that always brings joy to my life and fuels me to move on and overcome any obstacle I encounter in my journey. My little brother, Ali, the light of my life, how can I thank you?! My sisters, Mona, Khairia and Sahar, having three sisters like you, with the unique personality of each of you is marvelously overwhelming. Mona, thanks for always being the wise sister giving the advice in the right time and place. Khairia, just few minutes of chatting with you 'sharing your crazy thoughts', are more than enough to wipe off any stress in my life, thanks for always sharing that with me. Sahar, thanks for always being the 'funny' 'sincere' 'little' sister.

## Preface

This thesis is an outcome of a 4 year PhD study, which started in May 2011 at the Department of Geology, UiT the Arctic University of Norway, Tromsø, Norway. The work was financed by UiT the Arctic University of Norway, the Mohn Foundation, the Research Council of Norway through its Centres of Excellence funding scheme, project number 223259 and with additional support from the Norwegian Research School in Climate Dynamics (ResClim) and European Co-operation in Science and Technology (COST).

One year was assigned for 'duty work' including teaching, outreach activities and participation in marine cruises. I was a teaching assistant in the course GEO3111 'Reconstruction of Quaternary marine environments' and GEO3122 'Marine micropaleontology' during the fall of 2014 and in GEO2005 'Sedimentology' in the spring of 2012 and 2013. In addition, I have participated in five scientific cruises to different areas in the Nordic seas.

During my PhD, I have been on two research stays, the first at Bremen University for almost two months in summer 2012 and the second at Lamont Doherty Observatory of Columbia University for a ten months stay from September 2013 to June 2014. I have participated in several international workshops and summer schools including 'Climate Change in the Marine Realm' organized by AWI and Bremen University, 'Landscape and Climate' organized by Bjerknes Centre for Climate Research, Washington University and MIT, and The $^{11}$th Urbino summer school in paleoclimatology.

The results discussed in this thesis have been presented in many international and national conferences and meetings (e.g., AGU Fall Meeting 2013 and 2015, Goldschmidt Conference 2014 and IPODS-OC3 Meeting, 2014). This thesis consists of an introduction and three scientific articles. In these articles, we have generated records for the Norwegian Sea hydrography

spanning the past 135,000 years. These hydrographic records provide new information about the past changes in shallow subsurface and mid-depth temperatures, carbonate chemistry, nutrients and ventilation in the Norwegian Sea. The three articles are:

Mohamed M. Ezat, Tine L. Rasmussen, Jeroen Groeneveld, **Persistent intermediate water warming during cold stadials in the southeastern Nordic seas during the past 65 k.y.** Geology 2014; Volume 42 (8), 663-666.

Mohamed M. Ezat, Tine L. Rasmussen, Bärbel Hönisch, Jesper Olsen, Jeroen Groeneveld, Luke Skinner, **A 135 kyr record of subsurface $pCO_2$, nutrient levels and ventilation in the Norwegian Sea**. In preparation for submission to Nature Geoscience.

Mohamed M. Ezat, Tine L. Rasmussen, Bärbel Hönisch, Jeroen Groeneveld, **Downcore comparison of two planktic foraminiferal Mg/Ca cleaning protocols and reconstruction of the hydrographic changes in the southern Norwegian Sea during the past 135 kyr.** In preparation for submission to G-cubed.

## Table of contents

## 1. Introduction

In the last two decades, few issues have attracted the attention of public discourse more than 'global warming' or in other words the ongoing and projected changes in earth's climate state. From a scientific perspective, there is a consensus that the global temperatures are rising due to anthropogenic greenhouse gas emissions (e.g., Solomon et al., 2007). However, complex interactions between the different components of earth's climate system make the prediction of future climate a challenging task, especially on regional and local scales. One example that shows this complexity in the system is the slow-down in warming during the last decade, while the atmospheric $CO_2$ has been almost steadily increasing (e.g., Meehl et al., 2011). In addition to the rise in the average global temperature and its consequences as a result of increasing $CO_2$ emissions, the ocean pH has been decreasing referred to as 'ocean acidification' (e.g., Sabine et al., 2004). Increase in the acidity of the ocean has the potential to dramatically alter the marine ecosystem (e.g., Riebesell et al, 2000; Dèath et al., 2009). Past climate archives may provide an efficient tool to understand how the different components of the earth's climate system interact. By past climate archives, I mean all temporal records (covering several decades to billions of years back in time) retrieved from ocean or land, that can give information about climate-related parameters (e.g., Solomon et al., 2007; Zachos et al., 2001; Erba et al., 2010). The climate information are extracted from these records through 'proxies', which can be defined as indirect measurements of parameters that can give qualitative or quantitative information ideally about one climate-related parameter, but usually about a combination of parameters.

In this thesis, we looked at marine sediment archives from the high latitude North Atlantic in order to extract information about changes in seawater carbonate chemistry, ventilation, temperature and nutrients. The target is to reconstruct past changes in the exchange between the

eastern Nordic seas and the North Atlantic in connection with changes in climate and carbon cycle during the last 135,000 years. Our methods (proxies) are mainly based on the isotopic ($\delta^{11}B$, $\Delta^{14}C$, $\delta^{18}O$, $\delta^{13}C$) and elemental (Cd/Ca, Mg/Ca and B/Ca) composition of the fossil shells of planktic and benthic foraminifera. Foraminifera are unicellular organisms adapted to a wide range of marine environments and secrete calcium carbonate tests. The isotopic and elemental composition of foraminiferal tests is sensitive to specific environmental factors like sea water temperature (Mg/Ca), carbonate chemistry ($\delta^{11}B$, B/Ca), ventilation ($\Delta^{14}C$, $\delta^{13}C$) and content of nutrients (Cd/Ca, $\delta^{13}C$ ). The fossil tests of foraminifera, preserved on the sea floor, may then act as archives for ancient oceanographic conditions, when and where they lived. A detailed description of these proxies and their complications is introduced in papers II and III. I would like to emphasize that using a complex system i.e. 'geochemistry of foraminiferal shells' to infer information about another complex system 'earth's climate', requires an acknowledgment of the 'uncertainty' and how likely various sources of 'error' would affect acceptance/rejection of a proposed hypothesis. Starting my PhD in paleoclimate four years ago, it was a big shift from my master and bachelor interests and in fact the 'uncertainty statement' I wrote above might be the main take home message, I am carrying on out of my PhD-study for future work.

## 2. Background and objectives

Today, advection of heat and salt by northeastward inflow of Atlantic water (~8 Sv; 1 Sv = $10^6$ $m^3$ $s^{-1}$) across the Greenland-Scotland ridge into the Nordic seas and Arctic Ocean, where it loses heat and becomes fresher, and a southward return flow as cold and fresher surface outflow with the East Greenland Current (~1.3 Sv) as well as dense Iceland-Scotland (~3 Sv) and

Denmark Strait overflows (~3 Sv) represent the northern limb of the Atlantic Meridional Overturning Circulation (AMOC) (e.g., Hansen and Østerhus, 2000) (Fig. 1). The overflows from the Nordic seas contribute significantly to the North Atlantic Deep Water (NADW). This exchange of surface and deep water between the Arctic Mediterranean seas and North Atlantic is important for the global meridional ocean circulation and climate (e.g., Vellinga and Wood, 2002; Rhines et al., 2008) and is thought to have operated differently in the past in relation to changes in regional and global climate (e.g., Broecker et al., 1989; Rasmussen et al., 1996; Dokken and Jansen 1999; Ganopolski and Rahmstorf, 2001; Thornalley et al., 2011; Ezat et al., 2014; Skinner et al., 2014).

Millennial scale and abrupt climatic anomalies were a persistent feature during the last glaciation and deglaciation (e.g., Dansgaard et al., 1993; EPICA, 2006). Evidence for this climate instability first came from Greenland ice cores showing ~25 millennial-scale oscillations in air temperatures over Greenland, referred to as Dansgaard-Oeschger (DO) events (Dansgaard et al., 1993). A typical DO cycle there is characterized by an abrupt atmospheric warming of 8–16 °C from cold stadial to warmer interstadial conditions followed by a gradual cooling and eventually a sudden cooling back to stadial conditions (Huber et al., 2006). In North Atlantic and Nordic seas sediments, DO events are associated with the occurrence of Ice Rafted Debris (IRD). In particular, several layers anomalously rich in detrital carbonate were recorded in the North Atlantic called Heinrich events and are thought to be correlated with the coldest periods of the longest lasting stadials in the ice cores (e.g., Heinrich 1988; Bond et al., 1993; Hemming et al., 2004). The entire stadial periods during which a Heinrich event is recorded are defined as Heinrich stadials (HS). Apparent climatic reorganizations were recorded throughout the globe closely correlated with Greenland DO events, especially with those associated with Heinrich events (e.g., Voelker, 2002). However, this does not necessarily imply the same or connected

causal mechanisms (e.g., Wunch et al., 2006). The global expressions of DO events share some similar characteristics on a regional and global scale, but their detailed evolution differs (e.g., Gutjahr and Lippold, 2011; Standford et al., 2011; Bohm et al., 2015). Here we summarize the main climatic and carbon cycle observations for DO stadial 2 (also termed as HS1), which occurred during the early deglaciation (19–14.5 thousand years before present, hereafter 'ka'). We chose to focus on this event as it has received the greatest attention in our study.

Within this time interval of HS1 (19–14.5 ka), cooling over Greenland (Dansgaard et al., 1993), warming of the Antarctic region (EPICA, 2006), net global warming (Shakun et al., 2012), weakening of the Asian monsoons (Wang et al., 2001), southward shift of the intertropical convergence zone (Lea et al., 2003), apparent reorganizations of the AMOC (e.g., McManus et al., 2004; Skinner et al., 2014), delivery of armadas of icebergs into the North Atlantic (e.g., Hemming, 2004), rises in atmospheric $CO_2$ (e.g., Marcott et al., 2014) and abrupt decline in the $\delta^{13}C$ and $\Delta^{14}C$ of atmospheric $CO_2$ (e.g., Schmitt et al., 2012; Reimer et al., 2009) were recorded. In addition, extensive deglaciation of the European Alps (Denton et al., 1999) took place at the same time, while the northwestern Europe and major parts of the North Atlantic Ocean cooled down (e.g., Bond et al., 1993; Renssen and Isarin, 2001; Denton et al., 2005). At the end of stadial 2 and onset of interstadial 1 (at 14.5 ka), the air temperature abruptly increased over Greenland, while it slowly decreased over Antarctica.

Changes in the strength of ocean's meridional circulation, and particularly in the AMOC, are usually invoked in explaining these mysterious climate and carbon cycle variations through its influence on heat redistribution, global transmission of regional climate anomalies, air-sea $CO_2$ exchange and the efficiency of nutrient utilization (e.g., Stommel, 1961; Broecker, 1998; Ganopolsi and Rahmstorf, 2001; Vellinga and Wood, 2002; Clark et al., 2002; Anderson et al., 2009; Barker et al., 2011; Skinner et al., 2014;). Several pieces of evidence support an AMOC

instability during the last glacial and deglacial climatic anomalies; inferred based on proxies of distributions of nutrients (Cd/Ca, $\delta^{13}C$), water mass sources (Nd isotopes), degree of ventilation ($^{14}C$) and overturning rates ($^{231}Pa/^{230}Th$) (e.g., Sarnthein et al., 2000; McManus et al., 2004; Piotrowski et al., 2008; Roberts et al., 2010; Skinner et al., 2014). Whether the oceanic reorganizations were triggers or amplifiers for glacial/deglacial interhemispheric climatic anomalies remains a question (e.g., Broecker et al., 2003; Wunch et al., 2006).

A transient slowdown in the formation of NADW, probably caused by instability of the ice sheets, would have reduced the northward heat export cooling the northern Hemisphere and warming of the southern Hemisphere via a mechanism called the thermal bipolar seesaw (Broecker, 1998; Stocker and Johnsen, 2003). Associated sea ice retreat in the Southern Ocean and a reorganization of the atmospheric circulation (including southward shift and/or intensification of southern westerlies) may have caused venting of an abyssal $CO_2$-rich reservoir generated during the glacial period (e.g., Anderson et al., 2009; Skinner et al., 2010; Skinner et al., 2014). This glacial deep $CO_2$ reservoir thought to have been isolated for several thousands of years must have become $^{14}C$-depleted and with exceptionally low $\delta^{13}C$ values. Hence, venting of this reservoir may have caused the atmospheric rise in $CO_2$ and decline in $^{14}C$ and $\delta^{13}C$ of the atmospheric $CO_2$ during HS1 (e.g., Marchitto et al., 2007; Anderson et al., 2009; Skinner et al., 2010; Schmitt et al., 2012). Proposed mechanisms for enhanced $CO_2$ storage in the glacial deep ocean include an enhanced soft tissue-pump (Martin et al., 1990; Martinez-Garcia et al., 2014) and increased sea ice extension and ocean stratification (e.g., Stephens and Keeling, 2000). The extension and properties of this hypothesized $^{14}C$- and $\delta^{13}C$ depleted $CO_2$ reservoir in the glacial abyssal ocean and how and why it vented are still very open questions (e.g., Broecker and Clark, 2010; Anderson et al., 2010; Hain et al., 2011). While most studies aimed at understanding the deglacial rises in atmospheric $CO_2$ focus on the Southern Ocean (where most of the modern deep

water first see the sea surface), other areas such as in the North Pacific also seem to have played an important role (Rae et al., 2014).

Key evidence for the link between the carbon storage (release) in (from) the ocean and the evolution in the content and isotopic composition of atmospheric $CO_2$ during HS1 comes from the marine radiocarbon anomalies recorded at intermediate depth in the North Pacific and North Atlantic Ocean (e.g., Marchitto et al., 2007; Stott et al., 2009; Thornalley et al., 2011). Of particular interest to our study is the extreme and surprising mid-depth $^{14}C$ anomalies recorded south of Iceland. These anomalies have been interpreted as a remote signature of the upwelled $^{14}C$-depleted deep water from the Southern Ocean and northward transport by Antarctic Intermediate Water (AAIW) (Thornalley et al., 2011). AAIW is thought to have expanded further north in the North Atlantic than it does today due to reduction in the formation of NADW and/or changes in their preformed density gradients (e.g., Rickaby and Elderfield, 2005). However, the southern source of these $\Delta^{14}C$ anomalies south of Iceland remains in question (e.g., Sortor and Lund, 2011; Cleroux et al., 2011; Huang et al., 2014; Lund et al., 2015) as well as for those recorded in the North Pacific (e.g., De Pol-Holz et al., 2010). Another possible source for the $^{14}C$-depleted and nutrient-rich water masses found in the northern North Atlantic is outflow from an aged reservoir in the Nordic-Arctic basins (Cleroux et al., 2011; Skinner et al., 2014; Lund et al., 2015). Recently, Lund et al. (2015), based on a compilation of $\delta^{13}C$ records from the deep South Atlantic, found no evidence for increased ventilation of the deep ocean there during HS1, questioning the canonical view of venting of the Southern Ocean as the main trigger for the early deglacial rise in the atmospheric $CO_2$. Instead, they suggested a northern hemisphere source for the early deglacial rise in the atmospheric $CO_2$.

The stadials ended with a large and abrupt atmospheric warming in the northern high latitudes as seen in Greenland ice cores. In general, studies shows similar configuration and vigor of the AMOC during the interstadials compared to the present (e.g., McManus et al., 2004; Rasmussen and Thomsen, 2004; Piotrowski et al., 2008; Roberts et al., 2010; Thornalley et al., 2011; Skinner et al., 2014). The invigoration of NADW formation has been suggested to be the cause of the abrupt North Atlantic warmings at the onset of interstadials (e.g., Ganopolski and Rahmstorf, 2001) and attributed to buoyancy removal from NADW formation sites (e.g., Broecker et al., 1990) or freshening of AAIW (e.g., Weaver et al., 2003). Recent modeling studies suggested that the extent of sea ice and subsurface temperatures in the Nordic seas may have played an important role in the North Atlantic warmings and rapid recovery of the AMOC at the end of stadial periods (e.g., Li et al., 2005, 2010; Mignot et al., 2007; Brady and Otto-Bliesner et al., 2011; Singh et al., 2013).

Thus, reconstructing the evolution of the Arctic Mediterranean seas hydrography and their exchanges with North Atlantic is crucial to understand the glacial and deglacial anomalies in the climate and the carbon cycle. This PhD study is based on sediment core JM11-FI-19PC retrieved from the Faroe-Shetland Channel (62°49'N, 03°52'W; 1179 m water depth) (Fig. 1). The core location is ideal for the study of the exchange between the eastern Nordic seas and North Atlantic. In the Faroe-Shetland Channel the largest inflow of Atlantic water into the Nordic seas and one-third of the entire overflows from the Nordic seas into the North Atlantic takes place today (Hansen and Østerhus, 2000). In brief, in the present study we sought answers for the following questions aiming to bridge some knowledge gaps about past changes in the AMOC and its impact on the marine carbon cycle and regional climate from a northern angle.

1- How did the hydrographic properties evolve in the Norwegian Sea during the past 135 kyr? And what role they, if any, may have played in the recorded regional climatic anomalies?
2- How was the exchange of surface and deeper waters between the Norwegian Sea and the North Atlantic during the past 135 kyr?
3- Can the deglacial extreme $\Delta^{14}C$ anomalies recorded south of Iceland be explained by a deep outflow from Arctic Mediterranean seas across the Iceland-Scotland ridge?
4- The modern Norwegian Sea is among the most intense areas for $CO_2$ uptake (Takahashi et al., 2009), how did this operate during the past 135 kyr?

## 3. Approach

The objectives of this study are approached mainly via reconstructing the following water properties from the southern Norwegian Sea and comparing them with those from northern North Atlantic:

### 3.1. Seawater temperature and $\delta^{18}O$ (Method: Foraminiferal $\delta^{18}O$ and minor/trace elements)

Foraminiferal $\delta^{18}O$ values are a function of calcification temperature, seawater $\delta^{18}O$ and carbonate chemistry (e.g., Shackleton et al., 1967; Spero et al., 1997). Seawater $\delta^{18}O$ values at a specific location vary through time due to changes in global ice volume, salinity-related effects (evaporation/precipitation, meltwater and river runoff) and ocean circulation patterns (e.g., Dansgaard, 1964; Shackleton, 1967; Waelbroeck et al., 2011). Minor/trace element to calcium ratios measured in the same foraminiferal samples as $\delta^{18}O$ have the potential to provide

independent information about the calcification temperature (e.g., Nürnberg et al., 1996), salinity-related effects (e.g., Wit et al., 2013; Bahr et al., 2013) and carbonate chemistry (e.g., Yu and Elderfield, 2007a). In particular, parallel measurements of $\delta^{18}O$ and Mg/Ca on the same foraminiferal species may be used to infer information about the seawater $\delta^{18}O$ and temperature at the calcification depth and seasons of the foraminiferal species under analysis.

### 3.2. Seawater carbonate chemistry (Method: Foraminiferal $\delta^{11}B$)

The boron isotopic composition of biogenic carbonate is sensitive to seawater-pH. Briefly, from the two dominant dissolved boron species in seawater, boric acid [$B(OH)_3$] and borate [$B(OH)_4^-$], borate is the predominantly incorporated boron species into marine carbonate (Hemming and Hanson et al., 1992). The relative abundance of the two boron species as well as their boron isotopic composition changes with pH (Hershey et al., 1986). Culture experiments on planktic foraminifera gave an empirical support for using their boron isotopic composition as a proxy for pH (e.g., Sanyal et al., 1996), but species-specific offsets from the theoretical $\delta^{11}B$ of seawater borate were also observed, which is widely ascribed to 'vital effects' (e.g., Hönisch et al., 2003) and/or incorporation of boric acid (e.g., Klochko et al., 2009). A diffusion-reaction model has shown that this species-specific offset is constant over a wide range of pH values and thus does not compromise the use of planktic foraminiferal $\delta^{11}B$ as a pH proxy (Zeebe et al., 2003). If two of the six carbonate parameters (total Dissolved Inorganic Carbon (DIC), total alkalinity, carbonate ion concentration, bicarbonate ion concentration, pH and $CO_2$), are known in addition to temperature, pressure and salinity, the other parameters can be calculated (Zeebe and Wolf-Gladrow, 2001). The temperature and salinity may be estimated through a combination of foraminiferal $\delta^{18}O$ and Mg/Ca. Using reasonable assumptions about changes in total alkalinity, the other carbonate parameters can then be calculated.

As the ocean is the largest dynamic carbon reservoir on millennial time scale, it must have played a dominant role at glacial/interglacial variations in atmospheric $CO_2$. Constraining the seawater carbonate chemistry of the surface/deep ocean bears directly on the role of the ocean in shaping the atmospheric $CO_2$. In addition, it provides a non-conservative tracer of water masses and oceanic processes. In particular relevance to our study is the sea-ice formation process. Studies from the modern East Greenland current region showed that total dissolved inorganic carbon is rejected more efficiently than total alkalinity during sea-ice formation, causing the brines beneath the sea-ice to be enriched in $CO_2$ compared to normal seawater (e.g., Rysgaard et al., 2009). Seawater carbonate chemistry also is sensitive to changes in export production.

### 3.3. Seawater $^{14}C$ age (Method: Foraminiferal $\Delta^{14}C$)

Radiocarbon ($^{14}C$) is continually being produced in the atmosphere by cosmogenic interaction with nitrogen and is taken up by the ocean via air-sea $CO_2$ exchange. The radiocarbon content of seawater DIC is expressed as $^{14}C$ age or in $\Delta^{14}C$ units. The $^{14}C$ age of seawater DIC is a function of the air-sea $CO_2$ exchange at the surface ocean and subsequent radioactive decay of $^{14}C$ as the water circulates to the ocean's interior. Benthic foraminiferal species record the $^{14}C$ age of the ambient deep water, which is then a function of the time elapsed since this water was last in contact with the atmosphere. Planktic foraminifera record the seawater $^{14}C$ age at their shallow subsurface calcification depth, which is a balance between the equilibration with the atmosphere and mixing with deeper $^{14}C$ depleted waters. This provides the opportunity to estimate the changes in the ventilation age of water masses through time by comparing their $^{14}C$ age recorded in foraminifera with the contemporary atmospheric $^{14}C$ age. A challenging requirement for this approach is an accurate calendar chronology for the marine records.

## 4. Summary of papers

### Paper I

Mohamed M. Ezat, Tine L. Rasmussen, Jeroen Groeneveld, **Persistent intermediate water warming during cold stadials in the southeastern Nordic seas during the past 65 k.y.** Geology 2014; Volume 42 (8), 663-666.

In this paper we reconstruct the bottom water temperature (BWT) from the southern Norwegian Sea during the past 65 kyr based on Mg/Ca measurements in infaunal benthic foraminifera. The BWT record resolves most of the DO events, at least partly, during this time interval. The motivation of this work was to test a long-standing proposed hypothesis that the intermediate/deep water in the eastern Nordic seas and northern North Atlantic warmed up during the cold stadials. This hypothesis was suggested based on occurrence/increase of the abundance of a group of benthic foraminiferal faunas named as 'Atlantic species' (Rasmussen et al., 1996). Furthermore, a subsurface build-up of heat during the cold stadials is suggested to have been a key player in the onset of interstadials through destabilization of the water column stratification, causing melting of sea ice (Rasmussen and Thomsen, 2004), collapse of ice shelves (Marcott et al., 2011) and a rapid return to a vigorous mode of deep water formation in the Nordic seas (Brady and Otto-Bleiesner, 2011). This feature has also been frequently observed in fresh-water hosing (e.g., Brady and Otto-Bleiesner, 2011) and non-hosing (e.g., Singh et al., 2013) modeling experiments designed to simulate the abrupt glacial climate change. Our BWT record, which is the first Mg/Ca-based record from the Nordic seas on DO time scales, indeed shows prominent increases during the cold stadials (up to 5 °C) relative to the Holocene and interstadials. In agreement with previous studies (e.g., Rasmussen et al., 1999), we interpret the rise in BWT during stadials as a subsurface inflow of warm Atlantic water reaching >1.2 km water depth

below a well-developed halocline. We suggested that warm Atlantic water never ceased to flow into the Nordic seas during the glacial period; inflow at the surface during the Holocene and warm interstadials changed to subsurface and intermediate inflow during cold stadials. We conclude that 'it is the vertical shifts in the position of the warm Atlantic water that caused the abrupt surface warmings' based on the evidence of a gradual increase in BWT during the stadials and a sudden drop in BWT at the start of some interstadials. However, not all events follow this required pattern in our BWT record. In some part of the record (33.7 to 22.5 ka), we attribute this to the low temporal resolution in our record relative to the very short-lasting interstadials during this interval, as recorded in the Greenland ice cores. In any case, more and higher resolution BWT records are needed to further assess these hypotheses.

**Paper II**

Mohamed M. Ezat, Tine L. Rasmussen, Bärbel Hönisch, Jesper Olsen, Jeroen Groeneveld, Luke Skinner, **A 135 kyr record of subsurface $pCO_2$, nutrient levels and ventilation in the Norwegian Sea**. In preparation for submission to Nature Geoscience.

In this part of the study we were concerned with two questions:

1- The modern Norwegian Sea is among the most intense areas for $CO_2$ uptake (Takahashi et al., 2009), how did this operate during the past 135 kyr?

2- The deglacial extreme $\Delta^{14}C$ anomalies recorded south of Iceland (Thornalley et al., 2011) represents a benchmark observation to understand the deglacial evolution of the North Atlantic circulation and the ocean release/uptake of carbon, though, the source of these anomalies is not known. Have these $\Delta^{14}C$ anomalies originated from the Arctic Mediterranean seas via the Iceland-Scotland pathway?

For this, we generated records of shallow subsurface seawater $^{14}C$ ventilation age, $pCO_2$ and

nutrients using $\Delta^{14}C$, $\delta^{11}B$, Cd/Ca and $\delta^{13}C$ proxies measured in the planktic foraminiferal species *N. pachyderma* (s) and mid-depth $^{14}C$ ventilation age based on $\Delta^{14}C$ measurements in a specific group of benthic foraminiferal species.

The difference between the $pCO_2$ in the surface ocean and atmosphere ($\Delta pCO_{2sea\text{-}air}$) is a measure of the tendency of a water mass to exchange $CO_2$ with the atmosphere. Reconstructing $pCO_2$ in the surface ocean would then provide solid constrains on the ocean role in past changes in atmospheric $CO_2$. Reconstructions of sea surface $pCO_2$ from the western Equatorial Pacific (Palmer and Pearson, 2003), Eastern Pacific and Atlantic sector of the Southern Ocean (Martinez-Boti et al, 2015) suggested that $CO_2$ has escaped from the ocean during the deglaciation, when atmospheric $CO_2$ was increasing. The higher numbers of sea surface $pCO_2$ records from different ocean areas, the better the understanding of the ocean's role in control of the variations in atmospheric $CO_2$. Here in the Norwegian Sea, we document large increases in $\Delta pCO_{2sea\text{-}air}$ during some Heinrich stadials, correlating with rises in atmospheric $CO_2$. However, the relatively deeper habitat of *N. pachyderma* (s), as well as the probability of episodes of perennial/seasonal sea-ice cover during Heinrich stadials renders the direct interpretation of $\Delta pCO_{2sea\text{-}air}$ in terms of air-sea $CO_2$ exchange difficult. We suggested that the increases in the $pCO_2$ may represent episodes of enhanced sea ice formation (cf., Rysgaard et al., 2009). Also, the tight link between the increases in $CO_2$ and Cd/Ca peaks suggest that the $CO_2$ variations are, at least partly, due to changes in the level of nutrient utilization.

Our $^{14}C$ ventilation age reconstructions clearly preclude outflow of an 'old' water mass from the eastern Nordic seas to be a source of the extremely aged water masses found in the northern North Atlantic during the early and late HS1, while subsurface intrusions of these old water masses into the Nordic seas are more likely. During mid-HS1, a switch to well ventilated

intermediate water south of Iceland (Thornalley et al., 2011) and a decrease in the average high latitude North Atlantic reservoir age (Stern and Lisiecki 2013) were recorded. This occurred close in time to the $\Delta pCO_{2sea-air}$ peak in our record. As we speculate that the increase in the $pCO_2$ may indicate an enhanced period of sea ice formation, it seems possibly that the North Atlantic was flushed with relatively well ventilated outflows generated by salt rejection in the Nordic seas during mid-HS1.

**Paper III**

Mohamed M. Ezat, Tine L. Rasmussen, Bärbel Hönisch, Jeroen Groeneveld, **Downcore comparison of two planktic foraminiferal Mg/Ca cleaning protocols and reconstruction of the hydrographic changes in the southern Norwegian Sea during the past 135 kyr.** In preparation for submission to G-cubed.

The main target of this work is to reconstruct the shallow subsurface hydrography (temperature and seawater $\delta^{18}O$) for the last 135 kyr at the southern Norwegian Sea based on parallel measurements of Mg/Ca ratios and $\delta^{18}O$ in shells of the planktic foraminiferal species *Neogloboquadrina pachyderma* sinistral. We initially cleaned the foraminiferal samples prior to minor/trace element analyses using the 'Mg cleaning' method (Barker et al., 2003), but a later need to measure Cd and Ba (Ezat et al., second paper) led us to repeat the analyses using the 'full cleaning' method (Martin and Lea, 2002). The 'full cleaning' method includes two additional steps: reduction step with buffered solution of hydrous hydrazine and alkaline chelation step with alkaline diethylene-triamine-pentaacetic acid (DTPA) solution. While the reduction step is standard for Ba/Ca and Cd/Ca, it is not very clear if it is necessary, adequate or even damaging for the Mg/Ca analyses (Pena et al., 2005; Martin and Lea 2002; Rosenthal et al., 2004; Barker et al., 2003; Yu et al., 2007b). Although comparable Mg/Ca results were obtained from the two

cleaning protocols, significant decreases in the Mg/Ca ratios at some intervals were recorded when the 'full cleaning' method was used. The decreases in Mg/Ca may be due to efficient removal of contaminants or partial dissolution as a side effect from the extra cleaning (e.g., Barker et al., 2005). We compared the differences in Mg/Ca between the two cleaning methods with ratios of Al/Ca, Fe/Ca and Mn/Ca (as monitors of contamination), shell weights (as a preservation index) and % weight loss during the cleaning process (as an indicator of the laboratory dissolution). If the decrease in our down-core Mg/Ca was caused by dissolution as a side effect from the extra cleaning (e.g., Yu et al., 2007b), we would expect this decrease to predominate in samples where the sample loss during the cleaning process is higher. The decreases in Mg/Ca are also accompanied with decreases in Mn/Ca. Altogether this indicates that the 'Mg cleaning' method was not sufficiently effective in removing different contaminants and that the differences in Mg/Ca are mainly due to more efficient removal of Mn-contaminated coatings, when the 'full cleaning method' was applied. This may also apply to areas with similar depositional settings and thus we recommend, similar to previous studies (e.g., Barker et al., 2005), that a screening test for different cleaning protocols should be applied before deciding which cleaning protocol to use. We therefore used only Mg/Ca results from the full cleaning method. This is unfortunate, as those results are of much lower resolution than the results from the 'Mg cleaning' method. Mostly, our Mg/Ca record based on the full cleaning method is discontinuous and in certain intervals of low resolution and is not capable of resolving all glacial millennial scale climatic events.

The results show a decrease of about 1‰ in seawater $\delta^{18}O$, increase in the subsurface temperature and stable dominance of *N. pachyderma* (s) (>80%) during HS1 suggesting a strong stratification in the upper water column and a possible subsurface inflow of Atlantic water below a well-developed halocline, at least during the calcification seasons of *N. pachyderma* (s). Similar

decreases in seawater $\delta^{18}O$ are also recorded for the other resolved Heinrich stadials. In addition, our temperature estimates for the Eemian interglacial (~130–110 ka) are in a good agreement with previous estimates based on planktic foraminiferal assemblages and dinoflagellate cysts (Rasmussen et al., 2003; van Nieuwenhove et al., 2011) documenting a delay in the Eemian peak warmth compared to the North Atlantic and a late Eemian warming in the southeastern Nordic seas extending to the time of the summer insolation minimum at 60° N (e.g., Rasmussen et al., 2003). However, relatively high $\delta^{18}O_{seawater}$ during the early Eemian suggests a subsurface inflow of Atlantic water below a thin layer of polar water. Our bottom water temperature (BWT) reconstructions based on Mg/Ca measured in the benthic foraminiferal species *Melonis barleeanus* indicate early Eemian intermediate/deep circulation may have operated similarly to modern at this site.

## 5. Concluding remarks and Outlook

The overall objective of this study was to investigate the North Atlantic-Norwegian Sea exchanges in connection to the glacial and deglacial climatic and carbon cycle changes. Here we summarize our main findings and some suggestions for future work:

1- We generated the first record of Mg/Ca-based bottom water temperature (BWT) record on DO time scales from the Nordic seas. The record suggests that warm Atlantic water never ceased to flow into the Nordic seas during the glacial period; inflow at the surface during the Holocene and warm interstadials changed to subsurface and intermediate inflow during cold stadials. These hypothesized vertical shifts in the position of the warm Atlantic water may have caused the abrupt regional atmospheric warmings at the onset of interstadials, but higher temporal resolution BWT records from the Nordic seas as well as modelling exercises are required to evaluate these hypothesizes.

2- We produced shallow subsurface pH and $pCO_2$ records from the southern Norwegian Sea based on boron isotope measurements in the shells of the planktic foraminiferal species *N. pachyderma* (s). The direct interpretations of the $CO_2$ record in terms of air-sea $CO_2$ exchange were found to be difficult. Areas south of the Greenland-Scotland ridge, where other planktic species with known shallower habitat (e.g., *G. bulloides*) may be available for glacial and deglacial reconstructions should be investigated in the future. We suggest that the increases in $\Delta pCO_{2sea\text{-}air}$ during the resolved Heinrich Stadials may indicate high rates of sea ice formation and changes in the level of nutrient utilization. Based on $^{14}C$ ventilation age and carbonate chemistry reconstructions from the Norwegian Sea and northern North Atlantic for mid-HS1, we speculate that salt-rejection mode of intermediate deep water formation may have operated at this time and flushed the North Atlantic with relatively well-ventilated water from the Nordic seas.

3- Our $^{14}C$ ventilation age reconstructions for the intermediate waters in the southern Norwegian Sea clearly preclude outflow of an 'old' water mass from the eastern Nordic seas to be a source of the extremely aged water masses found in the northern North Atlantic during the early and late Heinrich Stadial 1. The Faroe Shetland Channel, our area of study, is a key area for exchanges between the Nordic seas and North Atlantic, but future work should cover other main gateways between the North Atlantic and Nordic seas.

4- Our record spans the past 135,000 years including the last interglacial 'the Eemian', the Weichselian glaciation and the Holocene interglacial. In this thesis we focused on the glacial and deglacial events and little attention is paid to the interglacial periods. Our Mg/Ca- based temperature reconstructions during the Eemian confirm the previous findings of early cooling and late warming in the eastern Nordic relative to the North

Atlantic. However, we document a shallow subsurface inflow of Atlantic water during the early Eemian, probably below a thin layer of polar water.

5- Comparing downcore Mg/Ca measurements in *N. pachyderma* (s) based on the use of two different cleaning protocols prior to the minor/trace element analyses yielded significantly different Mg/Ca results (for details see paper III).

**References**


Anderson, R. F., et al. (2009). Wind-Driven Upwelling in the Southern Ocean and the Deglacial Rise in Atmospheric $CO_2$. *Science, 323*(5920), 1443-1448.

Bahr, A., et al. (2013). Comparison of Ba/Ca and as freshwater proxies: A multi-species core-top study on planktonic foraminifera from the vicinity of the Orinoco River mouth. *Earth and Planetary Science Letters, 383*(0), 45-57.

Barker, S., Cacho, I., Benway, H., & Tachikawa, K. (2005). Planktonic foraminiferal Mg/Ca as a proxy for past oceanic temperatures: a methodological overview and data compilation for the Last Glacial Maximum. *Quaternary Science Reviews, 24*(7–9), 821-834.

Barker, S., Greaves, M., & Elderfield, H. (2003). A study of cleaning procedures used for foraminiferal Mg/Ca paleothermometry. *Geochemistry, Geophysics, Geosystems, 4*(9). doi: 10.1029/2003GC000559

Barker, S., et al. (2011). 800,000 Years of Abrupt Climate Variability. *Science, 334*(6054), 347-351.

Bohm, E., et al. (2015). Strong and deep Atlantic meridional overturning circulation during the last glacial cycle. *Nature, 517*(7532), 73-76.

Bond, G., et al. (1993). Correlations between climate records from North Atlantic sediments and Greenland ice. *Nature, 365*(6442), 143-147.

Brady, E., & Otto-Bliesner, B. (2011). The role of meltwater-induced subsurface ocean warming in regulating the Atlantic meridional overturning in glacial climate simulations. *Climate Dynamics, 37*(7-8), 1517-1532.

Broecker, W., & Clark, E. (2010). Search for a glacial-age $^{14}C$-depleted ocean reservoir. *Geophysical Research Letters, 37*(13). doi: 10.1029/2010GL043969

Broecker, W. S. (1998). Paleocean circulation during the Last Deglaciation: A bipolar seesaw? *Paleoceanography, 13*(2), 119-121.

Broecker, W. S. (2003). Does the Trigger for Abrupt Climate Change Reside in the Ocean or in the Atmosphere? *Science, 300*(5625), 1519-1522.

Broecker, W. S., Bond, G., Klas, M., Bonani, G., & Wolfli, W. (1990). A salt oscillator in the glacial Atlantic? 1. The concept. *Paleoceanography, 5*(4), 469-477.

Broecker, W. S., et al. (1989). Routing of meltwater from the Laurentide Ice Sheet during the Younger Dryas cold episode. *Nature, 341*(6240), 318-321.

Clark, P. U., Pisias, N. G., Stocker, T. F., & Weaver, A. J. (2002). The role of the thermohaline circulation in abrupt climate change. *Nature, 415*(6874), 863-869.

Cléroux, C., deMenocal, P., & Guilderson, T. (2011). Deglacial radiocarbon history of tropical Atlantic thermocline waters: absence of $CO_2$ reservoir purging signal. *Quaternary Science Reviews, 30*(15–16), 1875-1882.

Dansgaard, W. (1964). Stable isotopes in precipitation. *Tellus, 16*(4), 436-468.

Dansgaard, W., et al. (1993). Evidence for general instability of past climate from a 250-kyr ice-core record. *Nature, 364*(6434), 218-220.

De'ath, G., Lough, J. M., & Fabricius, K. E. (2009). Declining Coral Calcification on the Great Barrier Reef. *Science, 323*(5910), 116-119.

Denton, G. H., Alley, R. B., Comer, G. C., & Broecker, W. S. (2005). The role of seasonality in abrupt climate change. *Quaternary Science Reviews, 24*(10–11), 1159-1182.

Denton, G. H., et al. (1999). Interhemispheric Linkage of Paleoclimate during the Last Glaciation. *Geografiska Annaler. Series A, Physical Geography, 81*(2), 107-153.

De Pol-Holz, R., Keigwin, L., Southon, J., Hebbeln, D., & Mohtadi, M. (2010). No signature of abyssal carbon in intermediate waters off Chile during deglaciation. *Nature Geosci, 3*(3), 192-195.

Dokken, T. M., & Jansen, E. (1999). Rapid changes in the mechanism of ocean convection during the last glacial period. *Nature, 401*(6752), 458-461.

Erba, E., Bottini, C., Weissert, H. J., & Keller, C. E. (2010). Calcareous Nannoplankton Response to Surface-Water Acidification Around Oceanic Anoxic Event 1a. *Science, 329*(5990), 428-432.

Ezat, M. M., Rasmussen, T. L., & Groeneveld, J. (2014). Persistent intermediate water warming during cold stadials in the southeastern Nordic seas during the past 65 k.y. *Geology. 42*(8), 663-666.

Ezat, M. M., et al. A 135 kyr record of subsurface $pCO_2$, nutrient levels and ventilation in the Norwegian Sea. In preparation for submission to Naturegeoscience.

EPICA, (2006). One-to-one coupling of glacial climate variability in Greenland and Antarctica. Nature *444*, 195-198.

Ganopolski, A., & Rahmstorf, S. (2001). Rapid changes of glacial climate simulated in a coupled climate model. *Nature, 409*(6817), 153-158.

Gutjahr, M., & Lippold, J. (2011). Early arrival of Southern Source Water in the deep North Atlantic prior to Heinrich event 2. *Paleoceanography, 26*(2). doi: 10.1029/2011PA002114

Hain, M. P., Sigman, D. M., & Haug, G. H. (2011). Shortcomings of the isolated abyssal reservoir model for deglacial radiocarbon changes in the mid-depth Indo-Pacific Ocean. *Geophysical Research Letters, 38*(4). doi: 10.1029/2010GL046158

Hansen, B., & Østerhus, S. (2000). North Atlantic–Nordic Seas exchanges. *Progress in Oceanography, 45*(2), 109-208.

Huang, K.-F., Oppo, D. W., & Curry, W. B. (2014). Decreased influence of Antarctic intermediate water in the tropical Atlantic during North Atlantic cold events. *Earth and Planetary Science Letters, 389*(0), 200-208.

Heinrich, H. (1988). Origin and consequences of cyclic ice rafting in the Northeast Atlantic Ocean during the past 130,000 years. *Quaternary Research, 29*(2), 142-152.

Hemming, N. G., & Hanson, G. N. (1992). Boron isotopic composition and concentration in modern marine carbonates. *Geochimica et Cosmochimica Acta, 56*(1), 537-543.

Hemming, S. R. (2004). Heinrich events: Massive late Pleistocene detritus layers of the North Atlantic and their global climate imprint. *Reviews of Geophysics, 42*(1). doi: 10.1029/2003RG000128

Hershey, J. P., Fernandez, M., Milne, P. J., & Millero, F. J. (1986). The ionization of boric acid in NaCl, Na□Ca□Cl and Na□Mg□Cl solutions at 25°C. *Geochimica et Cosmochimica Acta, 50*(1), 143-148.

Huber, C., et al. (2006). Isotope calibrated Greenland temperature record over Marine Isotope Stage 3 and its relation to $CH_4$. *Earth and Planetary Science Letters, 243*(3–4), 504-519.

Hönisch, B., et al. (2003). The influence of symbiont photosynthesis on the boron isotopic composition of foraminifera shells. *Marine Micropaleontology, 49*(1–2), 87-96.

Hönisch, B., & Hemming, N. G. (2005). Surface ocean pH response to variations in $pCO_2$ through two full glacial cycles. *Earth and Planetary Science Letters, 236*(1–2), 305-314.

Jakobsen, P. K., Ribergaard, M. H., Quadfasel, D., Schmith, T., & Hughes, C. W. (2003). Near-surface circulation in the northern North Atlantic as inferred from Lagrangian drifters: Variability from the mesoscale to interannual. *Journal of Geophysical Research: Oceans, 108*(C8), 3251. doi: 10.1029/2002JC001554

Klochko, K., Cody, G. D., Tossell, J. A., Dera, P., & Kaufman, A. J. (2009). Re-evaluating boron speciation in biogenic calcite and aragonite using 11B MAS NMR. *Geochimica et Cosmochimica Acta, 73*(7), 1890-1900.

Lea, D. W., Pak, D. K., Peterson, L. C., & Hughen, K. A. (2003). Synchroneity of Tropical and High-Latitude Atlantic Temperatures over the Last Glacial Termination. *Science, 301*(5638), 1361-1364.

Li, C., Battisti, D. S., & Bitz, C. M. (2010). Can North Atlantic Sea Ice Anomalies Account for Dansgaard–Oeschger Climate Signals? *Journal of Climate, 23*(20), 5457-5475.

Li, C., Battisti, D. S., Schrag, D. P., & Tziperman, E. (2005). Abrupt climate shifts in Greenland due to displacements of the sea ice edge. *Geophysical Research Letters, 32*(19). doi: 10.1029/2005GL023492

Lund, D. C., Tessin, A. C., Hoffman, J. L., & Schmittner, A. (2015). Southwest Atlantic water mass evolution during the last deglaciation. *Paleoceanography*. doi: 10.1002/2014PA002657

Marchitto, T. M., Lehman, S. J., Ortiz, J. D., Flückiger, J., & van Geen, A. (2007). Marine Radiocarbon Evidence for the Mechanism of Deglacial Atmospheric $CO_2$ Rise. *Science, 316*(5830), 1456-1459.

Marcott, S. A., et al. (2014). Centennial-scale changes in the global carbon cycle during the last deglaciation. *Nature, 514*(7524), 616-619.

Marcott, S. A., et al. (2011). Ice-shelf collapse from subsurface warming as a trigger for Heinrich events. *Proceedings of the National Academy of Sciences, 108*(33), 13415-13419.

Martin, J. H., Gordon, R. M., & Fitzwater, S. E. (1990). Iron in Antarctic waters. *Nature, 345*(6271), 156-158.

Martin, P. A., & Lea, D. W. (2002). A simple evaluation of cleaning procedures on fossil benthic foraminiferal Mg/Ca. *Geochemistry, Geophysics, Geosystems, 3*(10), 1-8. doi: 10.1029/2001GC000280

Martinez-Boti, et al. (2015). Boron isotope evidence for oceanic carbon dioxide leakage during the last deglaciation. *Nature, 518*(7538), 219-222.

Martínez-García, et al. (2014). Iron Fertilization of the Subantarctic Ocean During the Last Ice Age. *Science, 343*(6177), 1347-1350.

McManus, J. F., Francois, R., Gherardi, J. M., Keigwin, L. D., & Brown-Leger, S. (2004). Collapse and rapid resumption of Atlantic meridional circulation linked to deglacial climate changes. *Nature, 428*(6985), 834-837.

Meehl, G. A., Arblaster, J. M., Fasullo, J. T., Hu, A., & Trenberth, K. E. (2011). Model-based evidence of deep-ocean heat uptake during surface-temperature hiatus periods. *Nature Clim. Change, 1*(7), 360-364.

Mignot, J., Ganopolski, A., & Levermann, A. (2007). Atlantic Subsurface Temperatures: Response to a Shutdown of the Overturning Circulation and Consequences for Its Recovery. *Journal of Climate, 20*(19), 4884-4898.

Mork, K. A., & Blindheim, J. (2000). Variations in the Atlantic inflow to the Nordic Seas, 1955–1996. *Deep Sea Research Part I: Oceanographic Research Papers, 47*(6), 1035-1057.

Nürnberg, D., Bijma, J., & Hemleben, C. (1996). Assessing the reliability of magnesium in foraminiferal calcite as a proxy for water mass temperatures. *Geochimica et Cosmochimica Acta, 60*(5), 803-814.

Orvik, K. A., & Niiler, P. (2002). Major pathways of Atlantic water in the northern North Atlantic and Nordic Seas toward Arctic. *Geophysical Research Letters, 29*(19). doi: 10.1029/2002GL015002

Palmer, M. R., & Pearson, P. N. (2003). A 23,000-Year Record of Surface Water pH and $PCO_2$ in the Western Equatorial Pacific Ocean. *Science, 300*(5618), 480-482.

Pena, L. D., Calvo, E., Cacho, I., Eggins, S., & Pelejero, C. (2005). Identification and removal of Mn-Mg-rich contaminant phases on foraminiferal tests: Implications for Mg/Ca past temperature reconstructions. *Geochemistry, Geophysics, Geosystems, 6*(9). doi: 10.1029/2005GC000930

Piotrowski, A. M., Goldstein, S. L., Hemming, S. R., Fairbanks, R. G., & Zylberberg, D. R. (2008). Oscillating glacial northern and southern deep water formation from combined neodymium and carbon isotopes. *Earth and Planetary Science Letters, 272*(1–2), 394-405.

Rae, J. W. B., et al. (2014). Deep water formation in the North Pacific and deglacial $CO_2$ rise. *Paleoceanography, 29*(6), 645-667.

Rasmussen, T. L., & Thomsen, E. (2004). The role of the North Atlantic Drift in the millennial timescale glacial climate fluctuations. *Palaeogeography, Palaeoclimatology, Palaeoecology, 210*(1), 101-116.

Rasmussen, T. L., Thomsen, E., Kuijpers, A., & Wastegård, S. (2003). Late warming and early cooling of the sea surface in the Nordic seas during MIS 5e (Eemian Interglacial). *Quaternary Science Reviews, 22*(8–9), 809-821.

Rasmussen, T. L., Thomsen, E., Labeyrie, L., & van Weering, T. C. E. (1996). Circulation changes in the Faeroe-Shetland Channel correlating with cold events during the last glacial period (58–10 ka). *Geology, 24*(10), 937-940.

Reimer, P. J., et al. (2009). IntCal09 and Marine09 radiocarbon age calibration curves, 0–50,000 years cal BP. *Radiocarbon 51*(4): 1111–1150.

Renssen, H., & Isarin, R. F. B. (1997). Surface temperature in NW Europe during the Younger Dryas: AGCM simulation compared with temperature reconstructions. *Climate Dynamics, 14*(1), 33-44.

Rhines, P., Häkkinen, S., & Josey, S. (2008). Is Oceanic Heat Transport Significant in the Climate System? In R. Dickson, J. Meincke, & P. Rhines (Eds.), *Arctic–Subarctic Ocean Fluxes* (pp. 87-109): Springer Netherlands.

Rickaby, R. E. M., & Elderfield, H. (2005). Evidence from the high-latitude North Atlantic for variations in Antarctic Intermediate water flow during the last deglaciation. *Geochemistry, Geophysics, Geosystems, 6*(5). doi: 10.1029/2004GC000858

Riebesell, U., et al. (2000). Reduced calcification of marine plankton in response to increased atmospheric $CO_2$. *Nature, 407*(6802), 364-367.

Roberts, N. L., Piotrowski, A. M., McManus, J. F., & Keigwin, L. D. (2010). Synchronous Deglacial Overturning and Water Mass Source Changes. *Science, 327*(5961), 75-78.

Rosenthal, Y., et al. (2004). Interlaboratory comparison study of Mg/Ca and Sr/Ca measurements in planktonic foraminifera for paleoceanographic research. *Geochemistry, Geophysics, Geosystems, 5*(4). doi: 10.1029/2003GC000650

Rysgaard, S., Bendtsen, J., Pedersen, L. T., Ramløv, H., & Glud, R. N. (2009). Increased $CO_2$ uptake due to sea ice growth and decay in the Nordic Seas. *Journal of Geophysical Research: Oceans, 114*(C9), C09011.

Sabine, C. L., et al. (2004). The Oceanic Sink for Anthropogenic $CO_2$. *Science, 305*(5682), 367-371.

Sanyal, A., et al. (1996). Oceanic pH control on the boron isotopic composition of foraminifera: Evidence from culture experiments. *Paleoceanography, 11*(5), 513-517.

Sarnthein, M. S., et al., (2000). in The Northern North Atlantic: A Changing Environment, P. R. Schafer, W. Schluter, J. Thiede, Eds. (Springer, Berlin, 2000), pp. 365–410.

Schmitt, J., et al. (2012). Carbon Isotope Constraints on the Deglacial $CO_2$ Rise from Ice Cores. *Science, 336*(6082), 711-714.

Shackleton, N. (1967). Oxygen Isotope Analyses and Pleistocene Temperatures Re-assessed. *Nature, 215*(5096), 15-17.

Shakun, J. D., et al. (2012). Global warming preceded by increasing carbon dioxide concentrations during the last deglaciation. *Nature, 484*(7392), 49-54.

Singh, H. A., Battisti, D. S., & Bitz, C. M. (2013). A Heuristic Model of Dansgaard–Oeschger Cycles. Part I: Description, Results, and Sensitivity Studies. *Journal of Climate, 27*(12), 4337-4358.

Skinner, L. C., Fallon, S., Waelbroeck, C., Michel, E., & Barker, S. (2010). Ventilation of the Deep Southern Ocean and Deglacial $CO_2$ Rise. *Science, 328*(5982), 1147-1151.

Skinner, L. C., Waelbroeck, C., Scrivner, A. E., & Fallon, S. J. (2014). Radiocarbon evidence for alternating northern and southern sources of ventilation of the deep Atlantic carbon pool during the last deglaciation. *Proceedings of the National Academy of Sciences, 111*(15), 5480-5484.

Solomon, S., et al. (2007). Technical summary. In Climate Change 2007: The Physical Science Basis. Contribution of Working Group I to the Fourth Assessment Report of the Intergovernmental Panel on Climate Change (eds S. Solomon, D. Qin, M. Manning, Z. Chen, M. Marquis, K. B. Averyt, M. Tignor & H. L. Miller), p. 91. Cambridge, UK: Cambridge University Press.

Sortor, R. N., & Lund, D. C. (2011). No evidence for a deglacial intermediate water $\Delta^{14}C$ anomaly in the SW Atlantic. *Earth and Planetary Science Letters, 310*(1–2), 65-72.

Spero, H. J., Bijma, J., Lea, D. W., & Bemis, B. E. (1997). Effect of seawater carbonate concentration on foraminiferal carbon and oxygen isotopes. *Nature, 390*(6659), 497-500.

Stanford, J. D., et al. (2011). A new concept for the paleoceanographic evolution of Heinrich event 1 in the North Atlantic. *Quaternary Science Reviews, 30*(9–10), 1047-1066.

Stephens, B. B., & Keeling, R. F. (2000). The influence of Antarctic sea ice on glacial-interglacial $CO_2$ variations. *Nature, 404*(6774), 171-174.

Stern, J. V., & Lisiecki, L. E. (2013). North Atlantic circulation and reservoir age changes over the past 41,000 years. *Geophysical Research Letters, 40*(14), 3693-3697.
Stocker, T. F., & Johnsen, S. J. (2003). A minimum thermodynamic model for the bipolar seesaw. *Paleoceanography, 18*(4). doi: 10.1029/2003PA000920
Stommel, H. (1961). Thermohaline Convection with Two Stable Regimes of Flow. *Tellus, 13*(2), 224-230.
Stott, L., Southon, J., Timmermann, A., & Koutavas, A. (2009). Radiocarbon age anomaly at intermediate water depth in the Pacific Ocean during the last deglaciation. *Paleoceanography, 24*(2). doi: 10.1029/2008PA001690
Takahashi, T., et al. (2009). Climatological mean and decadal change in surface ocean $pCO_2$, and net sea–air $CO_2$ flux over the global oceans. *Deep Sea Research Part II: Topical Studies in Oceanography, 56*(8–10), 554-577.
Thornalley, D. J. R., Barker, S., Broecker, W. S., Elderfield, H., & McCave, I. N. (2011). The Deglacial Evolution of North Atlantic Deep Convection. *Science, 331*(6014), 202-205.
Van Nieuwenhove, N., et al. (2011). Evidence for delayed poleward expansion of North Atlantic surface waters during the last interglacial (MIS 5e). *Quaternary Science Reviews, 30*(7–8), 934-946.
Vellinga, M., & Wood, R. (2002). Global Climatic Impacts of a Collapse of the Atlantic Thermohaline Circulation. *Climatic Change, 54*(3), 251-267.
Voelker, A. H. L. (2002). Global distribution of centennial-scale records for Marine Isotope Stage (MIS) 3: a database. *Quaternary Science Reviews, 21*(10), 1185-1212.
Waelbroeck, C., et al. (2011). The timing of deglacial circulation changes in the Atlantic. *Paleoceanography, 26*(3). doi: 10.1029/2010PA002007
Wang, Y. J., Cheng, H., Edwards, R. L., An, Z. S., Wu, J. Y., Shen, C.-C., & Dorale, J. A. (2001). A High-Resolution Absolute-Dated Late Pleistocene Monsoon Record from Hulu Cave, China. *Science, 294*(5550), 2345-2348.
Weaver, A. J., Saenko, O. A., Clark, P. U., & Mitrovica, J. X. (2003). Meltwater Pulse 1A from Antarctica as a Trigger of the Bølling-Allerød Warm Interval. *Science, 299*(5613), 1709-1713.
Wit, J. C., de Nooijer, L. J., Wolthers, M., & Reichart, G. J. (2013). A novel salinity proxy based on Na incorporation into foraminiferal calcite. *Biogeosciences, 10*(10), 6375-6387.
Wunsch, C. (2006). Abrupt climate change: An alternative view. *Quaternary Research, 65*(2), 191-203.
Yu, J., & Elderfield, H. (2007a). Benthic foraminiferal B/Ca ratios reflect deep water carbonate saturation state. *Earth and Planetary Science Letters, 258*(1–2), 73-86.
Yu, J., Elderfield, H., Greaves, M., & Day, J. (2007b). Preferential dissolution of benthic foraminiferal calcite during laboratory reductive cleaning. *Geochemistry, Geophysics, Geosystems, 8*(6). doi: 10.1029/2006GC001571
Zachos, J., Pagani, M., Sloan, L., Thomas, E., & Billups, K. (2001). Trends, Rhythms, and Aberrations in Global Climate 65 Ma to Present. *Science, 292*(5517), 686-693.
Zeebe, R. E., & Wolf-Gladrow, D.A. (2001). $CO_2$ in Seawater: Equilibrium, Kinetics, Isotopes. *Elsevier*.
Zeebe, R. E., Wolf-Gladrow, D. A., Bijma, J., & Hönisch, B. (2003). Vital effects in foraminifera do not compromise the use of $\delta^{11}B$ as a paleo-pH indicator: Evidence from modeling. *Paleoceanography, 18*(2). doi: 10.1029/2003PA000881

**Figure 1:** Map showing the major surface and bottom water currents in the northern North Atlantic and the Nordic seas (Hansen and Østerhus, 2000; Mork and Blindheim, 2000; Orvik and Niiler, 2002; Jakobsen et al., 2003). The star and circle indicate the location of core JM11-FI-19PC and cores studied in (Thornalley et al., 2011), respectively.

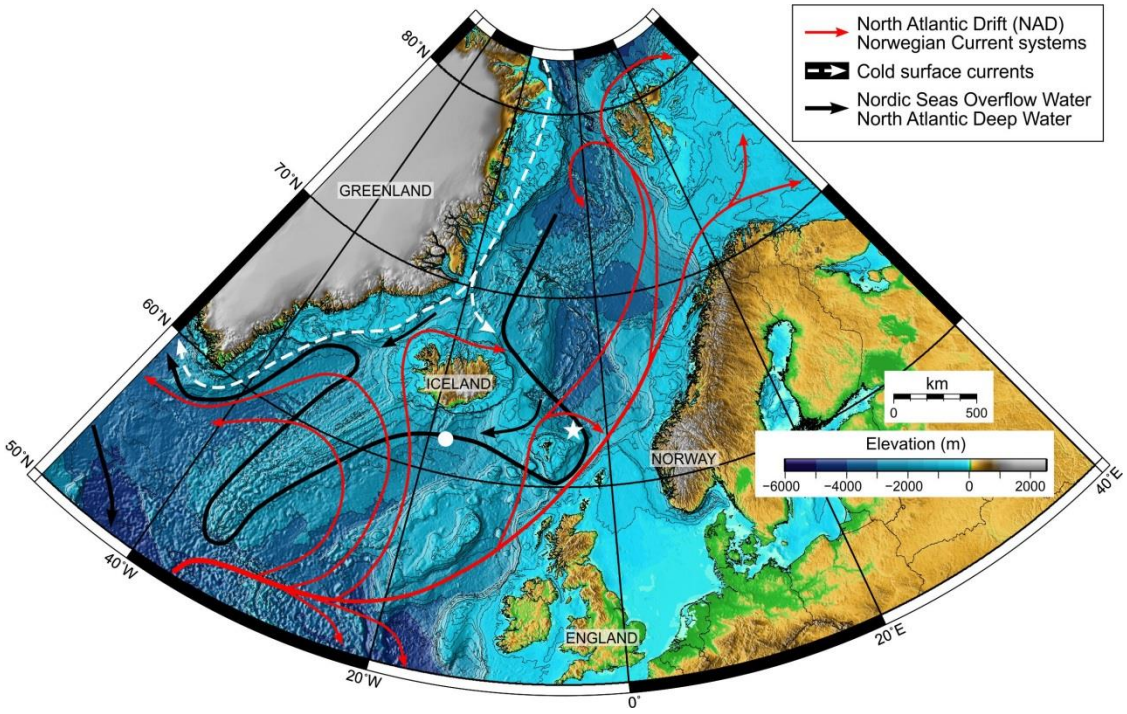

# Paper I

Geology, published online on 30 June 2014 as doi:10.1130/G35579.1

# Persistent intermediate water warming during cold stadials in the southeastern Nordic seas during the past 65 k.y.

Mohamed M. Ezat[1,2]*, Tine L. Rasmussen[1], and Jeroen Groeneveld[3]
[1]Centre for Arctic Gas Hydrate, Environment and Climate (CAGE), Uit, The Arctic University of Norway, NO-9037 Tromsø, Norway
[2]Department of Geology, Faculty of Science, Beni-Suef University, 62111 Beni-Suef, Egypt
[3]Center for Marine Environmental Sciences (MARUM), University of Bremen, Leobener Strasse, D-28359 Bremen, Germany

## ABSTRACT

**In the Nordic seas, conversion of inflowing warm Atlantic surface water to deep cold water through convection is closely linked with climate. During the last glacial period, climate underwent rapid millennial-scale variability known as Dansgaard-Oeschger (DO) events, consisting of warm interstadials and cold stadials. Here we present the first benthic foraminiferal Mg/Ca-$\delta^{18}O$ record from the Nordic seas in order to reconstruct the ocean circulation on DO time scales. The record confirms that convection similar to modern took place in the Nordic seas during interstadials with cold bottom water temperatures (BWTs) close to modern temperatures. The results show gradual and pronounced BWT increases of 2–5 °C during stadials, indicating a stop or near stop in convection. The BWT peaks are followed by an abrupt drop in temperature at the onset of interstadials, indicating the abrupt start of convection and renewed generation of cold deep water. The rise in BWT during stadials confirms earlier interpretations of subsurface inflow of warm Atlantic water below a halocline reaching >1.2 km water depth. The results suggest that warm Atlantic water never ceased to flow into the Nordic seas during the glacial period; inflow at the surface during the Holocene and warm interstadials changed to subsurface and intermediate inflow during cold stadials. Our results suggest that it is the vertical shifts in the position of the warm Atlantic water that cause the abrupt surface warmings.**

## INTRODUCTION

The North Atlantic Current transports warm and salty water masses into the Nordic seas, where they cool and sink to form North Atlantic Deep Water. The strength of deep water production influences the amount of heat transported northward, and has a major role in determining regional climate anomalies and their global telecommunication. Greenland ice cores reveal prominent and pervasive millennial-scale climatic oscillations, referred to as Dansgaard-Oeschger (DO) events, dating from the last glacial cycle. A typical DO cycle is characterized by an abrupt atmospheric warming of 8–16 °C from stadial (cold) to interstadial (warm) conditions followed by a gradual cooling and eventually a sudden cooling back to stadial conditions (Dansgaard et al., 1993; Huber et al., 2006). DO events are manifested in marine and continental records in the circum–North Atlantic region and throughout the globe (Voelker, 2002). Associated with the DO events is the anomalous occurrence of ice-rafted debris (IRD) across the North Atlantic Ocean, forming particularly thick detrital carbonate-bearing deposits known as Heinrich layers, during the six longest-lasting stadials (Heinrich stadials, HS) (Hemming, 2004). Several studies suggest a vital role of the Nordic seas in regulating climate during the last glacial period (e.g., Rasmussen et al., 1996; Dokken and Jansen, 1999; Singh et al., 2013; Petersen et al., 2013). Proxy studies from the Nordic seas have revealed prominent benthic foraminiferal $\delta^{18}O$ depletions of ~0.5‰–2‰ during stadials. The causes of the depletions in the benthic $\delta^{18}O$ signals are debated. Sinking of isotope-depleted brines formed due to sea ice production has been proposed (e.g., Dokken and Jansen, 1999); other explanations include warming of the intermediate water (e.g., Rasmussen and Thomsen, 2004) and hyperpycnal flow of sediment-rich freshwater (Stanford et al., 2011).

Oxygen isotopes in foraminiferal calcite are a function of calcification temperature and seawater $\delta^{18}O$; the latter is linked to glacio-eustatic changes and salinity (e.g., Skinner and Shackleton, 2005). The sea-level changes between the stadials and interstadials generally range between 20 and 30 m (Siddall et al., 2008). Global sea level can account only for ~0.25‰ $\delta^{18}O$ change ($\delta^{18}O_{sl}$ ~1.1‰/100 m; Fairbanks, 1989). This conversion does not account for the regional deviation of $\delta^{18}O_{sl}$ from the global mean due to spatiotemporal variability of the $\delta^{18}O_{sl}$ from the source to the study region (e.g., Friedrich and Timmermann, 2012). Especially during large ocean reorganization events, the regional deviation of $\delta^{18}O_{sl}$ could be significant at our site close to the northern ice sheets. The Mg/Ca measured from foraminiferal tests has the potential to determine the temperature component of the $\delta^{18}O$ signal. However, there are only very few benthic foraminiferal Mg/Ca records from the Nordic seas, and only for the period 18.7–14.2 ka (i.e., HS1) (Marcott et al., 2011).

In this study we present the first Mg/Ca-based bottom water temperature (BWT) record from the Nordic seas based on infaunal benthic foraminifera (*Melonis barleeanus* and *Cassidulina neoteretis*) covering the past 65 k.y. Although several studies (e.g., Raitzsch et al., 2008) showed a significant effect of carbonate ion saturation on Mg incorporation in epifaunal benthic foraminifera below 3 °C, infaunal species do not seem to be significantly influenced by carbonate ion saturation (e.g., Skinner et al., 2003; Elderfield et al., 2010). In addition, we estimate that the impact of salinity is minor (0.2–0.4 °C; e.g., Dissard et al., 2010). Accordingly, the variations in Mg/Ca are predominantly controlled by BWT.

## MATERIALS AND METHODS

The study is based on the upper 7 m of piston core JM11-FI-19PC (62°49′N, 03°52′W), retrieved from a water depth of 1179 m northwest of the Faroe Islands (during the 2011 R/V *Jan Mayen* cruise by the University of Tromsø) (Fig. 1A). Today, about one-third of the cold overflow crossing the Greenland-Scotland Ridge passes the core site (Hansen and Østerhus, 2000). The overflow water has a temperature of <–0.5 °C and a salinity of 34.91 psu (Hansen and Østerhus, 2000) (Fig. 1B); it flows underneath the warm Atlantic surface water of the North Atlantic Drift flowing into the Nordic seas (Fig. 1A).

The magnetic susceptibility was measured using a GEOTEK multisensor core logger. After logging, the core was split, scanned using X-ray fluorescence (XRF), and then sampled at 5 cm, 2.5 cm, or 1 cm intervals; ~300 benthic foraminifera were identified and counted from the size fraction >100 µm at 5 cm resolution. Warm-water species were grouped as Atlantic species (Rasmussen et al., 1996; see also the GSA Data Repository[1]). Tephra shards (rhyolitic and basaltic) were counted from the >100 µm size fraction. The concentration of tephra particles was calculated as the number of grains per gram dry weight sediment. Six tephra layers were identified by abundance counts (Table DR1 and Fig. DR1 in the Data Repository).

*E-mail: mohamed.ezat@uit.no.

[1]GSA Data Repository item 2014248, Tables DR1–DR4, Figures DR1–DR4, and supplemental information, is available online at www.geosociety.org/pubs/ft2014.htm, or on request from editing@geosociety.org or Documents Secretary, GSA, P.O. Box 9140, Boulder, CO 80301, USA.

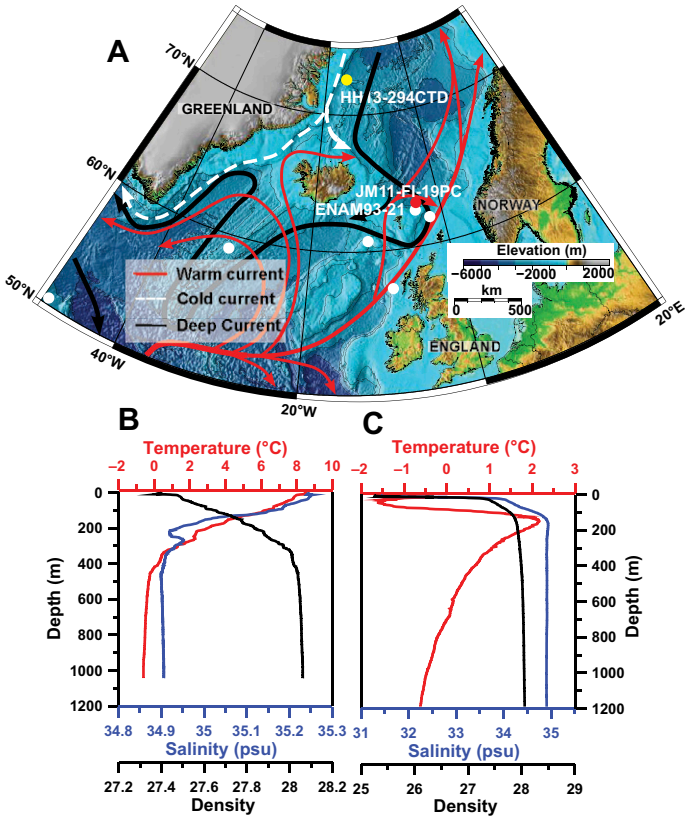


**Figure 1. A: Map of North Atlantic; location of core JM11-FI-19PC (red circle) and major surface and bottom water currents are indicated (Hansen and Østerhus, 2000). Cores containing Atlantic species (Rasmussen and Thomsen, 2004) are also indicated (white circles). B: Conductivity, temperature, depth (CTD) profile for site JM11-FI–19PC, April 2011. C: CTD profile from site HH13–294 (yellow circle in A), Iceland Sea, July 2013.**

Only pristine foraminiferal tests with no signs of dissolution of the benthic foraminiferal species *M. barleeanus* (35–75 tests, size fraction 150–315 µm) and *C. neoteretis* (70–100 tests, size fraction 150–250 µm) were selected for trace element and stable isotope analyses. The stable isotope analyses were performed using a Finnigan MAT 251 mass spectrometer with an automated carbonate preparation device at the Center for Marine Environmental Sciences (MARUM) at the University of Bremen (Germany). For trace elements, the foraminiferal tests were crushed and cleaned following the standard foraminiferal Mg/Ca cleaning protocol (Barker et al., 2003), centrifuged (10 min, 6000 rpm), and analyzed using an inductively coupled plasma–optical emission spectrometer (ICP-OES; Agilent Technologies, 700 Series with autosampler ASX-520 Cetac and micronebulizer). Instrumental precision of the ICP-OES was monitored by analysis of an in-house standard solution with Mg/Ca of 2.93 mmol/mol after every 5 samples ($\sigma$ = 0.012 mmol/mol). To allow interlaboratory comparison we analyzed an international limestone standard (ECRM752–1) with a reported Mg/Ca of 3.75 mmol/mol (Greaves et al., 2008). The average of the ECRM752–1 standard, which was routinely analyzed twice before each batch of 50 samples, was 3.753 mmol/mol. Analytical precision based on 3 replicate measurements of each foraminiferal sample (n = 225) was 0.09% ($1\sigma$ = 0.001 mmol/mol).

The Mg/Ca values were converted to BWT using species-specific calibration equations [*M. barleeanus* $Mg/Ca = 0.757 \pm 0.09 \times \exp(0.119 \pm 0.014 \times T)$], and [*C. neoteretis* $Mg/Ca = 0.864 \pm 0.07 \times \exp(0.082 \pm 0.020 \times T)$] (Kristjánsdóttir et al., 2007). The average estimated standard error for the calibration equations is 1.2 °C (Kristjánsdóttir et al., 2007). Seven replicate samples were cleaned and analyzed during different ICP-OES sessions, yielding an average difference of 0.056 mmol/mol (0.5 °C). The average difference in reconstructed BWT between both species at the same sampling depth is 0.7 °C (n = 22). The close match between the average reconstructed BWT for five core top samples (<2000 $^{14}$C yr; ~0.3 °C) and modern hydrographic conditions (~–0.5 °C) validates our benthic Mg/Ca and BWT reconstructions.

The age model is constructed by alignment of the JM11-FI–19PC record to the North Greenland Ice Core Project (NGRIP) ice core (Greenland Ice Core Chronology 2005 time scale, GICC05; Svensson et al., 2008) using well-dated tephra layers, magnetic susceptibility, and XRF scanner K/Ti ratios (Fig. DR1 and Table DR3). Radiocarbon dates (n = 11) were measured on monospecific planktonic foraminiferal samples and calibrated using the Calib7.01 and Marine13 software programs (Reimer et al., 2013) (Table DR2). The mid-point of the age ranges with $1\sigma$ error was calculated; 50 yr were added to match with the ice core time scale b2k (before 2 ka). The calibrated radiocarbon dates show strong consistency with our tuned age model (Fig. 2). The average deviation between calibrated radiocarbon dates and tuned-NGRIP ages is 500 yr, and is probably related to uncertainties in reservoir age corrections.

## RESULTS

The reconstructed BWT shows persistent intermediate water warming during the cold stadial events (Fig. 3C). BWT increased gradually during stadials to 2–3 °C and to 6 °C during Heinrich stadials, reaching the highest values at the transition to the interstadials and then being followed by an abrupt drop in temperature. This suggests that generation of cold overflows in the Nordic seas must have stopped or become much reduced to allow for such high BWT during cold stadials. In general, the BWT is low during the interstadials and approaches modern temperatures during the best resolved and largest interstadials (~0 °C). During interstadial 14, the BWT is ~–0.5 °C (Fig. 3C). Therefore, convection during interstadials might have been similar to today. A peculiar event with low BWT prior to HS2 is evidenced in late interstadial 3 above the Faroe Marine Ash Zone II (dated to 26.74 ka in the NGRIP ice core). BWT increased to 3 °C during HS2 and these rather high temperatures continued into the Last Glacial Maximum (LGM; ca. 22.5–19 ka), while interstadial 2 is barely visible (Fig. 3C).

Our BWT record does not capture the other brief interstadial events in late Marine Isotope Stage (MIS) 3 to early MIS 2 (ca. 33.7–22.5 ka), probably because of lower sampling resolution (>300 yr per sample). The interstadials during this period, as indicated from NGRIP $\delta^{18}$O values, were of short duration and were followed by abrupt cooling to stadial conditions with no prolonged gradual cooling phase as in earlier interstadials (Fig. 3F).

BWT increases gradually from the start of HS1 to >5 °C followed by a large and abrupt temperature drop at the transition to the Bølling-

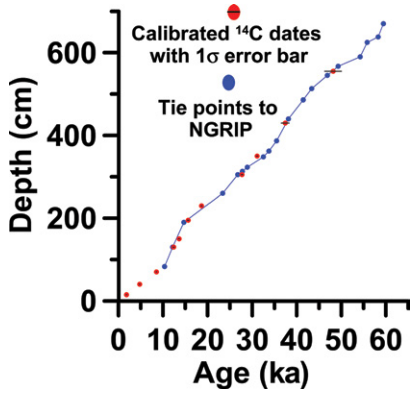


**Figure 2. Age-depth plot with independent calibrated radiocarbon ages using the Calib7.01 and Marine13 software programs (Reimer et al., 2013) (red circles) and ice core tuned ages (blue circles; NGRIP—North Greenland Ice Core Project).**

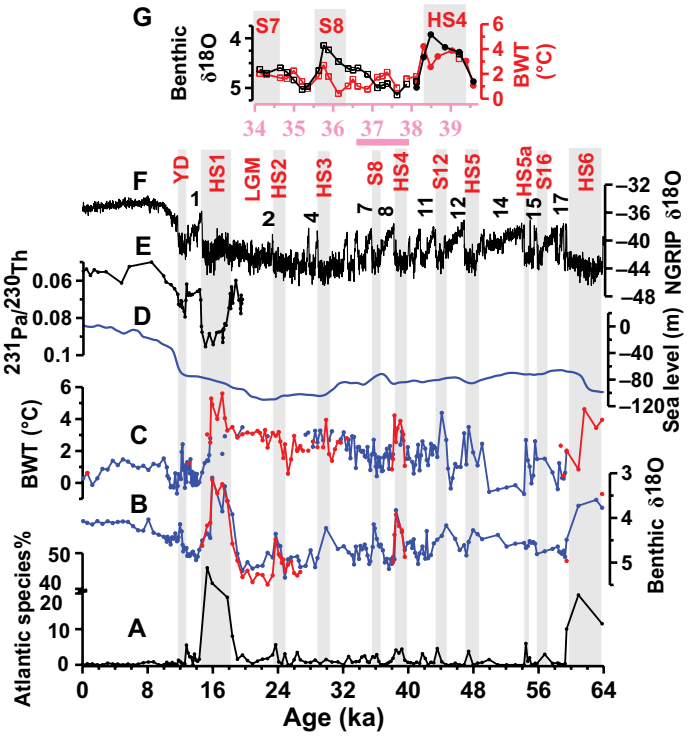


**Figure 3. Proxy records for core JM11-FI-19PC plotted versus North Greenland Ice Core Project (NGRIP) Greenland Ice Core Chronology 2005 (Svensson et al., 2008) time scale (b2k, years before A.D. 2000). A: Percent Atlantic species. Note break in the *y*-axis. B: Benthic $\delta^{18}O$ values measured on *Melonis barleeanus* (blue) and *Cassidulina neoteretis* (red). Note that JM11-FI–19PC $\delta^{18}O$ is closely following the $\delta^{18}O$ record of nearby core ENAM93–21 (Fig. DR3; see footnote 1). C: Mg/Ca-based bottom-water temperature (BWT) measured on *M. barleeanus* (blue) and *C. neoteretis* (red). D: Sea-level record from Grant et al. (2012). E: $^{231}Pa/^{230}Th_0$ record from Bermuda Rise (McManus et al., 2004) as proxy of Atlantic Meridional Overturning Circulation (AMOC) strength. Higher values refer to weaker rate of the AMOC. F: NGRIP ice core $\delta^{18}O$ values (Svensson et al., 2008). G: Detail of Dansgaard-Oeschger events 9–7 showing benthic $\delta^{18}O$ (black) and BWT (red) for *M. barleeanus* (squares) and *C. neoteretis* (circles). Gray bars mark Heinrich stadials (HS), stadials (S), Last Glacial Maximum (LGM), and Younger Dryas (YD). Numbers refer to interstadials.**

Allerød interstadial, likely reflecting sudden onset of convection and renewed inflow of Atlantic water at the surface. The Younger Dryas cold stadial shows a temperature increase to 2.5 °C (another stop or reduction in convection) and an abrupt decrease in temperature at the start of the Holocene, indicating strengthening of convection at the start of the Holocene. BWT increased from –0.5 °C to ~1 °C in the early Holocene and remained stable until 3 k.y. ago, when it decreased to ~0 °C.

## DISCUSSION

The presence of a group of subtropical-boreal benthic foraminiferal species termed "Atlantic species" in almost all stadials provides further evidence for intermediate water warming (Fig. 3A). These non-indigenous species were previously recorded from stadials in the Norwegian Sea and North Atlantic Ocean at intermediate depth (Rasmussen and Thomsen, 2004) (Fig. 1A). In core JM11-FI-19PC, the Atlantic species group composes ~5% of the benthic foraminiferal assemblages during most stadials. They are very abundant during HS6 (20%) and HS1 (45%), the two events with highest BWT (Figs. 3A and 3C). The occurrence of Atlantic species could be traced in the northern North Atlantic region, indicating that the North Atlantic Drift continued to flow across the North Atlantic and into the Nordic seas below a cold, light surface layer, warming the intermediate water masses as proposed in a conceptual model (Rasmussen and Thomsen, 2004).

Invasion of subtropical water throughout Sermilik Fjord, east of Greenland, underneath the polar water of the East Greenland Current with numerous floating icebergs (Straneo et al., 2010) may be a modern analogue to the reversed flow model of Rasmussen and Thomsen (2004). In Sermilik Fjord, Atlantic water with a temperature of 4.5 °C flows below a polar layer of –1.5 °C. Farther north in the Iceland Sea warm Atlantic water with a temperature of 2.2 °C is found underneath the East Greenland Current, which has a temperature below –1.5 °C (Fig. 1C). In a situation with spreading of polar water over the Nordic seas and the cessation or severe reduction in cold overflows, it is easy to picture a thickening and warming of the Atlantic water below the halocline reaching deeper locations than it does today in the Nordic seas. In addition, the general southward shift of mid-latitude storm tracks during the glaciation (e.g., Laîné et al., 2009) would have made the halocline more stable compared to modern conditions (Singh et al., 2013), and thus thickening of the Atlantic layer to deeper than 1000 m below the polar water would have been likely. The Atlantic water, being insulated by the thick polar water layer above the halocline, would lose almost no heat as it moves northward.

The benthic $\delta^{18}O$ changes at our site range from ~0.5‰ to 2‰. The BWT change we observe ranges from 2 °C to slightly more than 5.5 °C, which can explain as much as 1.5‰ (given that ~4 °C corresponds to 1‰ $\delta^{18}O$ change; e.g., Duplessy et al., 1980). The recorded temperature change can explain as much as 70% of the $\delta^{18}O$ variability in some events (e.g., Fig. 3G). Other processes must have occasionally played a role, especially at the transition from the LGM to HS1, where the temperature increase can explain only 20% of the observed benthic $\delta^{18}O$ change.

DO events are generally thought to be associated with changes in the Atlantic Meridional Overturning Circulation (AMOC) probably caused by increased input of freshwater reducing the formation of North Atlantic Deep Water (e.g., Ganopolski and Rahmstorf, 2001). Modeling studies (e.g., Brady and Otto-Bliesner, 2011) suggested that subsurface warming at high latitudes in the North Atlantic Ocean is probably a prerequisite for a rapid recovery of the AMOC. The warming of the intermediate water could trigger further collapse of marine-based glaciers and ice shelves (e.g., Marcott et al., 2011) that would have been maintaining the halocline (see Petersen et al., 2013). In addition, sea ice can be easily eroded by the release of stored ocean heat, and retreat of the sea ice edge in the Nordic seas is thought to have added to the abrupt atmospheric temperature increase (e.g., Gildor and Tziperman, 2003). Thus, the subsurface flow of Atlantic water into the Nordic seas and the intermediate water warming must have contributed substantially to the halocline collapse and the abrupt onset of interstadial conditions.

## CONCLUSIONS

Our new benthic foraminiferal Mg/Ca-$\delta^{18}O$ record from the southeastern Nordic seas shows prominent intermediate water warming during Heinrich stadials, the LGM, and some of the non-Heinrich stadials. The results show cold bottom water during interstadials and the Holocene. The increase in BWT during stadials can explain a large part of the concomitant depletions in benthic $\delta^{18}O$, but other factors must also have played a role.

Our results show that Atlantic water was continuously flowing into the Nordic seas during the past 65 k.y. During warm periods (the Holocene and interstadials) it was most likely at the surface and convection to cold deep water was fairly similar to today. During cold periods (stadials and Heinrich stadials) the Atlantic water was present as a subsurface and intermediate water mass, and generation of cold deep overflows would have been severely reduced. Our results suggest that the vertical shifts in the position of the warm Atlantic water in the Nordic seas have played a key role in the rapid climate change of the DO events.

**ACKNOWLEDGMENTS**

Ezat is funded by UiT, the Arctic University of Norway. The study is part of Paleo-Circus, funded by the Mohn Foundation and the Norwegian Research Council (CAGE; Centre of Excellence grant 223259). The study also received support from ResClim (Norwegian National Research School in Climate Dynamics) and European Cooperation in Science and Technology (COST). We thank J.P. Holm for designing the map and M. Forwick for running the X-ray fluorescence analyses. We also thank M. Segl and S. Pape (MARUM, University of Bremen) for technical support and U. Hoff, S. Jessen, and A. Smith for laboratory assistance and discussions.

**REFERENCES CITED**

Barker, S., Greaves, M., and Elderfield, H., 2003, A study of cleaning procedures used for foraminiferal Mg/Ca paleothermometry: Geochemistry Geophysics Geosystems, v. 4, no. 8407, doi:10.1029/2003GC000559.

Brady, E., and Otto-Bliesner, B., 2011, The role of meltwater-induced subsurface ocean warming in regulating the Atlantic meridional overturning in glacial climate simulations: Climate Dynamics, v. 37, p. 1517–1532, doi:10.1007/s00382-010-0925-9.

Dansgaard, W., et al., 1993, Evidence for general instability of past climate from a 250-kyr ice core record: Nature, v. 364, p. 218–220, doi:10.1038/364218a0.

Dissard, D., Gernot, N., Gert-Jan, R., and Jelle, B., 2010, Impact of seawater $pCO_2$ on calcification and Mg/Ca and Sr/Ca ratios in benthic foraminifera calcite: Results from culturing experiments with *Ammonia tepida*: Biogeosciences, v. 7, p. 81–93, doi:10.5194/bg-7-81-2010.

Dokken, T.M., and Jansen, E., 1999, Rapid changes in the mechanism of ocean convection during the glacial period: Nature, v. 401, p. 458–461, doi:10.1038/46753.

Duplessy, J.C., Moyes, J., and Pujol, C., 1980, Deep water formation in the North Atlantic Ocean during the last ice age: Nature, v. 286, p. 479–482, doi:10.1038/286479a0.

Elderfield, H., Greaves, M., Barker, S., Hall, I.R., Tripati, A., Ferretti, P., Crowhurst, S., Booth, L., and Daunt, C., 2010, A record of bottom water temperature and seawater $\delta^{18}O$ for the Southern Ocean over the past 440 kyr based on Mg/Ca of benthic foraminiferal *Uvigerina spp*: Quaternary Science Reviews, v. 29, p. 160–169, doi:10.1016/j.quascirev.2009.07.013.

Fairbanks, R.G., 1989, A 17,000-year glacio-eustatic sea level record: Influence of glacial melting rates on the Younger Dryas event and deep-ocean circulation: Nature, v. 342, p. 637–642, doi:10.1038/342637a0.

Friedrich, T., and Timmermann, A., 2012, Millennial-scale glacial meltwater pulses and their effect on the spatiotemporal benthic $\delta^{18}O$ variability: Paleoceanography, v. 27, PA3215, doi:10.1029/2012PA002330.

Ganopolski, A., and Rahmstorf, S., 2001, Rapid changes of glacial climate simulated in a coupled climate model: Nature, v. 409, p. 153–158, doi:10.1038/35051500.

Gildor, H., and Tziperman, E., 2003, Sea-ice switches and abrupt climate change: Royal Society of London Philosophical Transactions, v. 361, p. 1935–1944, doi:10.1098/rsta.2003.1244.

Grant, K.M., Rohling, E.J., Bar-Matthews, M., Ayalon, A., Medina-Elizalde, M., Bronk Ramsey, C., Satow, C., and Roberts, A.P., 2012, Rapid coupling between ice volume and polar temperature over the past 150,000 years: Nature, v. 491, p. 744–747, doi:10.1038/nature11593.

Greaves, M., et al., 2008, Interlaboratory comparison study of calibration standards for foraminiferal Mg/Ca thermometry: Geochemistry Geophysics Geosystems, v. 9, Q08010, doi:10.1029/2008GC001974.

Hansen, B., and Østerhus, S., 2000, North Atlantic–Norwegian Sea exchanges: Progress in Oceanography, v. 45, p. 109–208, doi:10.1016/S0079-6611(99)00052-X.

Hemming, S.R., 2004, Heinrich events: Massive late Pleistocene detritus layers of the North Atlantic and their global climate imprint: Reviews of Geophysics, v. 42, RG1005, doi:10.1029/2003RG000128.

Huber, C., Leuenberger, M., Spahni, R., Flückiger, J., Schwander, J., Stocker, T.F., Johnsen, S., Landais, A., and Jouzel, J., 2006, Isotope calibrated Greenland temperature record over Marine Isotope Stage 3 and its relation to $CH_4$: Earth and Planetary Science Letters, v. 243, p. 504–519, doi:10.1016/j.epsl.2006.01.002.

Kristjánsdóttir, G.B., Lea, D.W., Jennings, A.E., Pak, D.K., and Belanger, C., 2007, New spatial Mg/Ca-temperature calibrations for three Arctic, benthic foraminifera and reconstruction of north Iceland shelf temperature for the past 4000 years: Geochemistry Geophysics Geosystems, v. 8, Q03, doi:10.1029/2006GC001425.

Laîné, A., Kageyama, M., Salas-Mélia, D., Voldoire, A., Rivière, G., Ramstein, G., Planton, S., Tyteca, S., and Peterschmitt, J.Y., 2009, Northern Hemisphere storm tracks during the last glacial maximum in the PMIP2 ocean-atmosphere coupled models: Energetic study, seasonal cycle, precipitation: Climate Dynamics, v. 32, p. 593–614, doi:10.1007/s00382-008-0391-9.

Marcott, S.A., et al., 2011, Ice-shelf collapse from subsurface warming as a trigger for Heinrich events: National Academy of Sciences Proceedings, v. 108, p. 13415–13419, doi:10.1073/pnas.1104772108.

McManus, J.F., Francois, R., Gherardi, J.-M., Keigwin, L.D., and Brown-Leger, S., 2004, Collapse and rapid resumption of Atlantic meridional circulation linked to deglacial climate changes: Nature, v. 428, p. 834–837, doi:10.1038/nature02494.

Petersen, S.V., Schrag, D.P., and Clark, P.U., 2013, A new mechanism for Dansgaard-Oeschger cycles: Paleoceanography, v. 28, p. 24–30, doi:10.1029/2012PA002364.

Raitzsch, M., Kuhnert, H., Groeneveld, J., and Bickert, T., 2008, Benthic foraminifer Mg/Ca anomalies in South Atlantic core top sediments and their implications for paleothermometry: Geochemistry Geophysics Geosystems, v. 9, Q05010, doi:10.1029/2007GC001788.

Rasmussen, T.L., and Thomsen, E., 2004, The role of the North Atlantic Drift in the millennial timescale glacial climate fluctuations: Palaeogeography, Palaeoclimatology, Palaeoecology, v. 210, p. 101–116, doi:10.1016/j.palaeo.2004.04.005.

Rasmussen, T.L., Thomsen, E., Labeyrie, L., and van Weering, T.C.E., 1996, Circulation changes in the Faeroe-Shetland Channel correlating with cold events during the last glacial period (58–10 ka): Geology, v. 24, p. 937–940, doi:10.1130/0091-7613(1996)024<0937:CCITFS>2.3.CO;2.

Reimer, P.J., et al., 2013, IntCal13 and Marine13 radiocarbon age calibration curves 0–50,000 years cal BP: Radiocarbon, v. 55, p. 1869–1887, doi:10.2458/azu_js_rc.55.16947.

Siddall, M., Rohling, E.J., Thompson, W.G., and Waelbroeck, C., 2008, Marine isotope stage 3 sea level fluctuations: Data synthesis and new outlook: Reviews of Geophysics, v. 46, RG4003, doi:10.1029/2007RG000226.

Singh, H., Battisti, D., and Bitz, C., 2013, A heuristic model of the Dansgaard-Oeschger Cycles: Description, results, and sensitivity studies: Part I: Journal of Climate, doi:10.1175/JCLI-D-12-00672.1.

Skinner, L.C., and Shackleton N.J., 2005, An Atlantic lead over Pacific deep-water change across Termination I: Implications for the application of the marine isotope stage stratigraphy: Quaternary Science Reviews, v. 24, p. 571–580, doi:10.1016/j.quascirev.2004.11.008.

Skinner, L.C., Shackleton, N.J., and Elderfield, H., 2003, Millennial-scale variability of deep-water temperature and $\delta^{18}Odw$ indicating deep-water source variations in the northeast Atlantic, 0–34 cal. ka BP: Geochemistry Geophysics Geosystems, v. 4, doi:10.1029/2003GC000585.

Stanford, J.D., Rohling, E.J., Bacon, S., Roberts, A.P., Grousset, F.E., and Bolshaw, M., 2011, A new concept for the paleoceanographic evolution of Heinrich event 1 in the North Atlantic: Quaternary Science Reviews, v. 30, p. 1047–1066, doi:10.1016/j.quascirev.2011.02.003.

Straneo, F., Hamilton, G.S., Sutherland, D.A., Stearns, L.A., Davidson, F., Hammill, M.O., Stenson, G.B., and Rosing-Asvid, A., 2010, Rapid circulation of warm subtropical waters in a major glacial fjord in East Greenland: Nature Geoscience, v. 3, p. 182–186, doi:10.1038/ngeo764.

Svensson, A., et al., 2008, A 60 000 year Greenland stratigraphic ice core chronology: Climate of the Past, v. 4, p. 47–57, doi:10.5194/cp-4-47-2008.

Voelker, A.H.L., 2002, Global distribution of centennial-scale records for Marine Isotope Stage (MIS) 3: A database: Quaternary Science Reviews, v. 21, p. 1185–1212. doi:10.1016/S0277-3791(01)00139-1.

Manuscript received 13 February 2014
Revised manuscript received 15 May 2014
Manuscript accepted 17 May 2014

Printed in USA

Geology

# Persistent intermediate water warming during cold stadials in the southeastern Nordic seas during the past 65 k.y.

Mohamed M. Ezat, Tine L. Rasmussen and Jeroen Groeneveld

*Geology* published online 30 June 2014;
doi: 10.1130/G35579.1

**Supplemental Information for**

**'Persistent intermediate water warming during cold stadials in the SE Nordic seas during the last 65 kyr'**

**By**

Mohamed M. Ezat, Tine L. Rasmussen, Jeroen Groeneveld

**Table DR1.** Tephra layers in JM11-F1-19PC.

| Tephra horizons | Depth (cm) in JM11-FI-19PC | NGRIP Age (b2k) Svensson et al. (2008) |
|---|---|---|
| **Saksunarvatn tephra** | **83** | **10.347** |
| **Vedde ash** | **130** | **12.171** |
| **Faroe Marine Ash Zone (FMAZ) II** | **305** | **26.740** |
| **FMAZ III** | **440** | **38.122** |
| **FMAZ IV*** | **540** | |
| **North Atlantic Ash Zone (NAAZ) II**** | **~620** | **55.380** |

***** Located in the lower part of interstadial 12 (Wastegård and Rasmussen, 2014). It has not yet been located in the ice cores.
** Because of no distinct peak (Fig. DR1) it has not been included in the final age model.

**Table DR2.** Calibrated radiocarbon dates using the Calib7.01 and Marine13 programs (Reimer et al., 2013). The reservoir corrections of the Calib7.01 program were used.

| Depth (cm) in JM11-FI-19PC | Conventional Radiocarbon ages (kyr) | Calibrated Ages (kyr) | calibrated Ages ±1σ (b2k) | Laboratory code | Species |
|---|---|---|---|---|---|
| **15** | 2.229 ± 0.03 | 1.822 | 1.822 ±0.07 | UBA-21487 | *N. pachyderma s* |
| **40** | 4.570 ± 0.03 | 4.774 | 4.774 ±0.09 | UBA-21488 | *N. pachyderma s* |
| **70** | 8.083 ± 0.04 | 8.534 | 8.534 ±0.08 | UBA-21489 | *N. pachyderma s* |
| **130** | 10.905 ± 0.05 | 12.418 | 12.418 ±0.17 | UBA-21490 | *N. pachyderma s* |
| **150** | 12.186 ± 0.05 | 13.632 | 13.632 ±0.12 | UBA-21594 | *N. pachyderma s* |
| **195** | 13.493 ± 0.06 | 15.663 | 15.663 ±0.19 | UBA-21595 | *N. pachyderma s* |
| **230** | 15.786 ± 0.08 | 18.653 | 18.653 ±0.13 | UBA-21492 | *N. pachyderma s* |
| **305** | 23.962 ± 0.17 | 27.709 | 27.709 ±0.17 | UBA-21493 | *N. pachyderma s* |
| **350** | 27.459 ± 0.2 | 31.103 | 31.103 ±0.18 | UBA-21494 | *N. pachyderma s* |
| **430** | 33.614 ± 0.41 | 37.41 | 37.41 ±0.89 | UBA-21495 | *N. pachyderma s* |
| **555** | 46.045 ± 2.02 | 48.162 | 48.162 ±1.89 | UBA-21496 | *N. pachyderma s* |

**Table DR3.** Tie points of JM11-F1-19PC to NGRIP used in the construction of the age model. The final age model is based on a radiocarbon date from a core-top sample (15 cm, Table DR1), 4 tephra layers and 15 MS-K/Ti based tie points (see Fig. DR1). The ice core ages are taken from Svensson et al. (2008 and references therein).

| Tie Points | Depth (cm) in JM11-FI-19PC | NGRIP Age (b2k) Svensson et al. (2008) |
|---|---|---|
| **Saksunarvatn tephra** | 83 | 10.347 |
| **Vedde ash** | 130 | 12.171 |
| **IS 1 onset** | 190 | 14.692 |
| **IS 2 onset** | 260 | 23.340 |
| **FMAZ II** | 305 | 26.740 |
| **IS 3 onset** | 313 | 27.780 |
| **IS 4 onset** | 323 | 28.900 |
| **IS 5 onset** | 348 | 32.500 |
| **IS 6 onset** | 362 | 33.740 |
| **IS 7 onset** | 387 | 35.480 |
| **FMAZ III** | 440 | 38.122 |
| **IS 10 onset** | 486 | 41.460 |
| **IS 11 onset** | 513 | 43.340 |
| **IS 12 onset** | 545 | 46.860 |
| **IS 13 onset** | 567 | 49.280 |
| **IS 14 onset** | 590 | 54.220 |
| **IS 15 onset** | 625 | 55.800 |
| **IS 16 onset** | 638 | 58.280 |
| **IS 17 onset** | 670 | 59.440 |

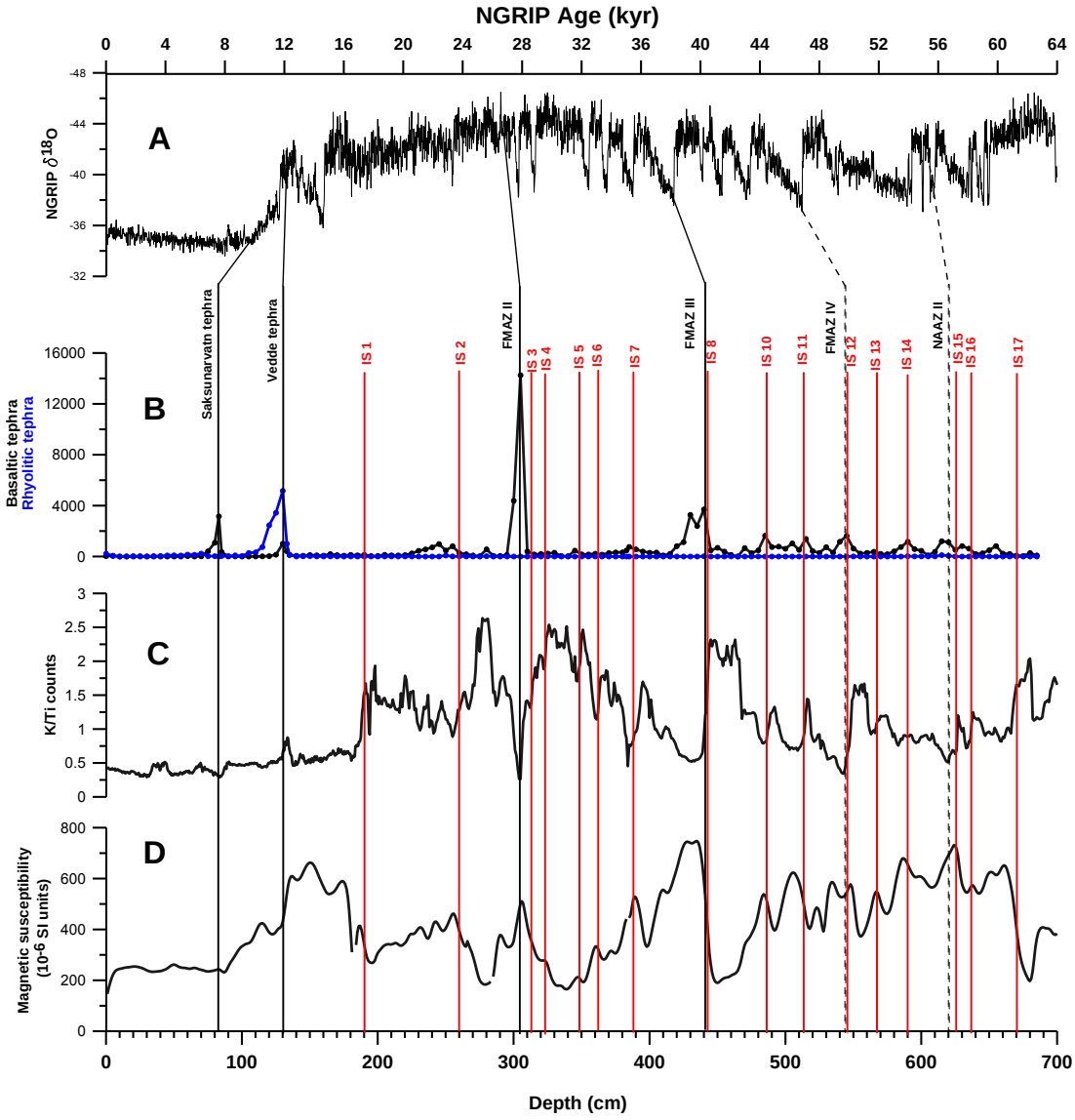


**Figure DR1.** Correlation of core JM11-F1-19PC to NGRIP based on location of tephra layers, magnetic susceptibility (MS) and XRF-K/Ti ratios. MS and K/Ti counts vary oppositely; high (low) MS correlates with low (high) K/Ti ratios during interstadials (stadials) (Rasmussen et al., 1996; Richter et al., 2006). Black and red lines mark the depths of the tephra and start of interstadials, respectively. Faroe Marine Ash Zone (FMAZ) IV and NAAZ II (North Atlantic Ash Zone) (dashed black lines) are used only as supporting tie points. Abbreviations: FMAZ (Faroe Marine Ash Zone), NAAZ (North Atlantic Ash Zone). NGRIP data are from Svensson et al. (2008).

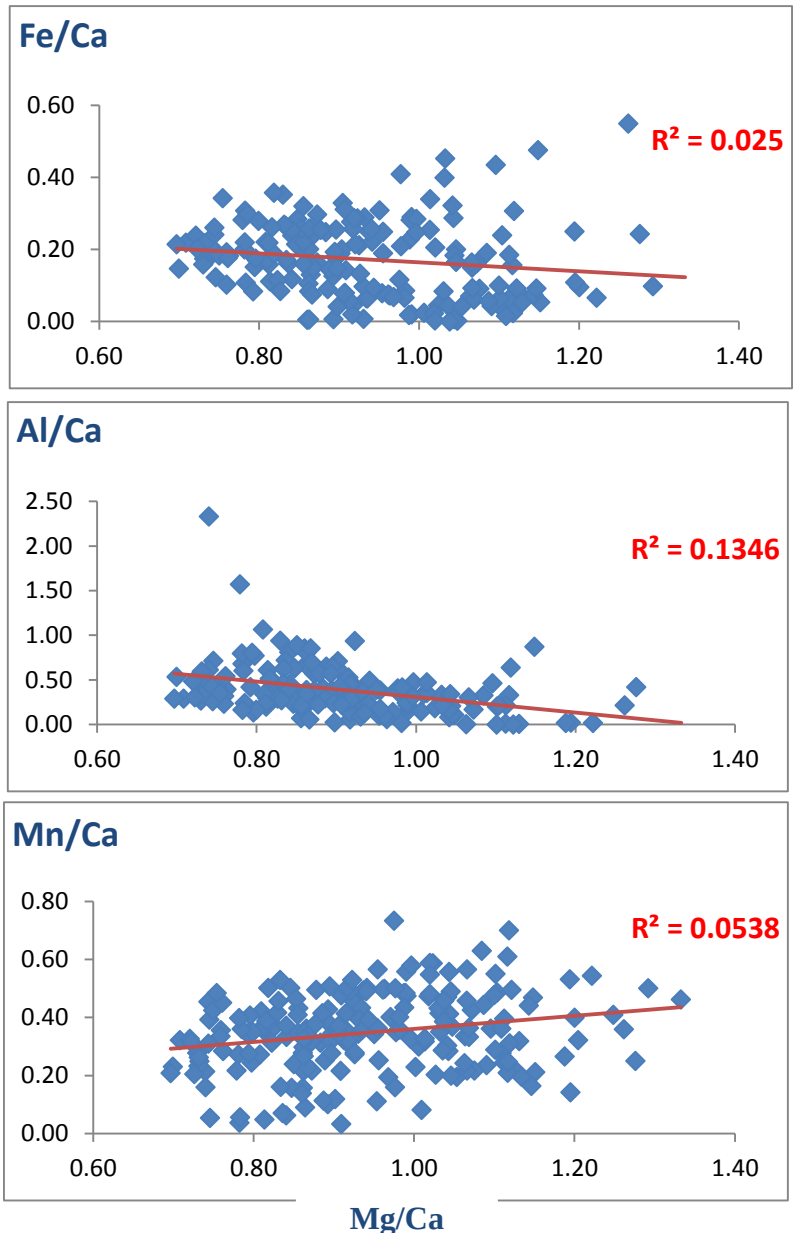


**Figure DR2. Plots of** Mg/Ca versus Fe/Ca, Al/Ca and Mn/Ca ratios for both *M. barleeanus* and *C. neoteretis* showing the absence of contamination by clay minerals and/or Mn-Fe-carbonates and oxyhydroxides (Boyle 1983; Barker et al 2003); for 13% of the samples the concentration of Fe, Al, and/or Mn was below the detection limit. All units are in mmol/mol.

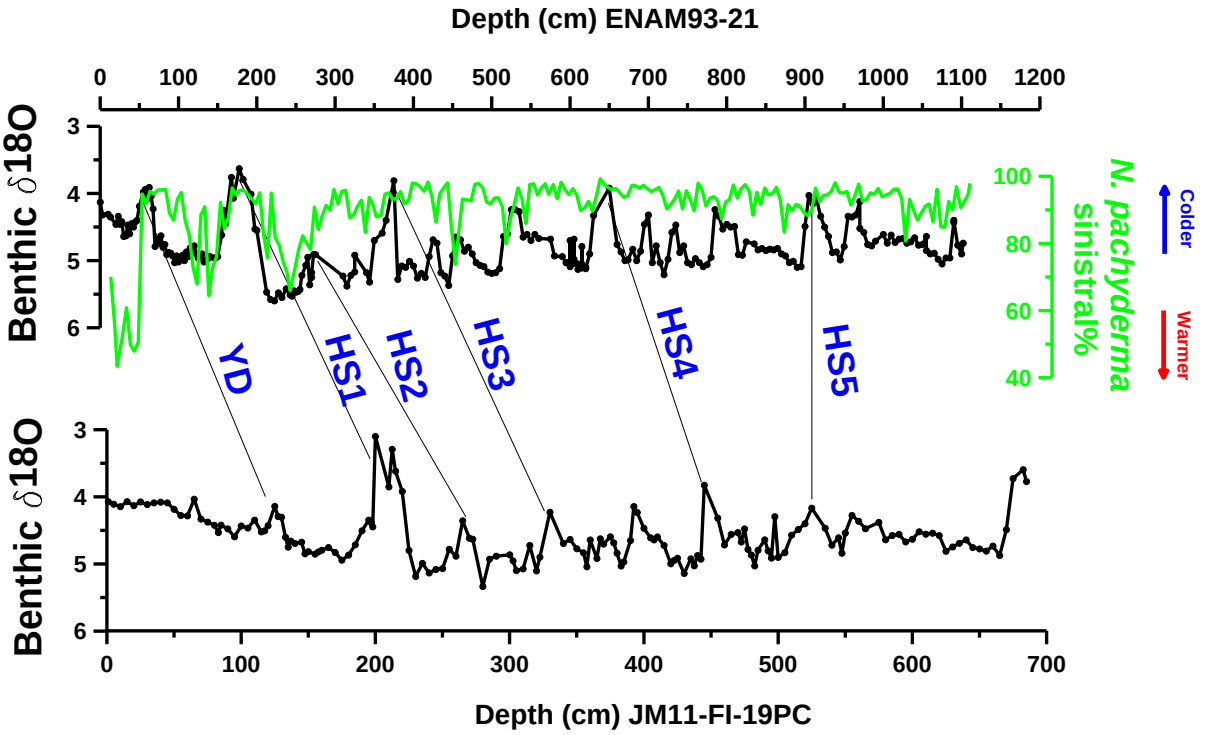


**Figure DR3. Correlation between benthic $\delta^{18}O$** records measured on ***Melonis barleeanus*** of JM11-F1-19PC and nearby core ENAM93-21 from 1020 m water depth (Rasmussen et al., 1996). The two records are very similar and with similar values. The magnetic susceptibility and XRF-K/Ti ratios for ENAM93-21 (Richter et al., 2006) are the same as in JM11-FI-19PC (Fig. DR. 1). The percentage of planktic species *N. pachyderma* sinistral for ENAM93-21 (green line) indicates relatively warmer surface/subsurface temperatures during the interstadials than in the stadials.

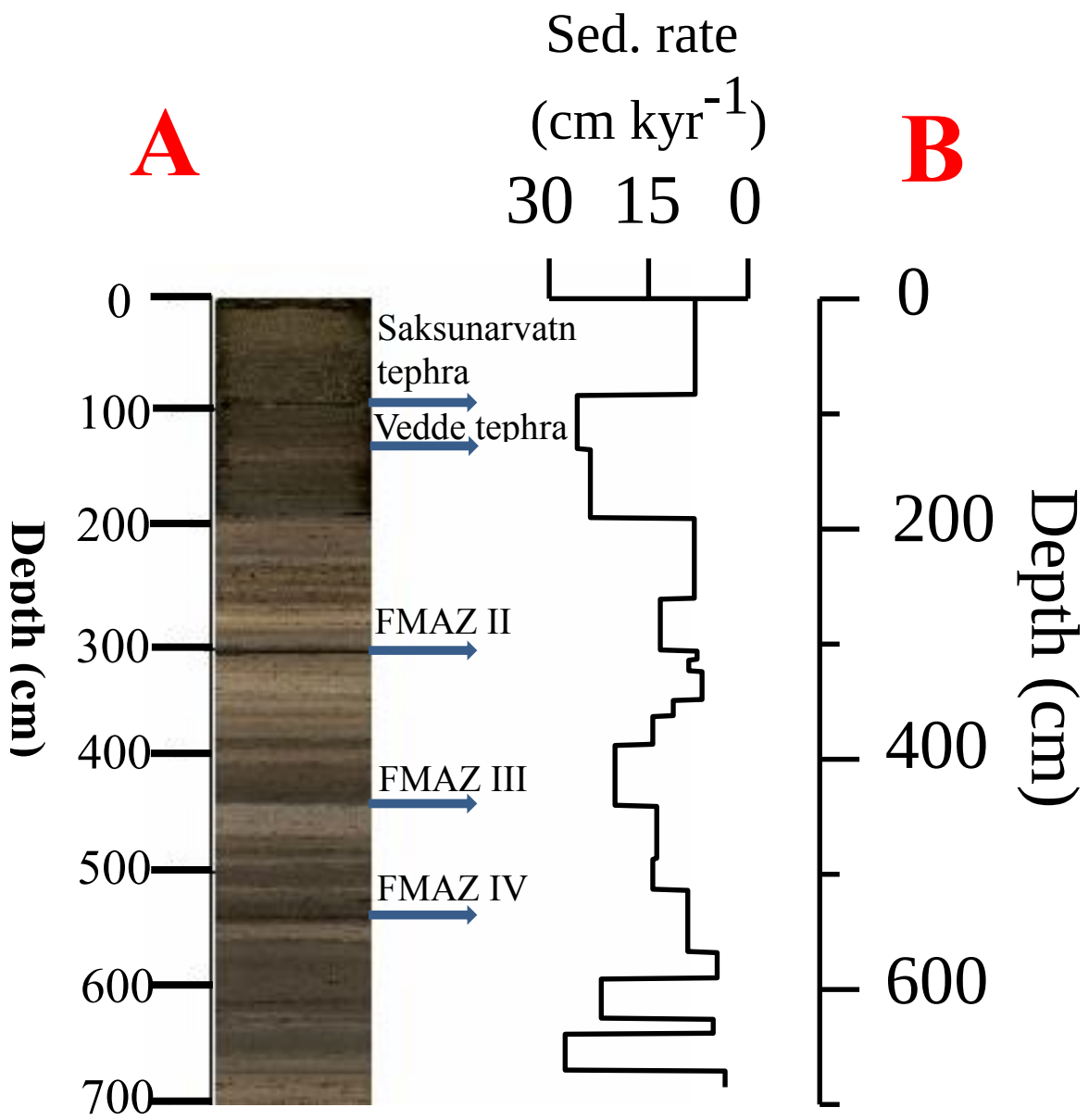


**Figure DR4. A. XRF-scanner image of the upper 7 m of JM11-FI-19PC.** The dark layers correlate with interstadials, while the light layers represent stadials/Heinrich events and the LGM. The same was recorded in ENAM93-21 (Rasmussen et al., 1998). Blue arrows refer to the tephra layers (see Table DR. 1). FMAZ: Faroe Marine Ash Zone. **B. Sedimentation rate of JM11-FI-19PC based on the tuned age model.**

**Atlantic species**

Benthic foraminiferal species linked to warm bottom water were grouped as ‘Atlantic Species’ (Rasmussen et al., 1996) and comprised predominantly specimens of *Epistominella decorata*, *Cibicidoides pachyderma* (*=C. aff C. floridanus*), *Gyroidina umbonata*, *Miliolinella irregularis*, *Sigmoilopsis schlumbergeri*, *Valvulineria sp.*, *Anomalinoides minimus*, *Eggerella bradyi*, *Bulimina costata*, and *Sagrina subspinescens*. The ecological preferences and systematics of those species assemblages are treated in detail in Rasmussen et al. (2003) and Rasmussen (2005). They are subtropical–boreal species adapted to low food supply. They do not occur in the Nordic seas today except two of them (*Gyroidina neosoldani*i and *Sigmoilopsis schlumbergeri*) that can be found on the shelf of western Norway in bottom water with a temperature >4 °C (Sejrup et al., 2004).

**Table DR 4. Mg/Ca data for core JM11-F1-19PC.**

| Depth (cm) | Age (kyr) | Mg/Ca (mmol/mol) | BWT (°C) | Species |
|---|---|---|---|---|
| **1** | 0.085 | 0.78 | 0.3 | *M. barleeanus* |
| **5** | 0.581 | 0.81 | 0.6 | *M. barleeanus* |
| **5** | 0.581 | 0.91 | 0.6 | *C. neoteretis* |
| **10** | 1.200 | 0.75 | -0.1 | *M. barleeanus* |
| **15** | 1.822 | 0.78 | 0.3 | *M. barleeanus* |
| **20** | 2.448 | 0.84 | 0.9 | *M. barleeanus* |
| **25** | 3.075 | 0.84 | 0.8 | *M. barleeanus* |
| **30** | 3.702 | 0.82 | 0.8 | *M. barleeanus* |
| **30** | 3.702 | 0.89 | 1.4 | *M. barleeanus* |
| **35** | 4.329 | 0.81 | 0.7 | *M. barleeanus* |
| **35** | 4.329 | 0.86 | 1.1 | *M. barleeanus* |
| **40** | 4.956 | 0.90 | 1.5 | *M. barleeanus* |
| **45** | 5.583 | 0.89 | 1.3 | *M. barleeanus* |
| **50** | 6.209 | 0.86 | 1.1 | *M. barleeanus* |
| **55** | 6.836 | 0.85 | 1.0 | *M. barleeanus* |
| **60** | 7.463 | 0.86 | 1.1 | *M. barleeanus* |
| **65** | 8.090 | 0.86 | 1.1 | *M. barleeanus* |
| **65** | 8.090 | 0.83 | 0.8 | *M. barleeanus* |
| **70** | 8.717 | 0.87 | 1.2 | *M. barleeanus* |
| **75** | 9.344 | 0.86 | 1.1 | *M. barleeanus* |
| **80** | 9.971 | 0.91 | 1.5 | *M. barleeanus* |

| | | | | |
|---|---|---|---|---|
| **83** | 10.347 | 0.85 | 1.0 | *M. barleeanus* |
| **85** | 10.425 | 0.80 | 0.4 | *M. barleeanus* |
| **90** | 10.619 | 0.78 | 0.3 | *M. barleeanus* |
| **95** | 10.813 | 0.73 | -0.3 | *M. barleeanus* |
| **100** | 11.007 | 0.74 | -0.2 | *M. barleeanus* |
| **105** | 11.201 | 0.73 | -0.3 | *M. barleeanus* |
| **110** | 11.395 | 0.87 | 1.2 | *M. barleeanus* |
| **110** | 11.395 | 0.81 | 0.6 | *M. barleeanus* |
| **115** | 11.589 | 0.70 | -0.7 | *M. barleeanus* |
| **117.5** | 11.686 | 0.74 | -0.2 | *M. barleeanus* |
| **120** | 11.783 | 0.81 | 0.6 | *M. barleeanus* |
| **125** | 11.977 | 0.79 | 0.4 | *M. barleeanus* |
| **127.5** | 12.074 | 0.78 | 0.2 | *M. barleeanus* |
| **130** | 12.171 | 0.95 | 1.9 | *M. barleeanus* |
| **133** | 12.289 | 1.01 | 2.4 | *M. barleeanus* |
| **135** | 12.368 | 0.84 | 0.8 | *M. barleeanus* |
| **137** | 12.447 | 0.86 | 1.1 | *M. barleeanus* |
| **140** | 12.565 | 0.73 | -0.3 | *M. barleeanus* |
| **142.5** | 12.663 | 0.86 | 1.1 | *M. barleeanus* |
| **145** | 12.762 | 0.76 | 0.1 | *M. barleeanus* |
| **147.5** | 12.860 | 0.88 | 1.3 | *M. barleeanus* |
| **150** | 12.959 | 0.84 | 0.9 | *M. barleeanus* |
| **152.5** | 13.057 | 0.86 | 1.1 | *M. barleeanus* |
| **152.5** | 13.057 | 0.96 | 1.2 | *C. neoteretis* |

| | | | | |
|---|---|---|---|---|
| **155** | 13.156 | 0.81 | 0.6 | *M. barleeanus* |
| **157.5** | 13.254 | 0.90 | 1.5 | *M. barleeanus* |
| **160** | 13.353 | 0.76 | 0.0 | *M. barleeanus* |
| **162.5** | 13.451 | 0.82 | 0.7 | *M. barleeanus* |
| **165** | 13.550 | 0.74 | -0.2 | *M. barleeanus* |
| **167.5** | 13.648 | 0.76 | 0.0 | *M. barleeanus* |
| **170** | 13.747 | 0.81 | 0.6 | *M. barleeanus* |
| **172.5** | 13.845 | 0.79 | 0.4 | *M. barleeanus* |
| **175** | 13.944 | 0.75 | -0.1 | *M. barleeanus* |
| **177.5** | 14.042 | 0.81 | 0.6 | *M. barleeanus* |
| **180** | 14.141 | 0.75 | -0.1 | *M. barleeanus* |
| **185** | 14.337 | 0.76 | 0.0 | *M. barleeanus* |
| **190** | 14.692 | 0.82 | 0.7 | *M. barleeanus* |
| **192.5** | 15.001 | 0.88 | 1.3 | *M. barleeanus* |
| **195** | 15.310 | 0.90 | 1.4 | *M. barleeanus* |
| **195** | 15.310 | 1.11 | 3.0 | *C. neoteretis* |
| **196** | 15.433 | 0.89 | 1.4 | *M. barleeanus* |
| **197** | 15.557 | 0.93 | 1.7 | *M. barleeanus* |
| **198** | 15.680 | 1.05 | 2.8 | *M. barleeanus* |
| **198** | 15.680 | 1.06 | 2.5 | *C. neoteretis* |
| **199** | 15.804 | 1.33 | 5.3 | *C. neoteretis* |
| **200** | 15.927 | 1.29 | 4.9 | *C. neoteretis* |
| **205** | 16.545 | 1.20 | 4.0 | *C. neoteretis* |
| **210** | 17.163 | 1.25 | 4.5 | *C. neoteretis* |

| | | | | |
|---|---|---|---|---|
| **210** | 17.163 | 1.37 | 5.6 | *C. neoteretis* |
| **210** | 17.163 | 0.94 | 1.8 | *M. barleeanus* |
| **212.5** | 17.472 | 1.21 | 4.1 | *C. neoteretis* |
| **212.5** | 17.472 | 1.07 | 2.9 | *M. barleeanus* |
| **215** | 17.781 | 1.13 | 3.3 | *C. neoteretis* |
| **220** | 18.398 | 1.15 | 3.5 | *C. neoteretis* |
| **225** | 19.016 | 1.09 | 2.8 | *C. neoteretis* |
| **225** | 19.016 | 1.07 | 2.9 | *M. barleeanus* |
| **230** | 19.634 | 1.15 | 3.5 | *M. barleeanus* |
| **230** | 19.634 | 1.11 | 3.1 | *C. neoteretis* |
| **235** | 20.251 | 1.12 | 3.2 | *C. neoteretis* |
| **240** | 20.869 | 1.11 | 3.1 | *C. neoteretis* |
| **245** | 21.487 | 1.13 | 3.3 | *C. neoteretis* |
| **247.5** | 21.796 | 1.12 | 3.1 | *C. neoteretis* |
| **250** | 22.105 | 1.08 | 2.7 | *C. neoteretis* |
| **252.5** | 22.413 | 1.13 | 3.3 | *C. neoteretis* |
| **255** | 22.722 | 1.04 | 2.2 | *C. neoteretis* |
| **255** | 22.722 | 1.07 | 2.9 | *M. barleeanus* |
| **260** | 23.340 | 1.12 | 3.1 | *C. neoteretis* |
| **265** | 23.718 | 1.10 | 3.0 | *C. neoteretis* |
| **270** | 24.096 | 1.12 | 3.2 | *C. neoteretis* |
| **272.5** | 24.284 | 1.07 | 2.6 | *C. neoteretis* |
| **277.5** | 24.662 | 0.89 | 1.6 | *C. neoteretis* |
| **280** | 24.851 | 0.98 | 2.4 | *C. neoteretis* |

| | | | | |
|---|---|---|---|---|
| **285** | 25.229 | 1.05 | 0.6 | *C. neoteretis* |
| **290** | 25.607 | 0.91 | 1.5 | *C. neoteretis* |
| **295** | 25.984 | 0.98 | 2.9 | *C. neoteretis* |
| **300** | 26.362 | 1.1 | 2.0 | *C. neoteretis* |
| **300** | 26.362 | 1.02 | 2.1 | *M. barleeanus* |
| **302.5** | 26.551 | 1.03 | 2.2 | *C. neoteretis* |
| **305** | 26.740 | 1.04 | 2.3 | *C. neoteretis* |
| **307.5** | 27.065 | 1.02 | 2.0 | *C. neoteretis* |
| **310** | 27.390 | 1.09 | 3.0 | *M. barleeanus* |
| **312.5** | 27.715 | 1.02 | 2.0 | *C. neoteretis* |
| **312.5** | 27.715 | 1.10 | 3.2 | *M. barleeanus* |
| **317.5** | 28.284 | 0.99 | 2.3 | *M. barleeanus* |
| **317.5** | 28.284 | 1.07 | 2.6 | *C. neoteretis* |
| **320** | 28.564 | 1.12 | 3.3 | *M. barleeanus* |
| **322.5** | 28.844 | 1.02 | 2.5 | *M. barleeanus* |
| **322.5** | 28.844 | 1.04 | 2.2 | *C. neoteretis* |
| **325** | 29.188 | 1.12 | 3.3 | *M. barleeanus* |
| **327.5** | 29.548 | 1.04 | 2.7 | *M. barleeanus* |
| **327.5** | 29.548 | 1.04 | 2.2 | *C. neoteretis* |
| **330** | 29.908 | 1.19 | 4.0 | *C. neoteretis* |
| **332.5** | 30.268 | 1.00 | 1.8 | *C. neoteretis* |
| **332.5** | 30.268 | 1.04 | 2.7 | *M. barleeanus* |
| **335** | 30.628 | 1.11 | 3.2 | *M. barleeanus* |
| **335** | 30.628 | 0.97 | 1.4 | *C. neoteretis* |

| | | | | |
|---|---|---|---|---|
| **337.5** | 30.988 | 1.03 | 2.1 | *C. neoteretis* |
| **340** | 31.348 | 1.07 | 2.6 | *C. neoteretis* |
| **342.5** | 31.708 | 1.06 | 2.5 | *C. neoteretis* |
| **342.5** | 31.708 | 1.05 | 2.7 | *M. barleeanus* |
| **345** | 32.068 | 1.10 | 3.2 | *M. barleeanus* |
| **347.5** | 32.428 | 0.97 | 2.1 | *M. barleeanus* |
| **347.5** | 32.428 | 1.09 | 2.8 | *C. neoteretis* |
| **350** | 32.677 | 1.05 | 2.7 | *M. barleeanus* |
| **352.5** | 32.899 | 0.91 | 1.5 | *M. barleeanus* |
| **355** | 33.120 | 1.07 | 2.9 | *M. barleeanus* |
| **357.5** | 33.341 | 1.07 | 2.9 | *M. barleeanus* |
| **360** | 33.563 | 0.85 | 0.9 | *M. barleeanus* |
| **362.5** | 33.775 | 0.99 | 2.2 | *M. barleeanus* |
| **365** | 33.949 | 0.99 | 2.3 | *M. barleeanus* |
| **367.5** | 34.123 | 0.96 | 2.0 | *M. barleeanus* |
| **370** | 34.297 | 0.96 | 2.0 | *M. barleeanus* |
| **372.5** | 34.471 | 0.96 | 2.0 | *M. barleeanus* |
| **375** | 34.645 | 0.93 | 1.7 | *M. barleeanus* |
| **377.5** | 34.819 | 0.92 | 1.6 | *M. barleeanus* |
| **380** | 34.993 | 0.99 | 2.3 | *M. barleeanus* |
| **383** | 35.202 | 0.89 | 1.4 | *M. barleeanus* |
| **385** | 35.341 | 0.83 | 0.8 | *M. barleeanus* |
| **387.5** | 35.505 | 0.93 | 1.8 | *M. barleeanus* |
| **390** | 35.630 | 0.94 | 1.8 | *M. barleeanus* |

| | | | | |
|---|---|---|---|---|
| **392.5** | 35.754 | 1.04 | 2.7 | *M. barleeanus* |
| **395** | 35.879 | 0.94 | 1.8 | *M. barleeanus* |
| **397.5** | 36.003 | 0.86 | 1.0 | *M. barleeanus* |
| **400** | 36.128 | 0.80 | 0.4 | *M. barleeanus* |
| **402** | 36.228 | 0.92 | 1.6 | *M. barleeanus* |
| **405** | 36.377 | 0.86 | 1.0 | *M. barleeanus* |
| **407.5** | 36.502 | 0.91 | 1.6 | *M. barleeanus* |
| **410** | 36.627 | 0.85 | 1.0 | *M. barleeanus* |
| **412.5** | 36.751 | 0.83 | 0.7 | *M. barleeanus* |
| **415** | 36.876 | 0.83 | 0.8 | *M. barleeanus* |
| **417.5** | 37.000 | 0.92 | 1.6 | *M. barleeanus* |
| **420** | 37.125 | 0.93 | 1.7 | *M. barleeanus* |
| **422.5** | 37.250 | 0.94 | 1.8 | *M. barleeanus* |
| **425** | 37.374 | 0.98 | 2.1 | *M. barleeanus* |
| **427.5** | 37.499 | 0.92 | 1.6 | *M. barleeanus* |
| **430** | 37.624 | 0.84 | 0.9 | *M. barleeanus* |
| **432.5** | 37.748 | 0.10 | 2.3 | *M. barleeanus* |
| **435** | 37.873 | 0.92 | 1.6 | *M. barleeanus* |
| **437.5** | 37.997 | 0.93 | 0.9 | *C. neoteretis* |
| **440** | 38.122 | 0.94 | 1.8 | *M. barleeanus* |
| **440** | 38.122 | 0.98 | 1.5 | *C. neoteretis* |
| **442.5** | 38.303 | 1.22 | 4.2 | *C. neoteretis* |
| **445** | 38.485 | 1.07 | 2.6 | *C. neoteretis* |
| **447.5** | 38.666 | 1.14 | 3.4 | *C. neoteretis* |

| | | | | |
|---|---|---|---|---|
| **452.5** | 39.029 | 1.19 | 3.9 | *C. neoteretis* |
| **452.5** | 39.029 | 1.00 | 2.4 | *M. barleeanus* |
| **455** | 39.210 | 1.11 | 3.2 | *M. barleeanus* |
| **457.5** | 39.392 | 1.04 | 2.7 | *M. barleeanus* |
| **457.5** | 39.392 | 1.11 | 3.0 | *C. neoteretis* |
| **460** | 39.573 | 0.94 | 1.1 | *C. neoteretis* |
| **462.5** | 39.755 | 0.91 | 1.5 | *M. barleeanus* |
| **465** | 39.936 | 0.99 | 2.2 | *M. barleeanus* |
| **467.5** | 40.118 | 0.91 | 1.5 | *M. barleeanus* |
| **472.5** | 40.480 | 0.89 | 1.3 | *M. barleeanus* |
| **475** | 40.662 | 0.81 | 0.6 | *M. barleeanus* |
| **477.5** | 40.843 | 0.87 | 1.1 | *M. barleeanus* |
| **480** | 41.025 | 0.92 | 1.7 | *M. barleeanus* |
| **482.5** | 41.206 | 1.01 | 2.4 | *M. barleeanus* |
| **482.5** | 41.206 | 0.99 | 2.3 | *M. barleeanus* |
| **485** | 41.387 | 0.83 | 0.8 | *M. barleeanus* |
| **487.5** | 41.564 | 0.93 | 1.7 | *M. barleeanus* |
| **490** | 41.739 | 1.03 | 2.6 | *M. barleeanus* |
| **495** | 42.087 | 0.98 | 2.2 | *M. barleeanus* |
| **497.5** | 42.261 | 0.90 | 1.4 | *M. barleeanus* |
| **500** | 42.435 | 0.86 | 1.1 | *M. barleeanus* |
| **505** | 42.783 | 1.01 | 2.5 | *M. barleeanus* |
| **507.5** | 42.957 | 0.94 | 1.8 | *M. barleeanus* |
| **510** | 43.131 | 0.10 | 2.3 | *M. barleeanus* |

| | | | | |
|---|---|---|---|---|
| **512.5** | 43.305 | 0.98 | 2.2 | *M. barleeanus* |
| **515** | 43.560 | 0.92 | 1.6 | *M. barleeanus* |
| **520** | 44.110 | 1.28 | 4.4 | *M. barleeanus* |
| **525** | 44.660 | 1.04 | 2.7 | *M. barleeanus* |
| **530** | 45.210 | 0.73 | -0.4 | *M. barleeanus* |
| **532** | 45.43 | 0.78 | 0.3 | *M. barleeanus* |
| **535** | 45.760 | 0.87 | 1.2 | *M. barleeanus* |
| **537** | 45.98 | 0.85 | 1.0 | *M. barleeanus* |
| **541** | 46.42 | 0.85 | 1.0 | *M. barleeanus* |
| **545** | 46.860 | 1.10 | 3.1 | *M. barleeanus* |
| **547.5** | 47.135 | 0.87 | 1.2 | *M. barleeanus* |
| **550** | 47.410 | 1.15 | 3.5 | *M. barleeanus* |
| **555** | 47.960 | 0.95 | 1.9 | *M. barleeanus* |
| **560** | 48.510 | 0.86 | 1.1 | *M. barleeanus* |
| **565** | 49.060 | 1.01 | 2.5 | *M. barleeanus* |
| **570** | 49.924 | 0.71 | -0.6 | *M. barleeanus* |
| **575** | 50.998 | 0.72 | -0.4 | *M. barleeanus* |
| **580** | 52.072 | 0.73 | -0.3 | *M. barleeanus* |
| **585** | 53.146 | 0.74 | -0.2 | *M. barleeanus* |
| **590** | 54.220 | 0.70 | -0.7 | *M. barleeanus* |
| **595** | 54.446 | 1.04 | 2.7 | *M. barleeanus* |
| **600** | 54.671 | 0.90 | 1.4 | *M. barleeanus* |
| **605** | 54.897 | 0.86 | 1.0 | *M. barleeanus* |
| **610** | 55.123 | 0.75 | -0.0 | *M. barleeanus* |

| | | | | |
|---|---|---|---|---|
| **615** | 55.349 | 0.80 | 0.5 | *M. barleeanus* |
| **620** | 55.574 | 1.03 | 2.6 | *M. barleeanus* |
| **625** | 55.800 | 0.90 | 1.5 | *M. barleeanus* |
| **630** | 56.754 | 0.91 | 1.5 | *M. barleeanus* |
| **635** | 57.708 | 0.82 | 0.7 | *M. barleeanus* |
| **640** | 58.353 | 0.72 | -0.4 | *M. barleeanus* |
| **645** | 58.534 | 0.88 | 1.2 | *M. barleeanus* |
| **650** | 58.715 | 1.05 | 2.3 | *C. neoteretis* |
| **655** | 58.896 | 0.79 | 0.3 | *M. barleeanus* |
| **660** | 59.078 | 0.78 | 0.3 | *M. barleeanus* |
| **660** | 59.078 | 0.90 | 0.5 | *C. neoteretis* |
| **665** | 59.259 | 0.82 | 0.6 | *M. barleeanus* |
| **670** | 59.440 | 0.96 | 2.0 | *M. barleeanus* |
| **670** | 59.440 | 1.02 | 2.0 | *C. neoteretis* |
| **675** | 60.893 | 0.93 | 0.8 | *C. neoteretis* |
| **677.5** | 61.620 | 1.26 | 4.6 | *C. neoteretis* |
| **682.5** | 63.073 | 1.15 | 3.5 | *C. neoteretis* |
| **685** | 63.800 | 1.20 | 4.0 | *C. neoteretis* |

**References**

Barker, S., Greaves, M., and Elderfield, H., 2003, A study of cleaning procedures used for foraminiferal Mg/Ca paleothermometry: Geochemistry Geophysics Geosystems**,** v. 4, no. 8407, doi: 10.1029/2003GC000559.

Boyle, E.A., 1983, Manganese carbonate overgrowths on foraminifera tests: Geochimica et Cosmochimica Acta**,** v. 47, p. 1815– 1819.

Rasmussen, T.L., 2005, Systematic paleontology and ecology of benthic foraminifera from the Plio-Pleistocene Kalithea Bay Section, Rhodes (Greece): Cushman Foundation for Foraminiferal Research Special Publication Series, v. 39, p. 53-157.

Rasmussen, T.L., and Thomsen, E., 2004, The role of the North Atlantic Drift in the millennial timescale glacial climate fluctuations: Palaeogeography, Palaeoclimatology, Palaeoecology, v. 210, p. 101–116, doi:10.1016/j.palaeo.2004.04.005.

Rasmussen, T.L., Thomsen, E., Kuijpers, A., Troelstra, S.R., Prins, M., 2003, Millennial-scale glacial variability versus Holocene stability: changes in planktic and benthic foraminifera faunas and ocean circulation in the North Atlantic during the last 60,000 years: Marine Micropaleontology, v. 47, p. 143–176.

Rasmussen, T.L., Thomsen, E., Van Weering, T.C.E., 1998, Cyclic changes in sedimentation on the Faeroe Drift 53-9 kyr BP related to climate variations: Geological Society Special Publication, v. 129. P. 255–267.

Rasmussen, T.L., Thomsen E., Labeyrie L., and van Weering T.C.E., 1996, Circulation changes in the Faeroe-Shetland Channel correlating with cold events during the last glacial period (58–10 ka): Geology, v. 24, p. 937– 940.

Reimer, P.J., and 29 others, 2013, IntCal13 and Marine13 Radiocarbon Age Calibration Curves 0–50,000 Years cal BP: Radiocarbon, v. 55, p. 1869–1887, doi:10.2458/azu_js_rc.55.16947.

Richter, T.O., et al., 2006, The Avaatech XRF Core Scanner: technical description and applications to NE Atlantic sediments. New Techniques in Sediment Core Analysis. Geol. Soc. London, Spec. publ., v. 267, p. 39–50 (2006).

Sejrup, H.P., Birks, H.J.B., Klitgaard Kristensen, D., Madsen, H., 2004, Benthonic foraminiferal distributions and quantitative transfer functions for the northwest European continental margin: Marine Micropaleontology, v. 53, p. 197–226.

Svensson, A., et al., 2008, A 60 000 year Greenland stratigraphic ice core chronology: Climate of the Past, v. 4, p. 47–57.

Wastegård, S., and Rasmussen, T.L., 2014, Faroe Marine Ash Zone IV – a new MIS 3 ash zone on the Faroe Islands margin. Geol. Soc. London, Spec. publ. in press.

# Paper II

# A 135 kyr record of subsurface $pCO_2$, nutrient levels and ventilation in the Norwegian Sea

Mohamed M. Ezat[1,2*], Tine L. Rasmussen[1], Bärbel Hönisch[3], Jesper Olsen[4], Jeroen Groeneveld[5], Luke Skinner[6]

[1] CAGE - Centre for Arctic Gas Hydrate, Environment and Climate, Department of Geology, UiT The Arctic University of Norway, NO-9037 Tromsø, Norway

[2] Department of Geology, Faculty of Science, Beni-Suef University, Beni-Suef, Egypt.

[3] Deapartment of Earth and Environmental Sciences and Lamont-Doherty Earth Observatory of Columbia University, Palisades, NY 10964, USA.

[4] Department of Physics and Astronomy, Aarhus University, DK-8000 Aarhus, Denmark.

[5] Center for Marine Environmental Sciences (MARUM), University of Bremen, Leobener Str., D-28359 Bremen, Germany.

[6] Godwin Laboratory for Palaeoclimate Research, Department of Earth Sciences, University of Cambridge, Cambridge CB2 3EQ, United Kingdom.

* e-mail: mohamed.ezat@uit.no

**Deglacial $\Delta^{14}C$ anomalies at mid-depth in the northern North Atlantic have been attributed to venting of an abyssal $CO_2$-rich and $^{14}C$-depleted reservoir in the Southern Ocean and northward transport via the Antarctic Intermediate Water (Thornalley et al., 2011). However, the southern source of these $\Delta^{14}C$ anomalies remains in question (e.g., Cléroux et al., 2011; Sortor and Lund, 2011; Huang et al., 2014). An alternative source could be the Nordic and Arctic basins (Cléroux et al., 2011; Skinner et al., 2014; Lund et al., 2015). On the basis of $\delta^{11}B$, $\Delta^{14}C$, Cd/Ca and $\delta^{13}C$, measured in the shells of the planktic foraminiferal species *Neogloboquadrina pachyderma* (sinistral) and $\Delta^{14}C$ measured in benthic foraminifera, we assess the evolution of subsurface seawater carbonate chemistry, ventilation age and nutrients in the southern Norwegian Sea. We find no evidence for a reservoir aged enough to explain the $\Delta^{14}C$ anomalies in the northern North Atlantic during the early and late Heinrich Stadial (HS) 1, while subsurface incursions of these old water masses into the Nordic seas are more likely. At mid-HS 1 (~16.5 ka), our results indicate southward export of relatively well-ventilated waters, possibly by brine formation, potentially ventilating the thermocline in the northern North Atlantic.**

Terrestrial and marine sediment records document abrupt shifts in the glacial and deglacial climate (e.g., Dansgaard et al., 1993). In particular, the last deglaciation was interrupted by two climatic anomalies, Heinrich stadial (HS) 1 and the Younger Dryas stadial (YD) were characterized by cooling over Greenland, warming of the Antarctic region and rise in atmospheric $CO_2$ (e.g., Petit et al., 1999; EPICA, 2006). Large scale reorganization of the Atlantic Meridional Overturning Circulation (AMOC) is thought to be a key player in these climatic transitions, through its influence on heat redistribution, global transmission of

regional climate anomalies, air-sea $CO_2$ exchange and the efficiency of nutrient utilization (e.g., Broecker, 1998; Sigman and Boyle 2000; Skinner et al., 2014). However, the physical, chemical and biological impact of AMOC changes during these climatic events remains unclear. In this study, we focus on variations in the mid-depth circulation in the North Atlantic, a key component of the AMOC, from a northern polar angle. The modern mid-depth circulation in the North Atlantic is mainly set up by the balance between the export of North Atlantic Deep Water (NADW) formed in the Labrador and Nordic seas and the northward return flow of the southern-sourced Antarctic Intermediate Water (AAIW), in which the AAIW does not expand north of 30° N.

In contrast, observations of elevated foraminiferal Cd/Ca and reduced $\delta^{13}C$ during HS1 and the YD suggest the extension of a nutrient rich water mass up to 60° N in the North Atlantic, possibly indicating that AAIW extended further north due to a reduction in the formation of NADW and/or changes in the preformed density gradient between AAIW and NADW (e.g., Rickaby and Elderfield, 2005). Moreover, extremely old ventilation ages have been observed for this water mass (hypothesized stadial AAIW) south of Iceland and employed as a remote fingerprint of upwelled $^{14}C$-depleted and $CO_2$-rich waters in the Southern Ocean (Thornalley et al., 2011), in agreement with the purging mechanism invoked to explain the stadial rises in atmospheric $CO_2$ (e.g., Skinner et al., 2010). Evidence from Nd isotope studies, however, debate whether the stadial AAIW was indeed more northerly expanded in the North Atlantic (Pahnke et al., 2008; Huang et al., 2014). Recently, Lund et al. (2015) studied a compilation of $\delta^{13}C$ records from the deep South Atlantic, and found no evidence for increased deep ocean ventilation during HS1, questioning the canonical view of Southern Ocean venting as the main pathway for the early deglacial rise in atmospheric $CO_2$. Instead, they suggested a northern hemisphere source for the early deglacial rise in the atmospheric $CO_2$.

An alternative source for the $^{14}C$-depleted and nutrient-rich water masses found in the northern North Atlantic is outflow from an aged reservoir in the Nordic-Arctic basins (Thornalley et al., 2011; Cléroux et al., 2011; Skinner et al., 2014; Lund et al., 2015). Thus, uncovering the stadial contribution from the Nordic seas is crucial to understand the evolution of deglacial North Atlantic circulation. So far, reconstructions from the Nordic seas show conflicting evidence and two opposite views of circulation patterns: a change of deep water formation from open convection to brine formation and southward propagation into the North Atlantic (e.g., Waelbroeck et al., 2011), or subsurface incursion of Atlantic water into the Nordic seas below a well-developed halocline (e.g., Rasmussen and Thomsen, 2004). To evaluate the above mentioned scenarios, we generated records of shallow subsurface $^{14}C$ ventilation age (ventilation age is defined as the time since the water was last equilibrated with the atmosphere), nutrient and seawater carbonate chemistry using $\Delta^{14}C$, Cd/Ca,$\delta^{13}C$ and $\delta^{11}B$ proxies measured in *N. pachyderma* (s). This species seems likely to reflect a thick part of the water column ranging from ~ 40 to 250 m (i.e., little bias due to regional or seasonal surface variability), which makes it a good tracer for water masses, but not ideal for inferring environmental conditions at the sea surface (Bauch et al., 1997; see Supplementary Information). Mid-depth ventilation ages are reconstructed based on $\Delta^{14}C$ measurements in a specific group of benthic foraminiferal species (Methods), but mid-depth nutrient levels and seawater carbonate chemistry is hampered by the low and scattered abundance of epifaunal benthic foraminiferal species in our record. The sediments are from core JM11-FI-19PC, retrieved from a water depth of 1179 m from the Faroe-Shetland Channel (Ezat et al., 2014) (Methods), where one-third of the Nordic seas outflow into the North Atlantic takes place today (Hansen and Østerhus, 2000). Our record encompasses the past 135,000 years.

$\delta^{11}B$ in planktic foraminifera shells is sensitive to seawater-pH (Hemming and Hanson et al., 1992), and in combination with temperature and salinity estimates from paired $\delta^{18}O$ and

Mg/Ca measurements, pH can be estimated from $\delta^{11}B$ (Supplementary Information). Further estimation of $pCO_2$ requires a second parameter of the carbon system, and we applied the modern local relationship between the salinity and total alkalinity to estimate the temporal changes in total alkalinity (Supplementary Information). We calculated the difference ($\Delta pCO_{2sea\text{-}air}$) between our reconstructed subsurface $pCO_2$ and atmospheric $CO_2$ from ice core measurements (Bereiter et al., 2015). Similar to earlier studies from tropical regions (e.g., Hönisch and Hemming 2005), our data show that glacial pH was elevated by ~0.2 units in the subsurface Norwegian Sea compared to the Holocene, but the record is punctuated by brief episodes of acidification during some Heinrich stadials (Fig. 1). The reconstructed subsurface $pCO_2$ shows lowest values of ~160 µatm during the Last Glacial Maximum (LGM), whereas it increased up to 320 µatm in HS1 (at ~16.5 ka), and then gradually dropped to ~210 µatm over the Bølling-Allerød interstadials (14.7–12.7 ka). The $\Delta pCO_{2sea\text{-}air}$ increased from ~-20 µatm during the LGM to ~100 µatm during HS1 (~16.5 ka) and gradually decreased towards the Bølling-Allerød interstadials. Similar prominent increases in $\Delta pCO_{2sea\text{-}air}$ occurred during the late part of HS11 during Termination II and during HS4 (Fig. 1).

Our $\delta^{13}C$ and Cd/Ca records generally show a good match, but important offsets throughout the record are also observed (Fig. 1). In general, high Cd/Ca and low $\delta^{13}C$ values refer to increase in nutrients (see Supplementary Information). The $\delta^{13}C$ record shows minimum values (~-0.4‰) during the Heinrich stadials HS1, HS3 and HS6 and ~-0.1‰ during HS11, HS4 and some non-Heinrich stadials. The highest Cd/Ca values are recorded during HS1, HS11 (~0.007 µmol/mol), HS3, YD (~0.004 µmol/mol) and HS4 (~ 0.0025 µmol/mol). Collectively, the $\delta^{13}C$ and Cd/Ca values refer to an increase in the nutrients during the resolved Heinrich stadials (Fig. 1). The ~0.5‰ decrease in $\delta^{13}C$ during the LGM (24–19 ka) compared to the Holocene with almost no concomitant change in Cd/Ca is likely due to the elevated pH (Fig. 1), which lowers the $\delta^{13}C$ recorded by planktic foraminifers relative to

$\delta^{13}C_{DIC}$ (Spero et al., 1997), and transfer of isotopically light terrestrial carbon (Keigwin and Boyle, 1989).

The most striking observation in our records is the simultaneous increase in $\Delta pCO_{2sea-air}$ and nutrients during parts of HS1, HS4 and HS11. $\Delta pCO_{2sea-air}$ is a measure of the tendency of a water mass to exchange $CO_2$ with the atmosphere (e.g., Takahashi et al., 2009). However, the relatively deeper habitat of *N. pachyderma* (s), as well as the probability of episodes of perennial/seasonal sea-ice cover during Heinrich stadials (e.g., Rasmussen and Thomsen 2004; Ezat et al., 2014) renders the direct interpretation of $\Delta pCO_{2sea-air}$ in terms of air-sea $CO_2$ exchange difficult. Possible interpretations include changes in the level of nutrient utilization and/or mixing with/surfacing of older and $CO_2$-rich water masses. Also, it could potentially be an indicator for high rate of sea ice formation as studies from the modern East Greenland region showed that total dissolved inorganic carbon is rejected more efficiently than total alkalinity during sea-ice formation, causing the brines beneath the sea-ice to be enriched in $CO_2$ compared to normal seawater (e.g., Rysgaard et al., 2009). We further discuss these possibilities within the frame of the ventilation age reconstructions.

The subsurface and mid-depth $^{14}C$ ventilation ages were reconstructed by comparing our planktic and benthic radiocarbon dates with the contemporary atmospheric radiocarbon ages from Bronk Ramsey et al. (2012). We will refer to ventilation ages as Planktic-Atmosphere (P-A), Benthic-Atmosphere (B-A) and benthic-planktic foraminifera (B-P) ages (Fig. 2i-k) (Methods). The ventilation age reconstructions show a gradual change from aged water masses at 21 ka (B-P=900 years, B-A= ~2100 years and P-A=~1200 years) to better-ventilated water masses at 18.5 ka (B-P=270 years, B-A= ~700 years and P-A=~400 years). The B-P, B-A and P-A ages at 18.5 ka are comparable to the modern values, which are 100, 500 and 400 years, respectively (Broecker and Peng, 1982). Comparable $^{14}C$ ventilation ages were recorded at mid-depth south of Iceland at 21 ka (Thornalley et al., 2011), but no

measurements exist for the period until 18 ka (Fig. 2b, c). There is a general trend towards increasing ventilation ages over HS1 at our site (Fig. 2), reaching maximum values (B-P=1000 years, B-A= ~1800 years and P-A=~800 years) at 15 ka. However, our ventilation ages are far lower than those recorded from south of Iceland during early and late HS1 (Fig. 2), thus precluding our area as the source of the extremely old water masses found south of Iceland. It is possible that the relatively old water masses during the early and late part of HS1 (18.5 to 17 and 15.5 to 14.5 ka) are due to episodic intrusions of old water from the south, although local aging or inflow from a relatively aged carbon pool in the Arctic Ocean cannot be excluded. Of particular interest is the interval of mid-HS1 (17 to 15.5 ka), where peaks in $CO_2$ and Cd/Ca do not coincide with older ventilation ages (Fig. 2). It is possible that this event represents an episode of enhanced sea-ice formation and southward export of high $CO_2$, but relatively well-ventilated brines. Minima in planktic $\delta^{18}O$ and B/Ca values are seen in our record and south of Iceland, but with a shift in timing of 1000 to 1500 years (Fig. 2), which may be due to errors in the age model. Synchronous with the decrease in the planktic $\delta^{18}O$ and B/Ca south of Iceland, the B-A and B-P ages decreased dramatically by 3000 years (Thornalley et al., 2011) to values similar to those we observe in the southern Norwegian Sea (Fig. 2). This ventilation event in the northern North Atlantic is likely caused by an outflow of better-ventilated water from the Nordic seas, as also suggested by Thornalley et al. (2011). High $CO_2$ at the calcification depth of *N. pachyderma* (s) at this time may be due to enhanced sea-ice formation, changes in the level of nutrient utilization or outflow of high $CO_2$, but younger waters from the Arctic Ocean. More and higher resolution records of $CO_2$ from the high latitude North Atlantic as well as modelling exercises are required to assess their effect on the evolution of atmospheric $CO_2$. Based on a compilation of planktic radiocarbon records from the high latitude North Atlantic, Stern and Lisiecki (2013) suggested a decrease in the reservoir ages (ventilation ages at the calcification depth of planktic foraminifera) around 16

ka. They interpreted this decrease by freshwater-induced stratification that isolated the upper part of the water column from the deeper and older waters and facilitated $CO_2$-equilibration with the atmosphere. Our low ventilation ages of a hypothesized southward outflow from the Norwegian Sea to the North Atlantic at the same time may explain some of the decrease in the northern North Atlantic reservoir ages at 16 ka. Finally, we observe interspecies differences in the benthic radiocarbon ages from a few hundred years to several thousand years (Fig. 3), adding evidence for caution in using 'mixed benthic species' for $^{14}C$ dates.

Our results clearly exclude outflow of an 'old' water mass from the Eastern Nordic seas to be a source of the extremely aged water masses found in the northern North Atlantic during the early and late HS1, while subsurface intrusions of these old water masses into the Nordic seas are more likely. For the event around 16.5 ka (mid-HS1) our results suggest southward export of relatively well-ventilated and $CO_2$-rich waters, possibly by brine formation, potentially ventilating the thermocline in the northern North Atlantic and which, may explain the decrease in high latitude North Atlantic reservoir age at that time.

**Figure Captions**

**Figure 1: Seawater carbonate chemistry and nutrient reconstructions from the Norwegian Sea. a,** $\delta^{11}B$ measured in *Neogloboquadrina pachyderma* (sinistral). **b,** Seawater-pH inferred from $\delta^{11}B$. **c,** Estimated subsurface $pCO_2$ at the calcification depth and season of *N. pachyderma* (s). **d,** Atmospheric $pCO_2$ from Antarctic ice cores (Bereiter et al., 2015 and references therein). **e,** The difference between reconstructed subsurface $pCO_2$ at our site and atmospheric $CO_2$, ($\Delta pCO_{2sea-air}$). **f,** Cd/Ca measured on *N. pachyderma* (s). **g,** $\delta^{13}C$ measured on *N. pachyderma* (s).

**Figure 2: Comparison of ventilation age reconstructions between the Norwegian Sea and northern North Atlantic. a,** Average regional surface reservoir age (=ventilation age at the calcification depth of planktic foraminifera) at high latitude North Atlantic from Stern and Liesecki (2013). **b,** Benthic-planktic $^{14}C$ difference south of Iceland (Thornalley et al., 2011). **c,** Mid-depth ventilation age south of Iceland (Thornalley et al., 2011). **d,** B/Ca (Yu et al., 2013) and. **e,** $\delta^{18}O$ (Thornalley et al., 2010) measured in *N. pachyderma* (s) south of Iceland. **f,** B/Ca, and **g,** $\delta^{11}B$ measured in *N. pachyderma* (s) in JM-FI-19PC. (see Fig. (S1) for a comparison between the $\delta^{11}B$ and B/Ca for all the records). **h,** Subsurface ventilation age. **j**, Benthic-planktic $^{14}C$ difference. **k,** Mid-depth ventilation age, closed and open circles are based on infaunal and epifaunal benthic species, respectively (see Fig. 3). Modern subsurface and mid-depth ventilation ages for the high latitude North Atlantic are indicated by blue circles. Pink, grey and dark grey shaded areas refer to periods with relatively well-ventilated, aged and extremely aged water masses, respectively. The yellow shaded interval indicates a period with a potential southward export of relatively well-ventilated water from the Norwegian Sea during mid Heinrich Stadial 1, possibly triggered by sea ice formation and brine rejection. If the timing difference between minima in planktic $\delta^{18}O$ and B/Ca between our record and the records south of Iceland are just an artefact due to errors in the age models, this will have an impact on the ventilation age estimations. However, this would not have a significant effect given the >3000 years shifts in the ventilation ages recorded south of Iceland during this interval.

**Figure 3: Planktic (black symbols) and benthic radiocarbon dates plotted versus calendar age.** Green symbols refer to benthic $^{14}C$ dates, mainly based on *Cassidulina neoteretis*, *Melonis barleeanus*, *Elphidium excavatum*, *Cassidulina reniforme* and *Astronion galloway* (hereafter infaunal group). Blue symbols indicate benthic $^{14}C$ dates, mainly

measured in *Cibicidoides floridanus* and *Cibicidoides* sp. (*Cibicidoides* group). Red symbols refer to radiocarbon dates measured in *Pyrgo serrata*, *Pyrgo depressa* and *Pyrgo* sp. The *Pyrgo* species dated 6000 to 8000 years older than the other benthic species from the same sample. Similar results of up to 2000 years older dates from *Pyrgo* species relative to other benthic species were also previously documented from Santa Barbara Basin, California (Magana et al., 2010). Here in the Norwegian Sea we observe a difference up to 8000 years and given the usual large size of these species, few specimens could have pronounced impact on the reconstructed ventilation ages. The *Cibicidoides* group gave $^{14}C$ dates that are about 300 years older than the infaunal group, which may be due to effects of bioturbation. We did not use the *Pyrgo sp.* dates for ventilation age reconstructions.

**References**


Bauch, D., Carstens, J., & Wefer, G. (1997). Oxygen isotope composition of living *Neogloboquadrina pachyderma* (sin.) in the Arctic Ocean. *Earth and Planetary Science Letters, 146*(1–2), 47-58.

Bereiter, B., et al. (2015). Revision of the EPICA Dome C $CO_2$ record from 800 to 600 kyr before present. *Geophysical Research Letters, 42*(2), 542-549.

Broecker, W. S. (1998). Paleocean circulation during the Last Deglaciation: A bipolar seesaw? *Paleoceanography, 13*(2), 119-121.

Broecker, W. S., & Peng, T. H. (1982). *Tracers in the Sea* (Eldigio Press, Palisades, NY).

Bronk Ramsey, C., et al. (2012). A Complete Terrestrial Radiocarbon Record for 11.2 to 52.8 kyr B.P. *Science, 338*(6105), 370-374.

Cléroux, C., deMenocal, P., & Guilderson, T. (2011). Deglacial radiocarbon history of tropical Atlantic thermocline waters: absence of $CO_2$ reservoir purging signal. *Quaternary Science Reviews, 30*(15–16), 1875-1882.

Dansgaard, W., et al. (1993). Evidence for general instability of past climate from a 250-kyr ice-core record. *Nature, 364*(6434), 218-220.

Ezat, M. M., Rasmussen, T. L., & Groeneveld, J. (2014). Persistent intermediate water warming during cold stadials in the southeastern Nordic seas during the past 65 k.y. *Geology, 42*(8), 663-666

Hansen, B., & Østerhus, S. (2000). North Atlantic–Nordic Seas exchanges. *Progress in Oceanography, 45*(2), 109-208.

Huang, K.-F., Oppo, D. W., & Curry, W. B. (2014). Decreased influence of Antarctic intermediate water in the tropical Atlantic during North Atlantic cold events. *Earth and Planetary Science Letters, 389*(0), 200-208.

Hönisch, B., & Hemming, N. G. (2005). Surface ocean pH response to variations in $pCO_2$ through two full glacial cycles. *Earth and Planetary Science Letters, 236*(1–2), 305-314.

Keigwin, L. D., & Boyle, E. A. (1989). Late quaternary paleochemistry of high-latitude surface waters. *Palaeogeography, Palaeoclimatology, Palaeoecology, 73*(1–2), 85-106.

Lund, D. C., Tessin, A. C., Hoffman, J. L., & Schmittner, A. (2015). Southwest Atlantic water mass evolution during the last deglaciation. *Paleoceanography*. doi: 10.1002/2014PA002657

EPICA (2006). One-to-one coupling of glacial climate variability in Greenland and Antarctica. (2006). *Nature, 444*(7116), 195-198.

Magana, A. L., et al. (2010). Resolving the cause of large differences between deglacial benthic foraminifera radiocarbon measurements in Santa Barbara Basin. *Paleoceanography, 25*(4).

Pahnke, K., Goldstein, S. L., & Hemming, S. R. (2008). Abrupt changes in Antarctic Intermediate Water circulation over the past 25,000 years. *Nature Geosci, 1*(12), 870-874.

Petit, J. R., et al. (1999). Climate and atmospheric history of the past 420,000 years from the Vostok ice core, Antarctica. *Nature, 399*(6735), 429-436.

Rasmussen, T. L., & Thomsen, E. (2004). The role of the North Atlantic Drift in the millennial timescale glacial climate fluctuations. *Palaeogeography, Palaeoclimatology, Palaeoecology, 210*(1), 101-116.

Rickaby, R. E. M., & Elderfield, H. (2005). Evidence from the high-latitude North Atlantic for variations in Antarctic Intermediate water flow during the last deglaciation. *Geochemistry, Geophysics, Geosystems, 6*(5). doi: 10.1029/2004GC000858

Rysgaard, S., Bendtsen, J., Pedersen, L. T., Ramløv, H., & Glud, R. N. (2009). Increased $CO_2$ uptake due to sea ice growth and decay in the Nordic Seas. *Journal of Geophysical Research: Oceans, 114*(C9), C09011.

Sigman, D. M., & Boyle, E. A. (2000). Glacial/interglacial variations in atmospheric carbon dioxide. *Nature, 407*(6806), 859-869.

Skinner, L. C., Fallon, S., Waelbroeck, C., Michel, E., & Barker, S. (2010). Ventilation of the Deep Southern Ocean and Deglacial $CO_2$ Rise. *Science, 328*(5982), 1147-1151.

Skinner, L. C., Waelbroeck, C., Scrivner, A. E., & Fallon, S. J. (2014). Radiocarbon evidence for alternating northern and southern sources of ventilation of the deep Atlantic carbon pool during the last deglaciation. *Proceedings of the National Academy of Sciences, 111*(15), 5480-5484.

Sortor, R. N., & Lund, D. C. (2011). No evidence for a deglacial intermediate water $\Delta^{14}C$ anomaly in the SW Atlantic. *Earth and Planetary Science Letters, 310*(1–2), 65-72.

Spero, H. J., Bijma, J., Lea, D. W., & Bemis, B. E. (1997). Effect of seawater carbonate concentration on foraminiferal carbon and oxygen isotopes. *Nature, 390*(6659), 497-500.

Stern, J. V., & Lisiecki, L. E. (2013). North Atlantic circulation and reservoir age changes over the past 41,000 years. *Geophysical Research Letters, 40*(14), 3693-3697.

Takahashi, T., et al. (2009). Climatological mean and decadal change in surface ocean $pCO_2$, and net sea–air $CO_2$ flux over the global oceans. *Deep Sea Research Part II: Topical Studies in Oceanography, 56*(8–10), 554-577.

Thornalley, D. J. R., Barker, S., Broecker, W. S., Elderfield, H., & McCave, I. N. (2011). The Deglacial Evolution of North Atlantic Deep Convection. *Science, 331*(6014), 202-205.

Thornalley, D. J. R., Elderfield, H., & McCave, I. N. (2011). Reconstructing North Atlantic deglacial surface hydrography and its link to the Atlantic overturning circulation. *Global and Planetary Change, 79*(3–4), 163-175.

Waelbroeck, C., et al. (2001). The timing of the last deglaciation in North Atlantic climate records. *Nature, 412*(6848), 724-727.

Yu, J., Thornalley, D. J. R., Rae, J. W. B., & McCave, N. I. (2013). Calibration and application of B/Ca, Cd/Ca, and $\delta^{11}B$ in *Neogloboquadrina pachyderma* (sinistral) to constrain $CO_2$ uptake in the subpolar North Atlantic during the last deglaciation. *Paleoceanography, 28*(2), 237-252.

**Methods**

Sediment core JM11-FI-19PC with a length of ~11 m, was recovered from the northwestern Faroe Islands slope (62°49'N, 03°52'W) at 1179 m water depth. The logging, scanning and sampling are described in Ezat et al. (2014). Pristine specimens with no visible signs of dissolution of *N. pachyderma* (s) were picked from the 150–250 μm size fractions for boron isotope (200–450 specimens), minor/trace element (70–160 specimens) and stable isotope analyses (~50 specimens). For boron isotope measurements, the foraminiferal shells were gently crushed, and cleaned following Barker et al. (2003). We measured the boron isotopes using a negative thermal ionization mass spectrometry at Lamont-Doherty Earth Observatory (LDEO) of Columbia University following the standard methods of Hemming and Hanson (1994) (see Supplemental Information for details). Two samples were repeated using the oxidative-reductive cleaning procedure from Pena et al. (2005), which yielded indistinguishable $\delta^{11}B$ values (Fig. S1).

For trace and minor element analyses, we followed the cleaning procedure of Martin and Lea (2002) including clay removal, reductive, oxidative, alkaline chelation and weak acid leaching steps with slight modifications from Pena et al. (2005). These modifications are related to the number of cold/hot water rinses after the reduction and DTPA steps. Also, the samples were rinsed with $NH_4OH$ (Lea and Boyle, 1993) instead of using 0.01N NaOH (Martin and Lea 2002) to remove the DTPA solution. The samples were then dissolved in 2% $HNO_3$ and finally analyzed by iCAPQ Inductively-Coupled Plasma Mass Spectrometry at LDEO. Based on repeated measurements of in-house standard solutions, the intra-run precision is < 1.4%, 1.9% and 2.1% for Mg/Ca, B/Ca and Cd/Ca, respectively. Five samples

were split after clay removal, reduction and oxidation steps; one half cleaned by the full cleaning procedure, while the alkaline chelation step was skipped for the other half. This was to test the influence of this rigorous step on Cd/Ca and B/Ca. The results with and without the alkaline chelation step showed an average difference of 0.0003 µmol/mol and 5 µmol/mol for Cd/Ca and B/Ca respectively (Table S1). The Mg/Ca values from the two cleaning methods are comparable but two samples showed a significant decrease in Mg/Ca, Fe/Ca, Mn/Ca and Al/Ca values. This might be due to a more efficient removal of contaminants that are rich in Mg but not in Cd or B (Table S1), but further tests are needed. All cleaning and loading steps for boron isotope and minor/trace element analyses were done in boron-free filtered laminar flow benches and all used boron-free Milli-Q water. The stable oxygen and carbon isotope analyses were performed using a Finnigan MAT 251 mass spectrometer with an automated carbonate preparation device at MARUM, University of Bremen. The external standard errors for the oxygen and carbon isotope analyses are 0.07‰ and 0.05‰, respectively. Values are reported relative to the Vienna Pee Dee Belemnite (VPDB), calibrated by using the National Bureau of Standards (NBS) 18, 19, and 20.

Monospecific samples of *N. pachyderma* (s) (~1000–1300 specimens; 150–250 µm size fraction) and samples of mixed benthic foraminifera were $^{14}$C dated by accelerator mass spectrometry (AMS) at the $^{14}$CHRONO Centre facility at Queen's University Belfast. Pre-treatment of the foraminiferal samples followed the approach by Nadeau et al. (2001). Samples were converted into graphite for AMS analysis on a Fe catalyst using the hydrogen reduction method (Vogel et al., 1987).

The identification of nine well-dated tephra layers in JM11-FI-19PC represents the backbone of our age model. The age model was subsequently refined by tying the start of DO interstadials (IS) as seen in the $\delta^{18}$O record of the Greenland ice cores (Rasmussen et al., 2014) with the sharp transitions in the magnetic susceptibility and K/Ti ratio measured by

XRF scanning (cf., Ezat et al., 2014; see Supplementary Information).

The $^{14}C$ ventilation ages were reconstructed by comparing the planktic and benthic radiocarbon dates with the contemporary atmospheric radiocarbon ages from Bronk Ramsey et al. (2012). A challenging requirement to this method is an accurate calendar chronology for the marine records. For this, we included a possible range of sediment age-depth models for the interval between 26 and 12 ka that enabled us to assess the influence of uncertainty in calendar ages on the ventilation age estimations. Figure (S8) shows that our main inferences about the ventilation changes in the Norwegian Sea may not be significantly influenced by the errors in the age-depth model. Another way to estimate the ventilation age of mid-depth/deep water is to compare the radiocarbon ages of co-existing benthic and planktic foraminifera, but the non-zero and very unlikely constant ventilation age for the subsurface water mass recorded by *N. pachyderma* (s) complicates this approach. As the complications of the two methods are independent, the very similar trends of the B-A and B-P ages (Fig. 2) support the reliability of our results.

**Acknowledgements**

We sincerely thank J. Ruprecht, P. DeMenocal, K. Esswein, M. Forwick, U. Hoff, J. Farmer, L. Pena, K. Allen, T. Dahl, E. Ellingsen, I. Hald, J. Sen, N. L. Rasmussen, M. Segl and S. Pape for valuable support in the laboratory and J. McManus, J. Farmer, U. Hoff, and H. Spero for helpful discussions. We thank D. Thornalley and J. Yu for sharing data. This research is funded by UiT, Arctic University of Norway, the Mohn Foundation and supported by the Research Council of Norway through its Centres of Excellence funding scheme, project number 223259.

**Author contributions**

M. M. E. conducted most of the lab work and wrote the first draft. All authors contributed with data and data analyses and wrote together the manuscript.

## Additional Information

Correspondence and requests for data should be addressed to M. M. E.

## Competing financial interests

The authors declare no competing financial interests.

## Additional References


Barker, S., Greaves, M., & Elderfield, H. (2003). A study of cleaning procedures used for foraminiferal Mg/Ca paleothermometry. *Geochemistry, Geophysics, Geosystems, 4*(9). doi: 10.1029/2003GC000559

Hemming, N. G., & Hanson, G. N. (1994). A procedure for the isotopic analysis of boron by negative thermal ionization mass spectrometry. *Chemical Geology, 114*(1–2), 147-156.

Lea, D. W., & Boyle, E. A. (1993). Determination of carbonate-bound barium in foraminifera and corals by isotope dilution plasma-mass spectrometry. *Chemical Geology, 103*(1–4), 73-84.

Martin, P. A., & Lea, D. W. (2002). A simple evaluation of cleaning procedures on fossil benthic foraminiferal Mg/Ca. *Geochemistry, Geophysics, Geosystems, 3*(10), 1-8. doi: 10.1029/2001GC000280

Nadeau, M. J., Grootes, P. M., Voelker, A., Bruhn, F., Duhr, A. & Oriwall, A. (2001). Carbonate 14C background: does it have multiple personalities? *Radiocarbon, 43*, 169–176.

Pena, L. D., Calvo, E., Cacho, I., Eggins, S., & Pelejero, C. (2005). Identification and removal of Mn-Mg-rich contaminant phases on foraminiferal tests: Implications for Mg/Ca past temperature reconstructions. *Geochemistry, Geophysics, Geosystems, 6*(9). doi: 10.1029/2005GC000930

Rasmussen, S. O., et al. (2014). A stratigraphic framework for abrupt climatic changes during the Last Glacial period based on three synchronized Greenland ice-core records: refining and extending the INTIMATE event stratigraphy. *Quaternary Science Reviews, 106*(0), 14-28.

Vogel, J. S., Southon, J. R., & Nelson, D. E. (1987). Catalyst and binder effects in the use of filamentous graphite for AMS. *Nuclear Instruments and Methods in Physics Research Section B: Beam Interactions with Materials and Atoms, 29*(1–2), 50-56.

**Figure 1**

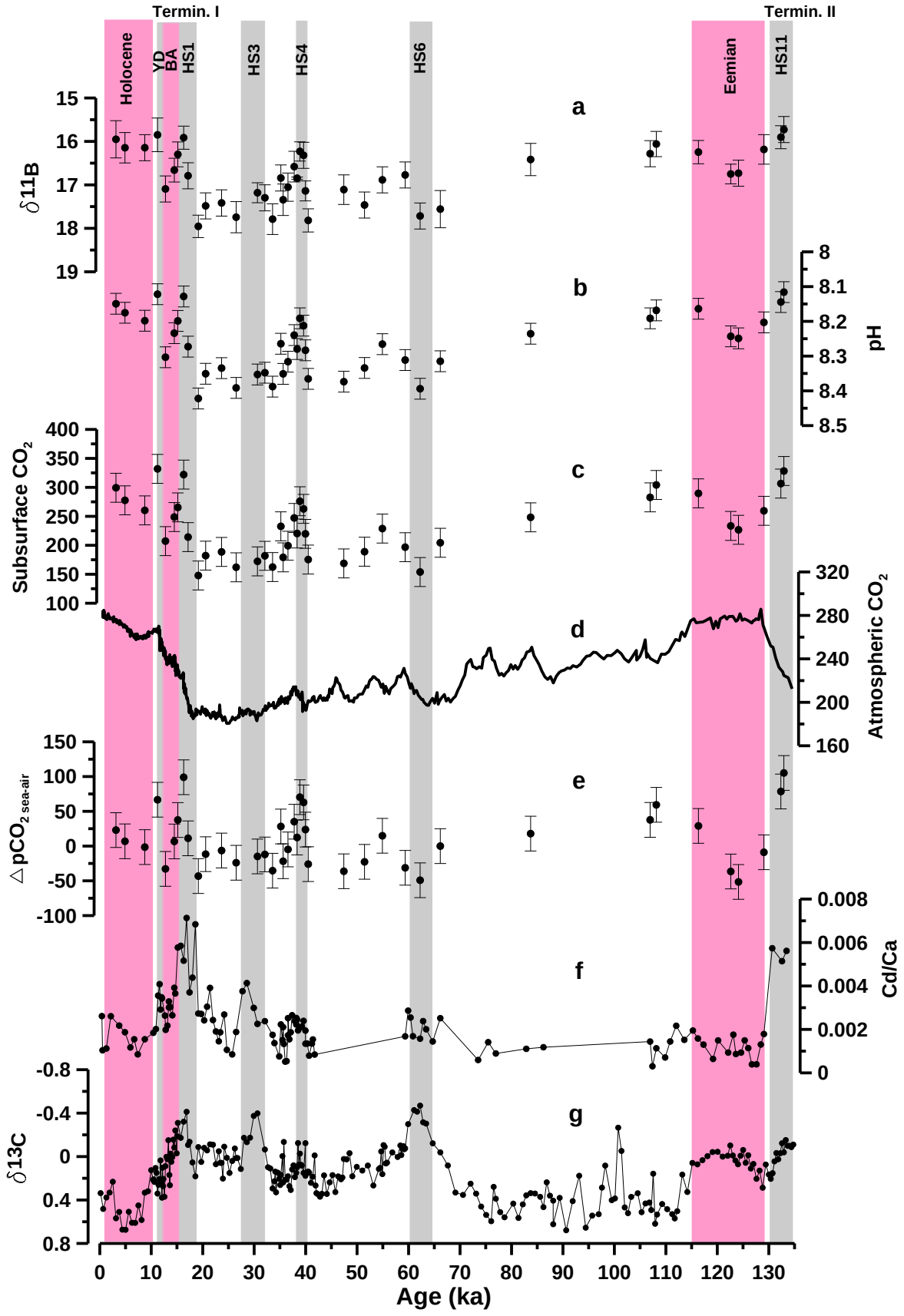
Termin. I
Termin. II
Holocene
YD
BA
HS1
HS3
HS4
HS6
Eemian
HS11
a
b
c
d
e
f
g
δ11B
pH
Subsurface CO2
Atmospheric CO2
△pCO2 sea-air
Cd/Ca
δ13C
Age (ka)

**Figure 2**

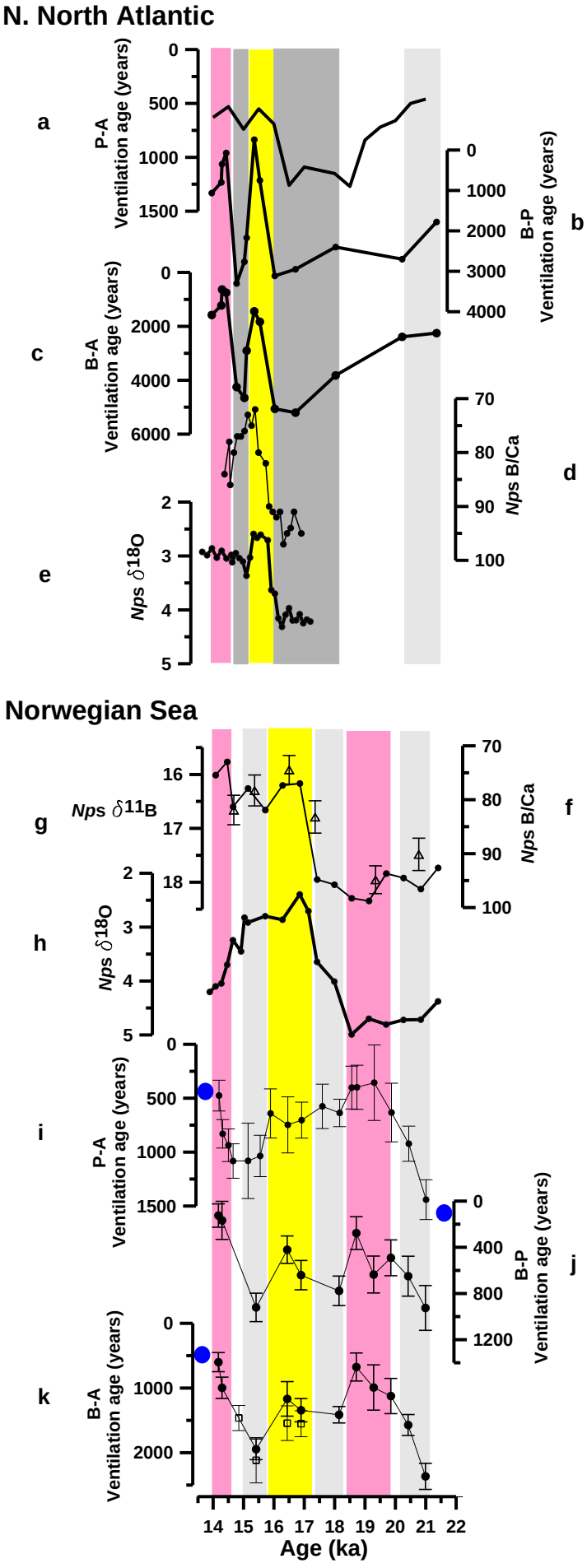
N. North Atlantic
a
P-A Ventilation age (years)
0
500
1000
1500
b
B-P Ventilation age (years)
0
1000
2000
3000
4000
c
B-A Ventilation age (years)
0
2000
4000
6000
d
Nps B/Ca
70
80
90
100
e
Nps δ18O
2
3
4
5
Norwegian Sea
g
Nps δ11B
16
17
18
f
Nps B/Ca
70
80
90
100
h
Nps δ18O
2
3
4
5
i
P-A Ventilation age (years)
0
500
1000
1500
j
B-P Ventilation age (years)
0
400
800
1200
k
B-A Ventilation age (years)
0
1000
2000
14 15 16 17 18 19 20 21 22
Age (ka)

**Figure 3**

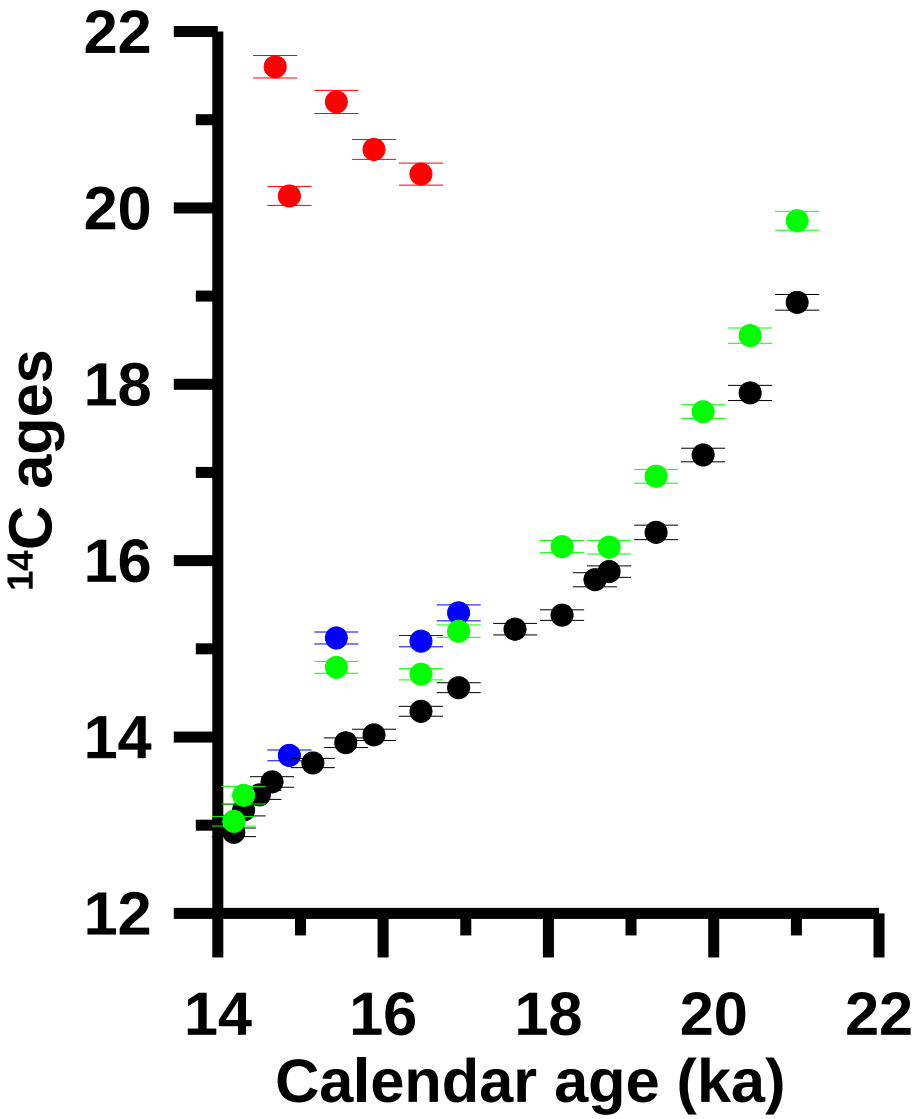

**Supplementary Information for**

**'A 135 kyr record of subsurface $pCO_2$, nutrient levels and ventilation in the Norwegian Sea'**

Mohamed M. Ezat, Tine L. Rasmussen, Bärbel Hönisch, Jesper Olsen, Jeroen Groeneveld, Luke Skinner

## 1. Boron isotope analysis

The foraminifer shells were gently crushed, weighed and cleaned following Barker et al. (2003). Thereafter, the samples were dried and weighed to determine the amount of acid for dissolution. Immediately prior to loading, samples were dissolved in 2M HCl, and then centrifuged to separate out any insoluble mineral grains. One µl of boron-free seawater followed by 2µl aliquot of the sample solution (with ca 1–1.5 ng B) were loaded onto outgassed Rhenium filaments, and then slowly evaporated at an ion current of 0.5A and mounted into the mass spectrometer. Five to ten aliquots were loaded per sample. Boron isotopes were measured as $BO_2^-$ ions on masses 43 and 42 using a Thermo Scientific Triton multi-collector thermal ionization mass spectrometer (TIMS) at the Lamont-Doherty Earth Observatory (LDEO) of Columbia University. Each sample aliquot was heated up slowly to 1000±20 °C and then 320 boron isotope ratios were measured over ~40 minutes. Boron isotope ratios are reported relative to the boron isotopic composition of SRM 951 boric acid standard, where $\delta^{11}B$ (‰) = (43/42sample / 43/42standard -1)*1000. This procedure (cf., Hemming and Hanson (1994)) enabled us to monitor the in-run mass fractionation and discard the samples that showed excessive fractionation if the 43/42 ratio increased by >0.004 (equal to ~1‰ $\delta^{11}B$) over the data acquisition time. Up to 10 sample aliquots were analyzed to minimize analytical uncertainty, which is reported as $2se = 2sd/\sqrt{n}$, where n is number of sample aliquots analyzed. The analytical uncertainty of each sample was then compared to the

long-term reproducibility of in-house vaterite standard (±0.34 for n=3 to ±0.19 for n=10) and the larger of the two uncertainties is reported. Two samples were repeated using the oxidative-reductive cleaning procedure from Pena et al. (2005), which yielded indistinguishable values (Fig. S1).

**2. Salinity and temperature reconstructions**

Foraminiferal $\delta^{18}O$ values are a function of calcification temperature, seawater $\delta^{18}O$ and carbonate chemistry (Emiliani 1955; Shackleton et al., 1967; Spero et al., 1997). Seawater $\delta^{18}O$ values at a specific location vary through time due to changes in global ice volume, salinity-related effects (evaporation/precipitation, meltwater and river runoff) and ocean circulation patterns (Craig, 1961; Dansgaard, 1964; Shackleton, 1967; Waelbroeck et al., 2011; Friedrich and Timmermann, 2012). The calcification temperatures were reconstructed using the Mg/Ca-temperature calibration of Elderfield and Ganssen, 2000: Mg/Ca=Pre-exponential constant * exp (0.1T) where the pre-exponential constant is calibrated to our core-top samples yielding a value of 0.4 and T is the temperature. We used the equation of Shackleton (1974) to calculate $\delta^{18}O_{SW}$ after correction for the global ice volume changes using the sea level record from Grant et al. (2012), assuming 1.1‰ increase in $\delta^{18}O$ values per 120 m drop in sea level (Adkins et al., 2002) (the temperature and seawater $\delta^{18}O$ are discussed elsewhere, Ezat et al., in preparation).

There is a quasi-linear regional relationship between the salinity and $\delta^{18}O_{SW}$ in the modern ocean as both parameters covary due to addition/removal of freshwater (e.g., LeGrande and Schmidt, 2006). The temporal changes in the $\delta^{18}O_{SW}$ composition of the freshwater sources and/or their relative contribution to a specific region, as well as changes in ocean circulation complicate using a local modern $\delta^{18}O_{SW}$-salinity relationship to infer past changes in salinity. Therefore, we estimated salinity using the $\delta^{18}O_{SW}$-salinity mixing line

from the Norwegian Sea (LeGrande and Schmidt, 2006) for most part of the record. For the deglaciations and Heinrich events, we used the $\delta^{18}O_{SW}$-salinity mixing line from Azetsu-Scott and Tan (1997). This mixing line is based on data from Kangerdlugssuaq fjord, East Greenland, where the dominant source of freshwater is glacial meltwater from tidewater glaciers with $\delta^{18}O$ values ranging from -30 to – -20‰, which is more representative of the sources of deglacial freshwater in the Norwegian Sea. We tried several different mixing models, which yielded salinity values within our estimated error (1psu).

It is also noteworthy that the applied correction for ice volume changes, using an eustatic sea level record, does not account for the spatiotemporal propagation of the $\delta^{18}O$ signal due to ice sheets growth/collapse into the global surface/deep ocean especially during periods of a reduced AMOC during Heinrich events (e.g., Friedrich and Timmermann, 2012). Given the close location of our site to the glacial continental ice sheets, this adds to the uncertainty in our salinity estimations. A correction for the effect of carbonate chemistry changes on the $\delta^{18}O$ based on the pH reconstructions from the same core record (section S4), and assuming a decrease of 0.22‰ in $\delta^{18}O$ per 0.2 units increase in pH (Zeebe, 1999), would decrease the $\delta^{18}O_{SW}$ for the LGM by 0.22‰. The impact of pH change elsewhere in the record is almost negligible. The effect of uncertainties in temperature and salinity on our pH and $pCO_2$ reconstructions is discussed in section (4).

**3. *Neogloboquadrina pachyderma* (sinistral)**

*N. pachyderma* (s) is the most dominant planktic species in the polar and subpolar areas and the only planktic species that can be used to generate continuous paleoceanographic records on glacial/interglacial timescales. However, identifying which water mass *N. pachyderma* (s) records remains a challenge. *N. pachyderma* (s) is thought to exhibit a wide and variable range of calcification depths in the Nordic seas from 40 to 250 m water depth,

vertical migration in the water column, encrustation, and maximum production during late spring to early autumn (e.g., Bauch et al., 1997; Simstich et al., 2003; Kozdon et al., 2009). In general, the signal recorded by *N. pachyderma* (s) seems likely to reflect a thick part of the water column (i.e., little bias due to regional or seasonal surface variability), which makes it a good tracer for water masses (see discussion in Bauch et al., 1997), but not ideal for inferring environmental conditions at the sea surface.

## 4. pH and $CO_2$ estimations

The boron isotopic composition of biogenic carbonate is sensitive to seawater-pH (for details see Hönisch and Hemming, 2007). Briefly, of the two dominant dissolved boron species in seawater, boric acid [$B(OH)_3$] and borate [$B(OH)_4^-$], borate is the species predominantly incorporated into marine carbonate (Hemming and Hanson et al., 1992). The relative abundance of the two boron species as well as their boron isotopic composition changes with pH (Hershey et al., 1986). Culture experiments with planktic foraminifera provide empirical support for using their boron isotopic composition as a proxy for pH (e.g., Sanyal et al., 1996), but species-specific offsets from the theoretical $\delta^{11}B$ of seawater borate were also observed, which is widely ascribed to 'vital effects' (e.g., Hönisch et al., 2003). A diffusion-reaction model (Zeebe et al., 2003) has shown that this species-specific offset ($\delta^{11}B_{C\text{-}B4}$) is constant over a wide range of pH values and thus does not compromise the use of planktic foraminiferal $\delta^{11}B$ as a pH proxy. We calculated the $\delta^{11}B_{C\text{-}B4}$ for *N. pachyderma* (s) by calibrating our core top foraminiferal $\delta^{11}B$ to a calculated pre-industrial pH using modern hydrographic carbonate data (total Dissolved Inorganic Carbon 'DIC', total alkalinity, phosphate, silicate, temperature, salinity; Key et al., 2010) from the southern Norwegian Sea. We corrected for the anthropogenic $CO_2$ effect by subtracting 50 µmol/kg from DIC (Jeansson et al., 2011). We used the hydrographic data collected during June 2002 and from

the 22nd of September to the 13th of October 2003) (i.e., within the assumed calcification season of *N. pachyderma* (s); e.g., Simstich et al. 2003; Jonkers et al., 2013) and at our assumed calcification depth (i.e., 40–120 m). The pre-industrial pH and subsequently $\delta^{11}B_{C\text{-}B4}$ were alternatively calculated based on hydrographic data from 50 and 200 m water depths to address the sensitivity of our calculated $pCO_2$ to the uncertainty in the calcification depth of *N. pachyderma* (s) (Fig. S2).

The $\delta^{11}B$ values measured in *N. pachyderma* (s) were translated into pH estimates using this equation:

$$pH = pK_B - \log(-(\delta^{11}B_{SW} - \delta^{11}B_{CaCO3} - \delta^{11}B_{CaCO3\text{-}B4}) / (\delta^{11}B_{SW} - \alpha^* (\delta^{11}B_{CaCO3} + \delta^{11}B_{CaCO3\text{-}B4}) - (\alpha\text{-}1)*1000))$$ (Hemming and Hanson, 1992),

where $pK_B$ is the equilibrium constant for the dissociation of boric acid for a given temperature and salinity (Dickson 1990), $\delta^{11}B_{SW}$ is the $\delta^{11}B$ of seawater (=39.61‰; Foster et al., 2010), and $\alpha$ is the fractionation factor for boron isotope exchange between boric acid and borate. Klochko et al. (2006) and Nir et al. (2015) determined the boron isotope fractionation factor in seawater $\alpha$~1.027. However, laboratory culture experiments with marine calcifiers over a wide pH-range display a lesser pH sensitivity than predicted from aqueous fractionation (e.g., Sanyal et al., 1996, 2000, 2001, Hönisch et al. 2004, Krief et al, 2010, Henehan et al. 2013). We therefore used the empirical fractionation factor for marine carbonates of ~1.020 and apply the temperature correction estimated by Kakihana et al. (1977). A sensitivity test to the use of different fractionation factors shows that any uncertainty in this estimate does not significantly affect our pH estimations (Fig. S3).

If two of the six carbonate parameters (total Dissolved Inorganic Carbon (DIC), total alkalinity, carbonate ion concentration, bicarbonate ion concentration, pH and $CO_2$), are

known in addition to temperature, pressure and salinity, the other parameters can be calculated (Zeebe and Wolf-Gladrow, 2001). We used the modern local salinity-total alkalinity relationship to estimate the total alkalinity (Alkalinity = 69.127 * Salinity – 116.42 ($R^2$= 0.76)). The $pCO_2$ is calculated using $CO_2$sys.xls (Pierrot et al., 2006), with the equilibrium constants $K_1$ and $K_2$ from Hanssen and Mehrbach, refit by Dickson and Millero (1987). The $K_{SO4}$ is from Dickson (1990), and the seawater boron concentration from Lee et al. (2010).

The net effect of uncertainty of 1‰ salinity (including its effect on the total alkalinity; 69 µmol/kg in total alkalinity per 1‰ salinity) and 1°C in temperature on the final $pCO_2$ calculations are ~ 9 and 12 µatm, respectively. The average analytical error in $\delta^{11}B$ (= ~0.3‰; equal to ~0.03 pH units) translates to an average uncertainty of ~18 µatm in downcore $pCO_2$ estimations. According to these sources of uncertainty, an average total error of 23 µatm is adopted.

**5. Nutrient proxies**

Foraminiferal Cd/Ca ratios were found to reflect the Cd concentrations in seawater (Boyle 1988; Keigwin and Boyle 1989), an element that shows strong similarity to the distribution of phosphorous (Boyle et al., 1976). Thus, foraminiferal Cd/Ca can be used to reconstruct the levels of phosphate in seawater (see for details, Elderfield and Rickaby, 2000), which provide clues to infer the changes in the level of nutrient utilization and/or changes in water masses (Elderfield and Rickaby, 2000; Rickaby and Elderfield, 2005). However, Rickaby and Elderfield (1999) also found a temperature control on the Cd incorporation into planktic foraminiferal shells. The $\delta^{13}C$ values in foraminiferal shells vary due to changes in nutrient cycling, air-sea gas exchange, carbonate chemistry and exchange between global carbon reservoirs (e.g., Broecker and Maier-Reimer 1992; Spero et al., 1997). As the non-

nutrient factors that affect both proxies are largely independent, a combination of the two proxies can be used as an indicator for the nutrient levels. Also, the absence of a correlation between our raw Cd/Ca data and Mg/Ca ratios, a temperature proxy, ($R^2$=0.0001; Fig. S4) supports the interpretation of the recorded Cd/Ca variability as changes in nutrient levels (Fig. S4).

**6. Age model**

The age model for JM11-FI-19PC core is based on well-dated tephra layers, magnetic susceptibility, K/Ti ratios measured by XRF-scanning (Ezat et al. 2014) and planktic and benthic foraminiferal $\delta^{18}O$ values. Tephrochronology represents one of the most accurate correlation tools between marine and continental climatic records (e.g., Davies et al., 2014). Six tephra layers were identified by abundance counts from the upper seven meters of JM11-FI-19PC (Ezat et al., 2014). Five of these tephra layers (Saksunarvatn tephra, Vedde ash, Faroe Marine Ash Zone (FMAZ) II, FMAZ III, North Atlantic Ash Zone (NAAZ) II) are well-known tephra from the study area and synchronized to their counterparts in the Greenland ice cores (e.g., Wastegård et al., 2006; Svensson et al., 2008; Davies et al., 2008, 2010 and references therein). A new tephra layer (FMAZ IV) was recently recorded in several records from the southern Norwegian Sea (Wastegård and Rasmussen, 2014). It dates c. 46,800 years BP and occurs in the lower part of Greenland interstadial 12 (see below), but has not yet been located in the Greenland ice cores. Electron microprobe analysis of major elemental composition also confirmed its presence in core JM11-FI-19PC (Wastegård and Rasmussen, 2014). Four tephra layers (5e-Low/BAS-IV, 5e Midt/RHY, 5C-Midt/BAS and 5a-top/BAS-I tephra layers) from the lower part of the core were identified under the binocular microscope in the size fractions >100 µm and 63–100 µm. The location of the tephra layers in relation to the magnetic susceptibility and via the correlation of the magnetic

susceptibility of JM11-FI-19PC with core LINK16 (Abbott et al., 2014) confirms the identification (Fig. S5). Due the heterogeneity in the elemental chemistry in the 5c-Midt/BAS tephra, Abbott et al. (2014) suggested that the basaltic particles within this layer were most likely transported by icebergs.

Marine Isotope stage 5e (the last interglacial 'Eemian') can be recognized by a clear development of a gradient in the benthic and planktic foraminiferal $\delta^{18}O$ values. This gradient is similar to the gradient of the Holocene section (Fig. S6). The lowermost part of JM11-FI-19PC with low planktic and benthic foraminiferal $\delta^{18}O$ values corresponds to HS11 in Termination II. We used the sharp increase in the benthic $\delta^{18}O$ values at 1030 cm core depth as an indication for the beginning of MIS 5e and we adopted an average sedimentation rate from the last deglaciation for HS11.

Within the firm constraints of the identified tephra layers, the age model was subsequently refined by tying the start of DO interstadials as seen in the $\delta^{18}O$ records from the Greenland ice cores with the increases in magnetic susceptibility (Fig. S6). The magnetic susceptibility from the region is thought to reflect changes in the strength of deep currents transporting the magnetic particles from the source (the Icelandic volcanic province) to the site of deposition (e.g., Rasmussen et al., 1996; Kissel et al., 1999). This has been confirmed by a comprehensive investigation to the magnetic properties and mineralogy of sediment cores from the Nordic seas and the North Atlantic for Marine Isotope Stage (MIS) 3 (Kissel et al., 1999). For MIS 5, 4 and 2, the relation appears more complicated. Other processes than bottom currents may be responsible for the transport of the magnetic particles (e.g., melt-out from icebergs). The variations in the magnetic susceptibility may also result from variant dilution due to changes in the amount of calcium carbonate and ice rafted debris. Thus, the interpretation of magnetic susceptibility in terms of bottom current strength for MIS 2, 4 and 5 needs further investigations (cf., Kissel et al., 1999).

The increases in the magnetic susceptibility recorded in our sediment core are more gradual than the abrupt transitions seen in the ice core records (Fig. S6). This can be due to the use of a loop sensor, which tends to smooth the signal over 5–10 cm intervals. Therefore, we use the K/Ti ratio, which has better temporal resolution and which shows more abrupt changes. The magnetic susceptibility and the K/Ti ratios vary oppositely in our area (Richter et al., 2006); during interstadials high magnetic susceptibility correlates with low K/Ti ratios. This is due to an enhanced deposition of bottom current transported basaltic material derived from the Icelandic volcanic province (Rasmussen et al., 1996; Richter et al., 2006). During stadials low MS correlates with high K/Ti ratios due to increased contribution of continentally derived material, possibly through ice rafting from Fennoscandia (Rasmussen et al., 1996; Richter et al., 2006). The XRF-scanner measurements are subject to artifacts due to variations in grain size, interstitial water content and variable thickness of water films that form below the cover of the plastic foil during the analysis (e.g., Tjallingii et al., 2007; Weltje and Tjallingii, 2008; Hennekam and de Lange, 2012). The comparison of the XRF-counts with both water content and element counts of Cl and S (elements that are predominantly present in porewater) can provide indirect information about the variable thickness of the water film formed under the plastic foil (for details see e.g., Hennekam and de Lange, 2012). In brief, high and variable counts of Cl and S in the upper and lower parts of the core with strong correlation with the K and Ti counts suggest that the elemental counts from these core intervals are highly affected by the variations in the water content and variations in the thickness of the water film (Fig. S7). Between 170 cm and 730 cm, the Cl and S counts are low with no correlation to the K/Ti ratios (Fig. S7). In addition, there is no correlation between the K/Ti ratios and grain size or water content. We therefore decided to use the K/Ti ratio only for this interval (Fig. S7). The final age model is based on a radiocarbon date from a core-top sample (at 15 cm), 7 tephra layers and 21 MS-K/Ti based tie points, and a benthic

$\delta^{18}O$ tie point at the start of MIS 5e (Fig. S7). The correlation between magnetic susceptibility and planktic $\delta^{18}O$ records of JM11-FI-19PC to nearby sediment cores ENAM93-21 and MD95-2009 (62°44'N, 03°52'W; 1020 m water depth) and to the $\delta^{18}O$ records of Greenland ice cores is very close (Fig. S8).

**Figure Captions**

**Figure S1: Comparison between $\delta^{11}B$ and B/Ca measured in *N. pachyderma* (sinistral).** There is a general good agreement between $\delta^{11}B$ and B/Ca throughout the record especially across LGM-HS1, but some offsets do also exist. The B/Ca in planktic foraminifera is shown to vary with seawater carbonate chemistry but a quantitative assessment is complicated (Allen et al., 2012). The two red circles represent $\delta^{11}B$ replicate samples cleaned with the reductive-oxidative cleaning method from Pena et al. (2005), while we followed the cleaning method of Barker et al. (2003) for the other $\delta^{11}B$ analyses (black circles). The two cleaning methods yielded indistinguishable values for these two samples.

**Figure S2: a, A sensitivity test of the downcore $pCO_2$ estimations for the uncertainty in the calcification depth of *N. pachyderma* (s) including its effect on the choice of the depth of modern hydrographic data used to calculate $\delta^{11}B_{C\text{-}B4}$ (see section S4).** In this study we assumed a calcification depth range from 40 to 120 m water depth (black line). Alternatively, we calculated $\delta^{11}B_{C\text{-}B4}$ based on data from 50 m water depth (red line) and 250 m water depth (blue line). This test shows no significant influence of the uncertainty in the calcification depth of *N. pachyderma* (s) on our $pCO_2$ calculations.

**Figure S3: Sensitivity study to test the difference in downcore $pCO_2$ between using the empirical boron isotope fractionation into marine carbonates (black dots and line)**

**(Kakihana et al., 1977) and boron isotope fractionation predicted from dissolved boron in seawater (red dots and line) (Klochko et al. 2006) (see section S4 for details).**

**Figure S4: Cross-plot of Cd/Ca and Mg/Ca.** Absence of correlation between both proxies hints to no significant dependency of our downcore Cd/Ca on temperature.

**Figure S5: A correlation between magnetic susceptibility between core LINK16 and the lower part (=135 to 75 kyr BP) of core JM11-FI-19PC.** In this interval we identified 4 tephra layers by vision. These tephra layers were recorded in nearby core LINK16 and confirmed by major and trace element analyses (ref). Therefore, we can confirm the location of these tephra layers in our record by correlation of magnetic susceptibility between the two cores.

**Figure S6: Correlation of core JM11-F1-19PC to Greenland ice cores based on location of tephra layers (Davies et al., 2008; 2010), magnetic susceptibility (MS), XRF-K/Ti and benthic (red) and planktic (black) $\delta^{18}O$**. The black and blue vertical lines refer to the locations of tephra layers and onset of interstadials in JM11-FI-19PC, respectively. Abbreviations: FMAZ (Faroe Marine Ash Zone), NAAZ (North Atlantic Ash Zone). Greenland ice core data from (Rasmussen et al., 2014; Seierstad et al., 2014 and references therein).

**Figure S7: XRF-scanner K, Ti, S and Cl counts plotted with % water content and size fraction >100 µm.**

**Fig. S8: Subsurface (a) and mid depth (b) ventilation ages based on different calendar age scenarios (dashed lines) for the time interval between 22 and 14 ka.** The solid green

lines refer to average ventilation age from different possibilities. The solid black lines refer to ventilation ages presented in Figure 2**.** We will further estimate a best guess and a maximum/minimum range of sediment age-depth models using the Bayesian calibration and age-modeling program Bchron (Parnell et al., 2008).

**Table S1: A test for the influence of the alkaline chelation (using DTPA) step on the Cd/Ca, B/Ca and Mg/Ca.**

## References


Abbott, P. M., et al. (2014). Re-evaluation and extension of the Marine Isotope Stage 5 tephrostratigraphy of the Faroe Islands region: The cryptotephra record. *Palaeogeography, Palaeoclimatology, Palaeoecology, 409*(0), 153-168.

Adkins, J. F., McIntyre, K., & Schrag, D. P. (2002). The Salinity, Temperature, and $\delta^{18}O$ of the Glacial Deep Ocean. *Science, 298*(5599).

Azetsu-Scott, K., & Tan, F. C. (1997). Oxygen isotope studies from Iceland to an East Greenland Fjord: behaviour of glacial meltwater plume. *Marine Chemistry, 56*(3–4), 239-251.

Barker, S., Greaves, M., & Elderfield, H. (2003). A study of cleaning procedures used for foraminiferal Mg/Ca paleothermometry. *Geochemistry, Geophysics, Geosystems, 4*(9). doi: 10.1029/2003GC000559

Bauch, D., Carstens, J., & Wefer, G. (1997). Oxygen isotope composition of living *Neogloboquadrina pachyderma* (sin.) in the Arctic Ocean. *Earth and Planetary Science Letters, 146*(1–2), 47-58.

Boyle, E. A. (1988). Cadmium: Chemical tracer of deepwater paleoceanography. *Paleoceanography, 3(4),* 471-489.

Boyle, E. A., Sclater, F., & Edmond, J. M. (1976). On the marine geochemistry of cadmium. *Nature, 263(5572),* 42-44.

Broecker, W. S., & Maier-Reimer, E. (1992). The influence of air and sea exchange on the carbon isotope distribution in the sea. *Global Biogeochemical Cycles, 6(3),* 315-320.

Craig, H. (1961). Isotopic Variations in Meteoric Waters. *Science, 133*(3465), 1702-1703.

Dansgaard, W. (1964). Stable isotopes in precipitation. *Tellus, 16*(4), 436-468.

Davies, S. M., et al. (2014). A North Atlantic tephrostratigraphical framework for 130–60 ka b2k: new tephra discoveries, marine-based correlations, and future challenges. *Quaternary Science Reviews, 106*(0), 101-121.

Davies, S. M., et al. (2010). Tracing volcanic events in the NGRIP ice-core and synchronising North Atlantic marine records during the last glacial period. *Earth and Planetary Science Letters, 294*(1–2), 69-79.

Davies, S. M., et al. (2008). Identification of the Fugloyarbanki tephra in the NGRIP ice core: a key tie-point for marine and ice-core sequences during the last glacial period. *Journal of Quaternary Science, 23*(5), 409-414.

Dickson, A. G., & Millero, F. J. (1987). A comparison of the equilibrium constants for the dissociation of carbonic acid in seawater media. *Deep Sea Research Part A. Oceanographic Research Papers, 34*(10), 1733-1743.

Dickson, A. G. (1990). Thermodynamics of the dissociation of boric acid in synthetic seawater from 273.15 to 318.15 K. *Deep Sea Research Part A. Oceanographic Research Papers, 37*(5), 755-766.

Elderfield, H., & Ganssen, G. (2000). Past temperature and $\delta^{18}O$ of surface ocean waters inferred from foraminiferal Mg/Ca ratios. *Nature, 405*(6785), 442-445.

Elderfield, H., & Rickaby, R. E. M. (2000). Oceanic Cd/P ratio and nutrient utilization in the glacial Southern Ocean. *Nature, 405*(6784), 305-310.

Emiliani, C. (1955). Pleistocene Temperatures. *The Journal of Geology, 63*(6), 538-578.

Ezat, M. M., Rasmussen, T. L., & Groeneveld, J. (2014). Persistent intermediate water warming during cold stadials in the southeastern Nordic seas during the past 65 k.y. *Geology, 42*(8), 663-666.

Ezat, M. M., Rasmussen, T. L., Hönisch, B., Groeneveld, J. Downcore comparison of two planktic foraminiferal Mg/Ca cleaning protocols and reconstruction of the hydrographic changes in the southern Norwegian Sea during the past 135 kyr. In preparation.

Foster, G. L., Pogge von Strandmann, P. A. E., & Rae, J. W. B. (2010). Boron and magnesium isotopic composition of seawater. *Geochemistry, Geophysics, Geosystems, 11*(8). doi: 10.1029/2010GC003201

Friedrich, T., & Timmermann, A. (2012). Millennial-scale glacial meltwater pulses and their effect on the spatiotemporal benthic $\delta^{18}O$ variability. *Paleoceanography, 27*(3), PA3215. doi: 10.1029/2012PA002330

Grant, K. M., et al. (2012). Rapid coupling between ice volume and polar temperature over the past 150,000 years. *Nature, 491*(7426), 744-747.

Hemming, N. G., & Hanson, G. N. (1992). Boron isotopic composition and concentration in modern marine carbonates. *Geochimica et Cosmochimica Acta, 56*(1), 537-543.

Hemming, N. G., & Hanson, G. N. (1994). A procedure for the isotopic analysis of boron by negative thermal ionization mass spectrometry. *Chemical Geology, 114*(1–2), 147-156.

Hennekam, R., & de Lange, G. (2012). X-ray fluorescence core scanning of wet marine sediments: methods to improve quality and reproducibility of high-resolution paleoenvironmental records. *Limnology and Oceanography: Methods, 10*(12), 991-1003.

Hershey, J. P., Fernandez, M., Milne, P. J., & Millero, F. J. (1986). The ionization of boric acid in NaCl, Na□Ca□Cl and Na□Mg□Cl solutions at 25°C. *Geochimica et Cosmochimica Acta, 50*(1), 143-148.

Hönisch, B., et al. (2003). The influence of symbiont photosynthesis on the boron isotopic composition of foraminifera shells. *Marine Micropaleontology, 49*(1–2), 87-96. 6

Hönisch, B., et al. (2004). Assessing scleractinian corals as recorders for paleo-pH: Empirical calibration and vital effects. *Geochimica et Cosmochimica Acta, 68*(18), 3675-3685.

Hönisch, B., Hemming, N. G., & Loose, B. (2007). Comment on "A critical evaluation of the boron isotope-pH proxy: The accuracy of ancient ocean pH estimates" by M. Pagani, D. Lemarchand, A. Spivack and J. Gaillardet. Geochimica et Cosmochimica Acta, *71(6*), 1636-1641.

Jeansson, E., et al. (2011). The Nordic Seas carbon budget: Sources, sinks, and uncertainties. Global Biogeochemical Cycles, *25(4)*, GB4010. doi: 10.1029/2010GB003961

Jonkers, L., Jiménez-Amat, P., Mortyn, P. G., & Brummer, G.-J. A. (2013). Seasonal Mg/Ca variability of N. pachyderma (s) and G. bulloides: Implications for seawater temperature reconstruction. Earth and Planetary Science Letters, *376(0)*, 137-144.

Kakihana, H., Kotaka, M., Satoh, S., Nomura, M., & Okamoto, M. (1977). Fundamental studies on the ion-exchange of boron isotopes. Bulletin of the Chemical Society of Japan, *50*, 158–163.

Keigwin, L. D., & Boyle, E. A. (1989). Late quaternary paleochemistry of high-latitude surface waters. Palaeogeography, Palaeoclimatology, Palaeoecology, *73(1–2)*, 85-106.

Key, R. M., et al. The CARINA data synthesis project: introduction and overview. *Earth Syst. Sci. Data*, *2*(1), 105-121.

Kissel, C., et al. (1999). Rapid climatic variations during marine isotopic stage 3: magnetic analysis of sediments from Nordic Seas and North Atlantic. *Earth and Planetary Science Letters, 171*(3), 489-502.

Klochko, K., Cody, G. D., Tossell, J. A., Dera, P., & Kaufman, A. J. (2009). Re-evaluating boron speciation in biogenic calcite and aragonite using 11B MAS NMR. *Geochimica et Cosmochimica Acta, 73*(7), 1890-1900.

Klochko, K., Kaufman, A. J., Yao, W., Byrne, R. H., & Tossell, J. A. (2006). Experimental measurement of boron isotope fractionation in seawater. *Earth and Planetary Science Letters, 248*(1–2), 276-285.

Kozdon, R., Ushikubo, T., Kita, N. T., Spicuzza, M., & Valley, J. W. (2009). Intratest oxygen isotope variability in the planktonic foraminifer N. pachyderma: Real vs. apparent vital effects by ion microprobe. *Chemical Geology, 258*(3–4), 327-337.

Lee, K., et al. (2010). The universal ratio of boron to chlorinity for the North Pacific and North Atlantic oceans. *Geochimica et Cosmochimica Acta, 74*(6), 1801-1811.

LeGrande, A. N., & Schmidt, G. A. (2006). Global gridded data set of the oxygen isotopic composition in seawater. *Geophysical Research Letters, 33*(12), L12604. doi: 10.1029/2006GL026011

Nir, O., Vengosh, A., Harkness, J. S., Dwyer, G. S., & Lahav, O. (2015). Direct measurement of the boron isotope fractionation factor: Reducing the uncertainty in reconstructing ocean paleo-pH. *Earth and Planetary Science Letters, 414*(0), 1-5.

Parnell, A. C., Haslett, J., Allen, J. R. M., Buck, C. E., & Huntley, B. (2008). A flexible approach to assessing synchroneity of past events using Bayesian reconstructions of sedimentation history. *Quaternary Science Reviews, 27*(19–20), 1872-1885.

Pena, L. D., Calvo, E., Cacho, I., Eggins, S., & Pelejero, C. (2005). Identification and removal of Mn-Mg-rich contaminant phases on foraminiferal tests: Implications for Mg/Ca past temperature reconstructions. *Geochemistry, Geophysics, Geosystems, 6*(9). doi: 10.1029/2005GC000930

Pierrot, D., Lewis, E., & Wallace., D. W. R. (2006). MS Excel program developed for $CO_2$ system calculations. ORNL/CDIAC-105, *Carbon Dioxide Information Analysis Center*, Oak Ridge National Laboratory, U.S. Department of Energy, Oak Ridge, TN.

Rasmussen, S. O., et al. (2014). A stratigraphic framework for abrupt climatic changes during the Last Glacial period based on three synchronized Greenland ice-core records: refining and extending the INTIMATE event stratigraphy. *Quaternary Science Reviews, 106*(0), 14-28.

Rasmussen, T. L., Thomsen, E., Labeyrie, L., & van Weering, T. C. E. (1996). Circulation changes in the Faeroe-Shetland Channel correlating with cold events during the last glacial period (58–10 ka). *Geology, 24*(10), 937-940.

Richter, T. O., et al. (2006). The Avaatech XRF Core Scanner: technical description and applications to NE Atlantic sediments. *Geological Society, London, Special Publications, 267*(1), 39-50.

Rickaby, R. E. M., & Elderfield, H. (1999). Planktonic foraminiferal Cd/Ca: Paleonutrients or paleotemperature? *Paleoceanography, 14*(3), 293-303.

Rickaby, R. E. M., & Elderfield, H. (2005). Evidence from the high-latitude North Atlantic for variations in Antarctic Intermediate water flow during the last deglaciation. *Geochemistry, Geophysics, Geosystems, 6*(5). doi: 10.1029/2004GC000858

Sanyal, A., et al. (1996). Oceanic pH control on the boron isotopic composition of foraminifera: Evidence from culture experiments. *Paleoceanography, 11*(5), 513-517.

Seierstad, I. K., et al. (2014). Consistently dated records from the Greenland GRIP, GISP2 and NGRIP ice cores for the past 104 ka reveal regional millennial-scale $\delta^{18}O$ gradients with possible Heinrich event imprint. *Quaternary Science Reviews, 106*(0), 29-46.

Shackleton, N. (1967). Oxygen Isotope Analyses and Pleistocene Temperatures Re-assessed. *Nature, 215*(5096), 15-17.

Simstich, J., Sarnthein, M., & Erlenkeuser, H. (2003). Paired $\delta^{18}O$ signals of *Neogloboquadrina pachyderma* (s) and Turborotalita quinqueloba show thermal stratification structure in Nordic Seas. *Marine Micropaleontology, 48*(1–2), 107-125.

Spero, H. J., Bijma, J., Lea, D. W., & Bemis, B. E. (1997). Effect of seawater carbonate concentration on foraminiferal carbon and oxygen isotopes. *Nature, 390*(6659), 497-500.

Svensson, A., et al. (2008). A 60 000 year Greenland stratigraphic ice core chronology. *Clim. Past, 4*(1), 47-57.

Tjallingii, R., Röhl, U., Kölling, M., & Bickert, T. (2007). Influence of the water content on X-ray fluorescence core-scanning measurements in soft marine sediments. *Geochemistry, Geophysics, Geosystems, 8*(2). doi: 10.1029/2006GC001393

Waelbroeck, C., et al. (2011). The timing of deglacial circulation changes in the Atlantic. *Paleoceanography, 26*(3). doi: 10.1029/2010PA002007

Wastegård, S., & Rasmussen, T. L. (2014). Faroe Marine Ash Zone IV: a new MIS 3 ash zone on the Faroe Islands margin. *Geological Society, London, Special Publications, 398*(1), 81-93.

Wastegård, S., Rasmussen, T. L., Kuijpers, A., Nielsen, T., & van Weering, T. C. E. (2006). Composition and origin of ash zones from Marine Isotope Stages 3 and 2 in the North Atlantic. *Quaternary Science Reviews, 25*(17–18), 2409-2419.

Weltje, G. J., & Tjallingii, R. (2008). Calibration of XRF core scanners for quantitative geochemical logging of sediment cores: Theory and application. *Earth and Planetary Science Letters, 274*(3–4), 423-438.

Zeebe, R. E., & Wolf-Gladrow, D.A. (2001). $CO_2$ in Seawater: Equilibrium, Kinetics, Isotopes. *Elsevier*.

Zeebe, R. E. (1999). An explanation of the effect of seawater carbonate concentration on foraminiferal oxygen isotopes. *Geochimica et Cosmochimica Acta, 63*(13–14), 2001-2007.

Zeebe, R. E., Wolf-Gladrow, D. A., Bijma, J., & Hönisch, B. (2003). Vital effects in foraminifera do not compromise the use of $\delta^{11}B$ as a paleo-pH indicator: Evidence from modeling. *Paleoceanography, 18*(2). doi: 10.1029/2003PA000881

**Figure S1**

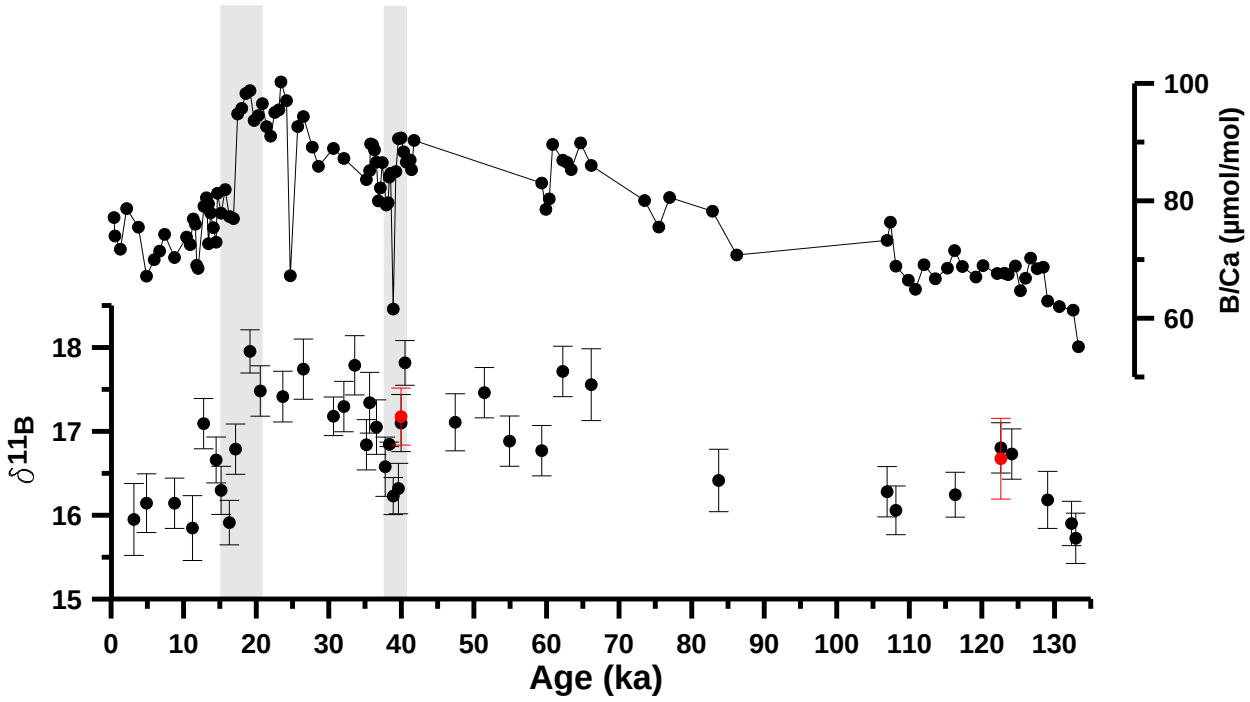
100
80
60
B/Ca (µmol/mol)
18
17
16
15
δ11B
0
10
20
30
40
50
60
70
80
90
100
110
120
130
Age (ka)

**Figure S2**

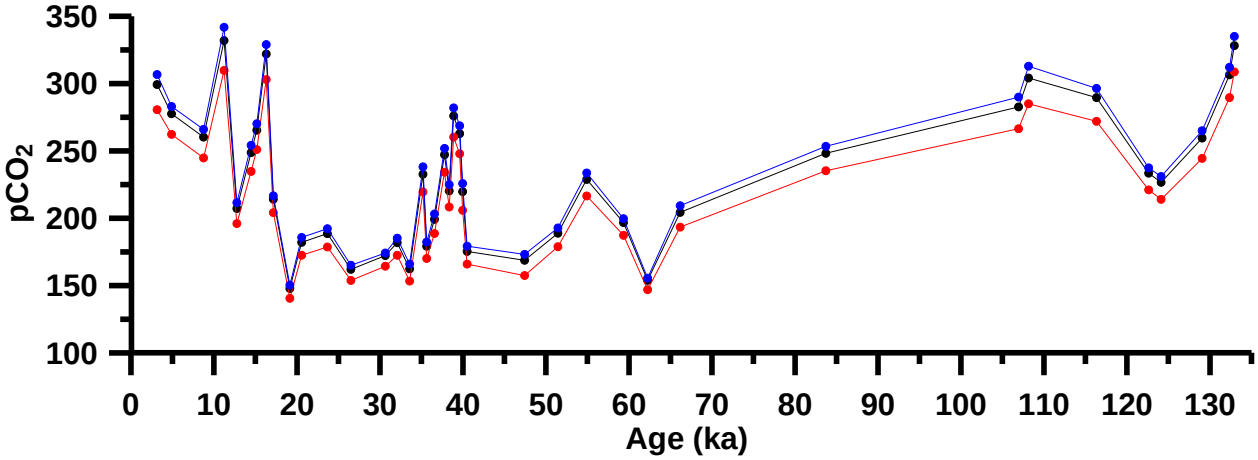
pCO2
350
300
250
200
150
100
0
10
20
30
40
50
60
70
80
90
100
110
120
130
Age (ka)

**Figure S3**

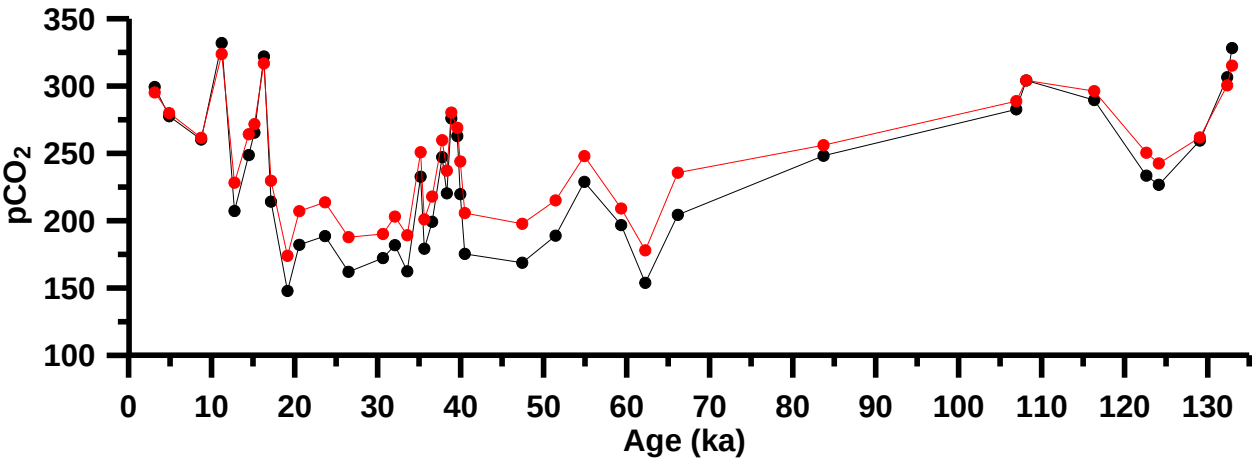
350
300
250
200
150
100
pCO2
0
10
20
30
40
50
60
70
80
90
100
110
120
130
Age (ka)

**Figure S4**

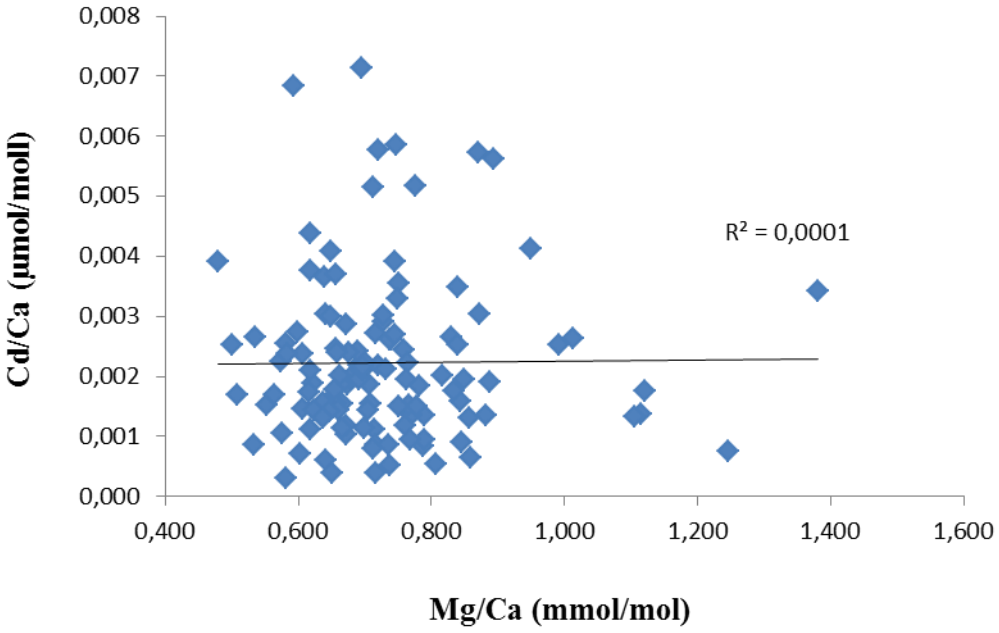
0,008
0,007
0,006
0,005
0,004
0,003
0,002
0,001
0,000
Cd/Ca (µmol/moll)
R² = 0,0001
0,400
0,600
0,800
1,000
1,200
1,400
1,600
Mg/Ca (mmol/mol)

**Figure S5**

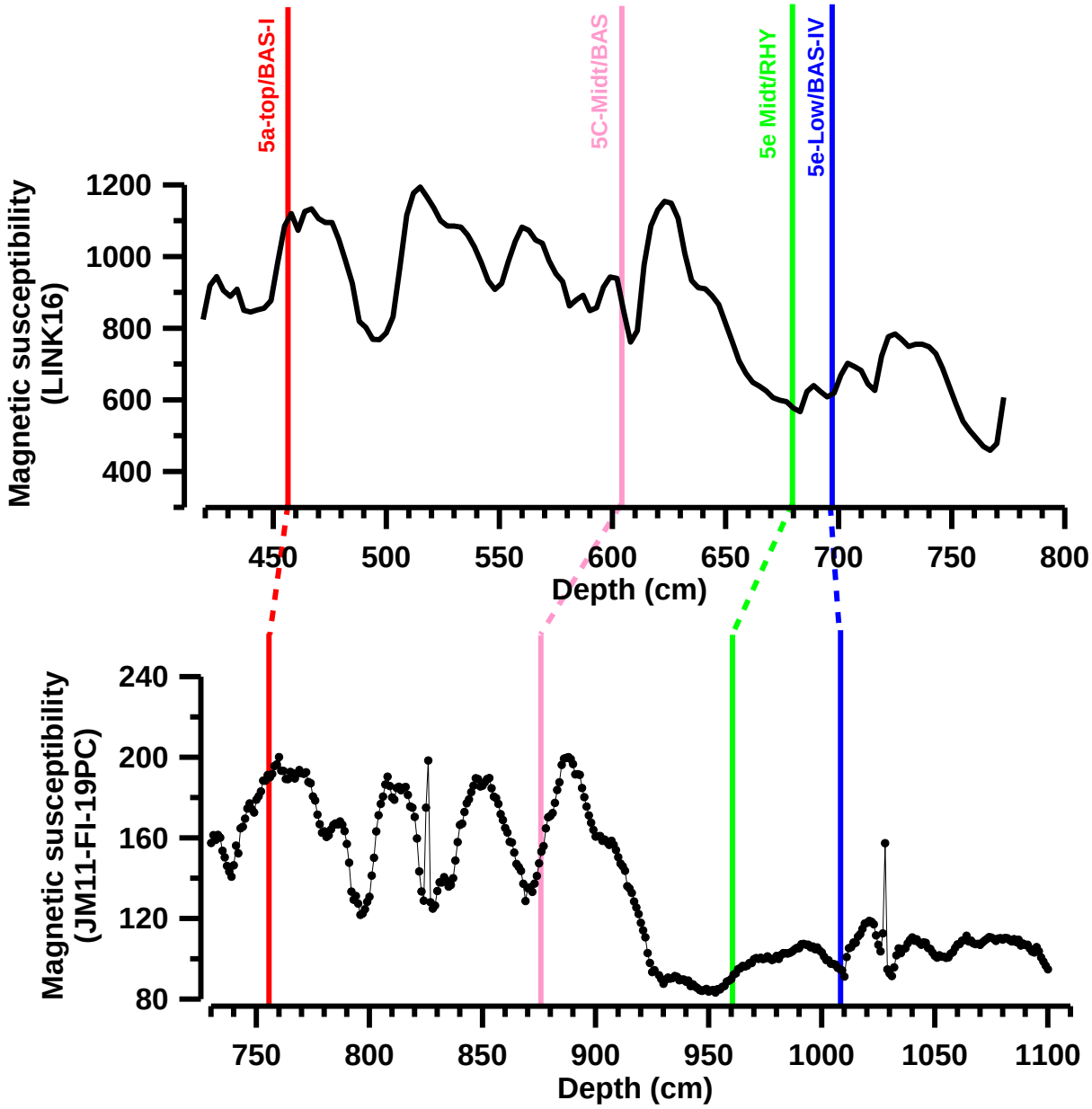
5a-top/BAS-I
5C-Midt/BAS
5e Midt/RHY
5e-Low/BAS-IV
Magnetic susceptibility (LINK16)
1200
1000
800
600
400
450
500
550
600
650
700
750
800
Depth (cm)
Magnetic susceptibility (JM11-FI-19PC)
240
200
160
120
80
750
800
850
900
950
1000
1050
1100
Depth (cm)

**Figure S6**

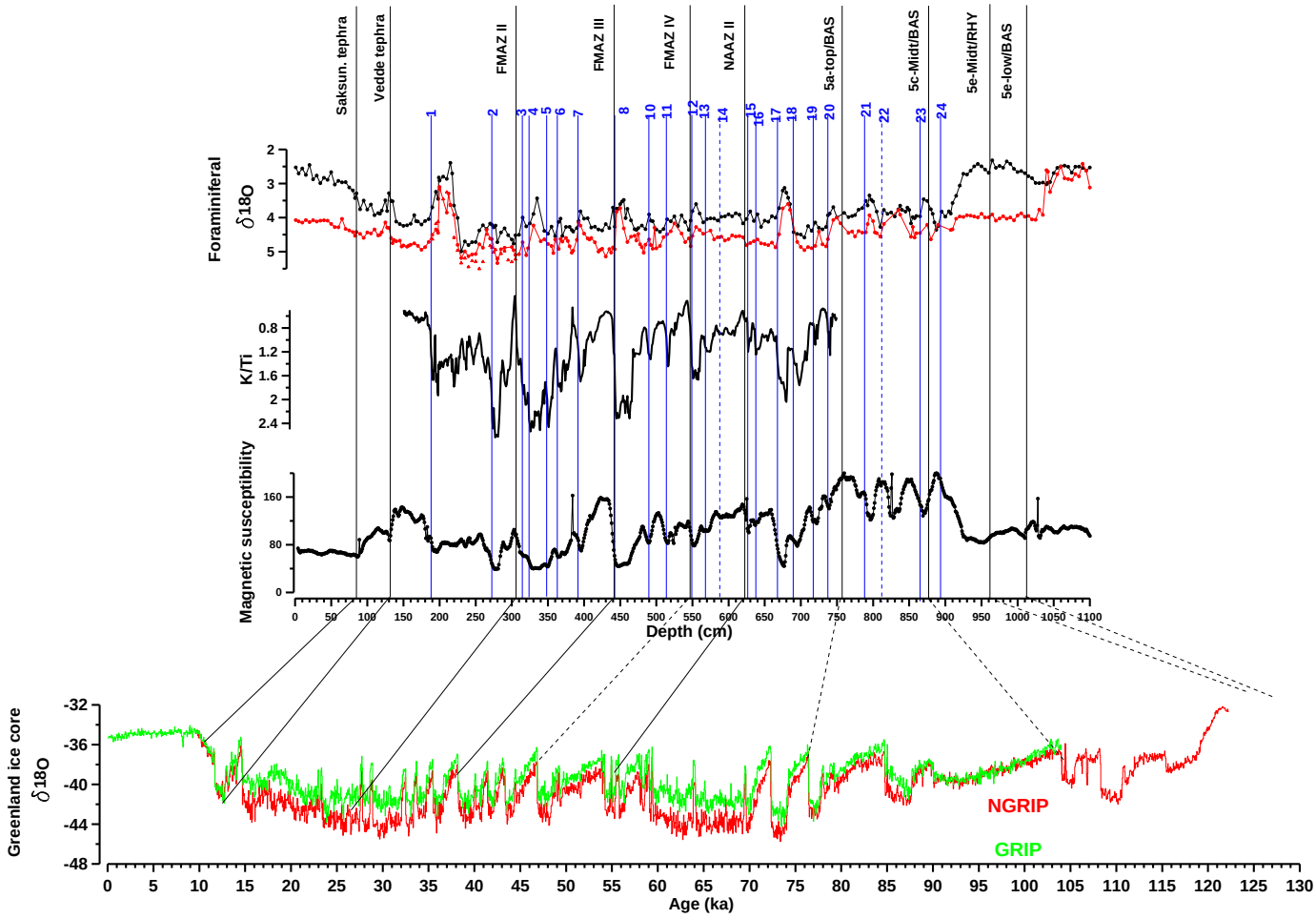
Saksun. tephra
Vedde tephra
FMAZ II
FMAZ III
FMAZ IV
NAAZ II
5a-top/BAS
5c-Midt/BAS
5e-Midt/RHY
5e-low/BAS
Foraminiferal δ18O
K/Ti
Magnetic susceptibility
Depth (cm)
Greenland ice core δ18O
NGRIP
GRIP
Age (ka)

**Figure S7**

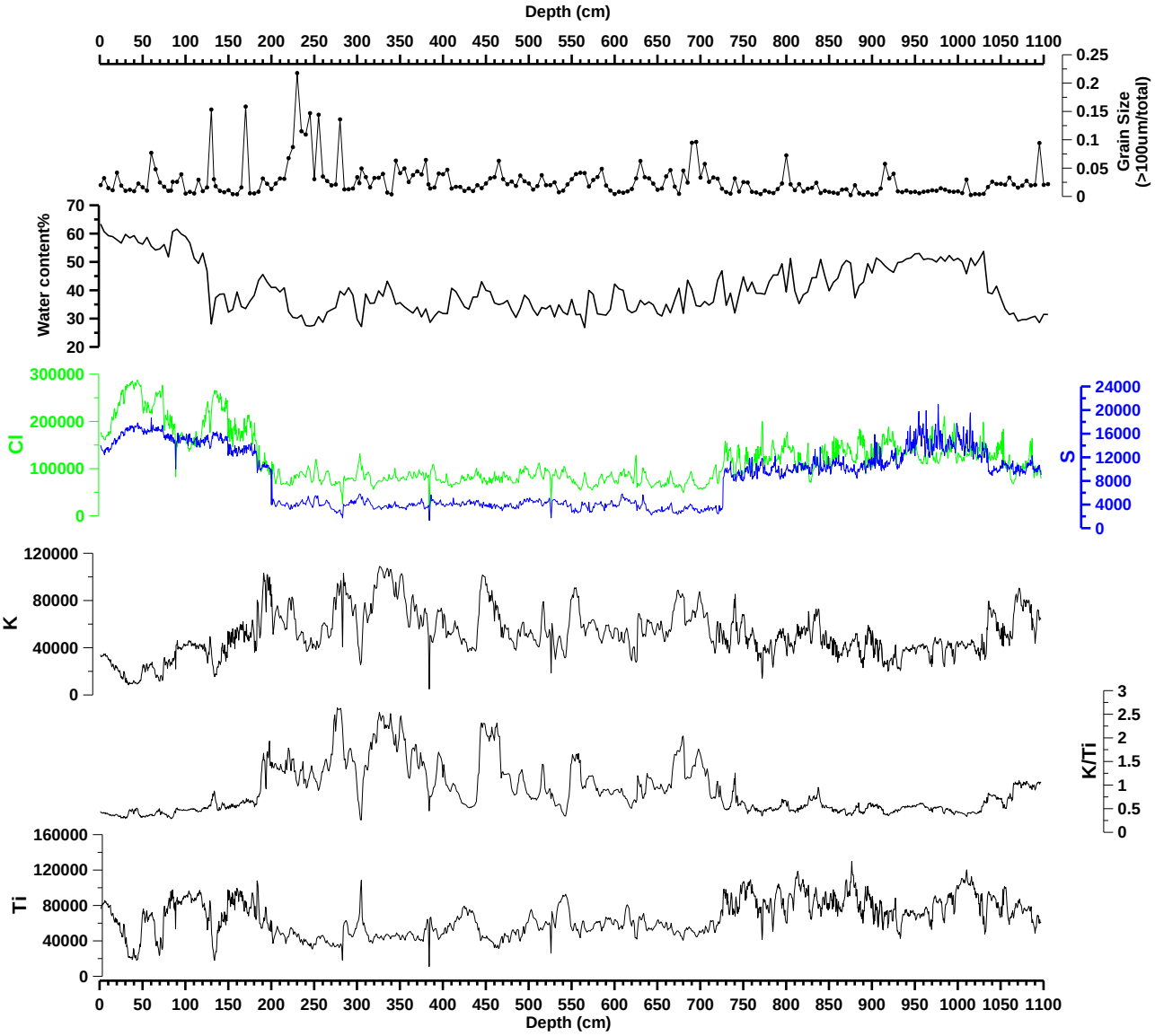
Depth (cm)
0 50 100 150 200 250 300 350 400 450 500 550 600 650 700 750 800 850 900 950 1000 1050 1100
Grain Size (>100um/total)
0 0.05 0.1 0.15 0.2 0.25
Water content%
20 30 40 50 60 70
Cl
0 100000 200000 300000
S
0 4000 8000 12000 16000 20000 24000
K
0 40000 80000 120000
K/Ti
0 0.5 1 1.5 2 2.5 3
Ti
0 40000 80000 120000 160000
Depth (cm)

**Figure S8**

a

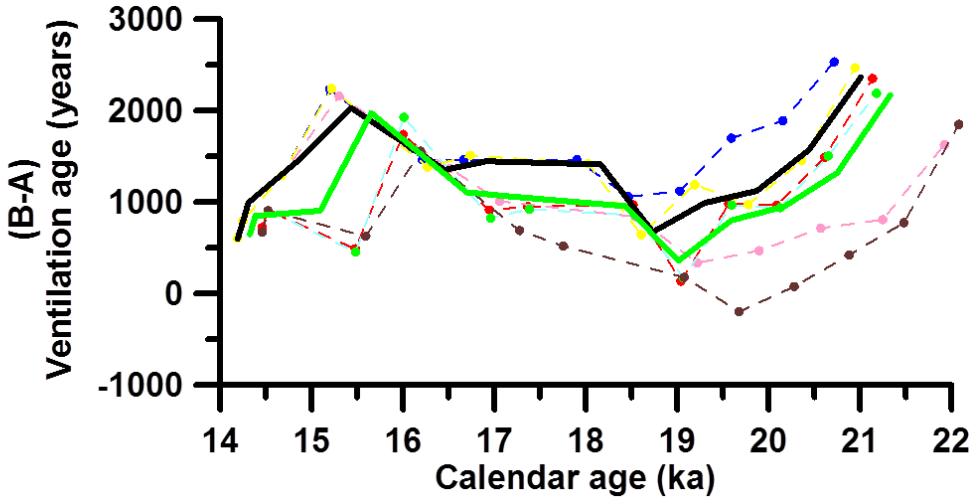
3000
2000
1000
0
-1000
(B-A)
Ventilation age (years)
14
15
16
17
18
19
20
21
22
Calendar age (ka)

b

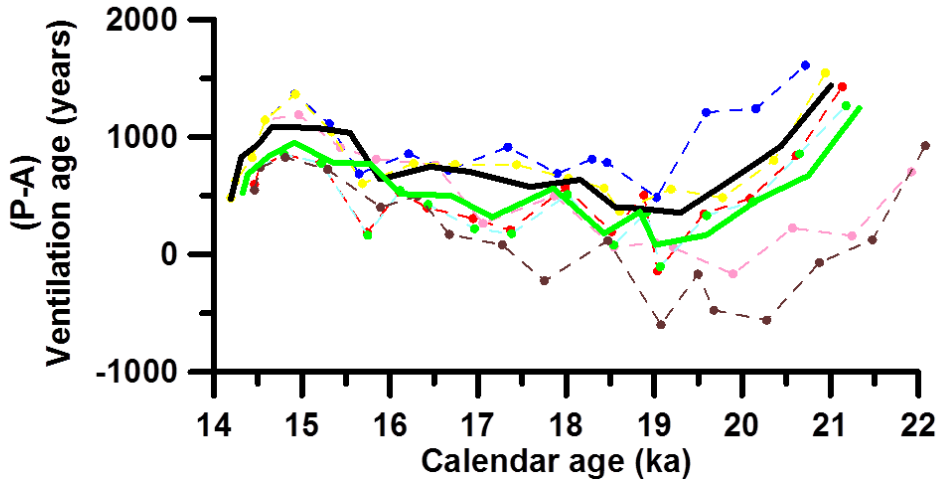
2000
1000
0
-1000
(P-A)
Ventilation age (years)
14
15
16
17
18
19
20
21
22
Calendar age (ka)

**Table S1**

| Depth | B/Ca | Mg/Ca | Al/Ca | Mn/Ca | Fe/Ca | Cd/Ca | DTPA step |
|---|---|---|---|---|---|---|---|
| Cm | umol/mol | mmol/mol | umol/mol | umol/mol | umol/mol | umol/mol | |
| 215 | 77,0 | 0,695 | 4 | 92 | 14 | 0,0071 | Yes |
| 215 | 76,4 | 0,922 | 118 | 121 | 41 | 0,0074 | No |
| | | | | | | | |
| 345 | 87,2 | 0,607 | 2 | 89 | 35 | 0,0024 | Yes |
| 345 | 87,6 | 0,646 | 168 | 97 | 30 | 0,0026 | No |
| | | | | | | | |
| 490 | 90,3 | 0,788 | 43 | 25 | 48 | 0,0008 | Yes |
| 490 | 82,7 | 1,272 | 297 | 30 | 227 | 0,0013 | No |
| | | | | | | | |
| 670 | 78,6 | 0,671 | 9 | 75 | 36 | 0,0029 | Yes |
| 670 | 78,2 | 0,725 | 64 | 84 | 46 | 0,0030 | No |
| | | | | | | | |
| 682,5 | 86,6 | 0,583 | 2 | 31 | 21 | 0,0024 | Yes |
| 682,5 | 84,1 | 0,672 | 28 | 35 | 26 | 0,0026 | No |

# Paper III

**Downcore comparison of two planktic foraminiferal Mg/Ca cleaning protocols and reconstruction of the hydrographic changes in the southern Norwegian Sea during the past 135 kyr**

Mohamed M. Ezat[1,2], Tine L. Rasmussen[1], Bärbel Hönisch[3], Jeroen Groeneveld[4]

[1] CAGE - Centre for Arctic Gas Hydrate, Environment and Climate, Department of Geology, UiT, The Arctic University of Norway, NO-9037 Tromsø, Norway

[2] Department of Geology, Faculty of Science, Beni-Suef University, Beni-Suef, Egypt.

[3] Deapartment of Earth and Environmental Sciences and Lamont-Doherty Earth Observatory of Columbia University, Palisades, NY 10964, USA.

[4] Center for Marine Environmental Sciences (MARUM), University of Bremen, Leobener Str., D-28359 Bremen, Germany.

## Abstract

The subsurface hydrography in the southern Norwegian Sea during the past 135,000 years was investigated using parallel measurements of Mg/Ca and $\delta^{18}O$ in shells of the planktic foraminiferal species *Neogloboquadrina pachyderma* sinistral. Two cleaning methods were applied prior to Mg/Ca analysis, 'Mg Cleaning' (Barker et al., 2003) and 'full cleaning' (Martin and Lea, 2002) methods. Although comparable results were obtained, significant decreases in the Mg/Ca at some intervals were recorded, when the 'full cleaning' method was used relative to the 'Mg cleaning' method. Comparison of the differences in Mg/Ca with Al/Ca, Fe/Ca and Mn/Ca, as monitors of contamination, as well as the shell weight of *N. pachyderma* (s) and weight loss % during the cleaning demonstrates that the decreases in Mg/Ca are likely due to a more efficient removal of Mn-contaminant coatings of

the shells, when the 'full cleaning' procedure is applied. We further combined Mg/Ca and B/Ca from the 'full cleaning' method with $\delta^{18}O$ values to constrain the calcification temperature and seawater $\delta^{18}O$ in the past. A decrease of about 1‰ in seawater $\delta^{18}O$, increase in the subsurface temperature and dominance of *N. pachyderma* (s) (>80%) during Heinrich Stadial (HS)1 suggests a strong stratification in the upper water column and a possible subsurface inflow of Atlantic water below a developed halocline, at least during the calcification seasons of *N. pachyderma* (s). Similar decreases in seawater $\delta^{18}O$ are also recorded for the other resolved Heinrich stadials (HS3, -4, -6 and -11). In addition, our temperature estimates confirm the delay of the Eemian 'MIS 5e' warm peak in the Eastern Nordic seas compared to the North Atlantic and a late warming extending to the time of the summer insolation minimum at 60° N (e.g., Rasmussen et al., 2003a). However, relatively high values of seawater $\delta^{18}O$ during the early Eemian suggest a subsurface inflow of Atlantic water below a thin layer of polar water. Bottom water temperature (BWT) reconstructed based on Mg/Ca measured in the benthic foraminiferal species *Melonis barleeanus* reveal cold temperatures during the early Eemian similar to the late Holocene indicating that early Eemian intermediate/deep circulation may have operated similar to modern at this site.

## 1. Introduction

Advection of relatively warm and saline Atlantic water into the Nordic seas and outflow of deep water into the North Atlantic are among the key oceanic processes that determine the hydrographic properties and circulation dynamics in the high latitude North Atlantic (e.g., Hansen and Østerhus, 2000). This exchange of surface and deep waters between the North Atlantic, the Nordic seas and the Arctic Ocean represents the northernmost part of the Atlantic Meridional Overturning Circulation (AMOC), an important component of

the earth's climate system. Changes in ocean circulation, and particularly in the AMOC, affect heat distribution, global transmission of regional climate anomalies and sea-air $CO_2$ exchange (e.g., Broecker, 1998; Wunsch et al., 2006; Sigman and Boyle, 2000), and are thus widely considered in explaining millennial scale and abrupt climatic anomalies during the late Pleistocene (e.g., Barker et al., 2011). Past archives of hydrographic changes at key areas of exchange between the North Atlantic and the Nordic seas could provide solid constraints to understand the past changes in AMOC and their linkage to climate change.

In this study, we analyzed Mg/Ca and $\delta^{18}O$ in the planktic foraminiferal species *N. pachyderma* (s) in order to reconstruct the subsurface hydrography for the last 135 kyr BP including the last interglacial 'the Eemian', the last glacial Dansgaard-Oeschger (DO) events and the Holocene interglacial. The study is based on sediment core JM-FI-19PC collected from the Northwest of the Faroe Islands (62°49'N, 03°52'W; 1179 m water depth), where the largest Atlantic water inflow into the Nordic seas and a significant outflow of deep water into the North Atlantic take place today (Figure 1). One striking feature in the Nordic seas records is the large decrease of 0.5 to 2.5‰ in both planktic and benthic foraminiferal $\delta^{18}O$, correlating with the millennial-scale climate swings (e.g., Rasmussen et al., 1996; Meland et al., 2008). Foraminiferal $\delta^{18}O$ values are a function of calcification temperature, seawater $\delta^{18}O$ ($\delta^{18}O_{SW}$) and carbonate chemistry (Emiliani 1955; Shackleton et al., 1967; Spero et al., 1997). $\delta^{18}O_{SW}$ values at a specific location vary through time due to changes in global ice volume, salinity-related effects (evaporation/precipitation, meltwater and river runoff) and ocean circulation patterns (Craig, 1961; Dansgaard, 1964; Shackleton, 1967; Waelbroeck et al., 2011; Friedrich and Timmermann, 2012). Differentiating between the various signals is a challenge, but imperative for our understanding of the temporal variability in foraminiferal $\delta^{18}O$. Minor/trace element to calcium ratios measured in the same foraminiferal samples as $\delta^{18}O$ have the potential to provide independent information about the calcification

temperature (e.g., Nürnberg et al., 1996), salinity- related effects (e.g., Wit et al., 2013; Hönisch et al., 2011; Bahr et al., 2013) and carbonate chemistry (e.g., Yu and Elderfield, 2007; Yu et al., 2007a; Raitzsch et al., 2008). In particular, Mg/Ca have been widely used in parallel with $\delta^{18}O$ measurements to constrain calcification temperatures and $\delta^{18}O_{SW}$ (e.g., Elderfield and Ganssen, 2000; Skinner et al., 2003; Thornalley et al., 2009).

Laboratory experiments have shown that the incorporation of Mg into planktic foraminiferal $CaCO_3$ is primarily controlled by temperature, while other factors such as salinity and carbonate chemistry play a minor role (e.g., Nürnberg et al., 1996; Russell et al., 2004; Hönisch et al., 2013, Spero et al., 2015). However, the primary Mg/Ca signal, as most other minor/trace element to Ca ratios, can be significantly modified by partial dissolution (e.g., Dekens et al., 2002; Regenberg et al., 2006), as well as contamination with organics, adsorbed clays and post-depositional overgrowths (Boyle, 1981). Two main procedures, the 'Mg cleaning' and 'Cd cleaning' methods are currently used to clean foraminiferal samples prior to minor/trace element analyses in order to remove the different contaminants (Boyle and Keigwin, 1985; Barker et al., 2003; for review see Barker et al., 2005). The main difference is that the 'Cd cleaning' method includes an additional reduction step with buffered solution of hydrous hydrazine. The reduction step is a standard procedure for Cd/Ca and Ba/Ca analyses (Boyle and Keigwin, 1985), and because all elements can be analyzed simultaneously, it is tempting to apply the same cleaning procedure and measure all elements together. However, there is a debate whether the reduction step is necessary, adequate or even damaging for the Mg/Ca analyses (Pena et al., 2005; Martin and Lea 2002; Rosenthal et al., 2004; Barker et al., 2003; Yu et al., 2007b). Finally, another additional step, which is specific for Ba/Ca analyses additionally requires treatment of the foraminiferal samples with alkaline diethylene-triamine-pentaacetic acid (DTPA) to remove authigenic barite (e.g., Lea and

Boyle, 1991; Martin and Lea, 2002). Hereafter, this latter cleaning method will be described as the 'full cleaning' method.

For minor/trace element analyses in *N. pachydema* (s), we initially cleaned the foraminiferal samples using the 'Mg cleaning' method (Barker et al., 2003), but a later need to measure Cd and Ba (Ezat et al., second manuscript) led us to repeat the analyses using the 'full cleaning' method (Martin and Lea, 2002). Although comparable Mg/Ca results were obtained, significant decreases in the Mg/Ca at some intervals were recorded when the 'full cleaning' method was used. Therefore, we first document the differences in down-core *N. pachydema* (s) Mg/Ca using the two different cleaning methods and subsequently, we discuss the variations in downcore Mg/Ca and $\delta^{18}O$ records in terms of paleoceanographic changes. In addition, we analyzed Mg/Ca and $\delta^{18}O$ in the benthic foraminiferal species *Melonis barleeanus* from the last interglacial 'Eemian' period (~130 to 110 kyr BP) in order to reconstruct the Bottom Water Temperature (BWT).

## 2. **Methods**

The magnetic susceptibility was measured using a GEOTEK Multi-Sensor Core Logger. After logging, the core was opened, split, X-rayed, XRF-scanned and sampled at 5 cm intervals. Samples were weighed, freeze-dried and weighed again before wet sieving (Ezat et al., 2014). Only pristine foraminiferal specimens with no visible signs of dissolution were selected for minor/trace element and stable isotope analyses.

### 2.1. Minor/trace element analyses for *N. pachydema* (s)

For the first set of trace/minor element analyses in *N. pachyderma* (s), the foraminiferal tests (50–100 specimens, size fraction 150 to 250 µm) were gently crushed and cleaned following the 'Mg cleaning' method (Barker et al., 2003) with a slight modification:

the removal of coarse grained silicate was omitted and instead the samples were centrifuged after dissolution (10 min, 6000 rpm) to separate any insoluble particles. The samples were analyzed using an ICP-OES (Agilent Technologies, 700 Series with autosampler (ASX-520 Cetac) and micro-nebulizer) at the Department of Geosciences, University of Bremen. Instrumental accuracy of the ICP-OES was monitored by analysis of an in-house standard solution with a Mg/Ca of 2.93 mmol/mol after every five samples (long term average of 2.917 mmol/mol, standard deviation ($\sigma$) = 0.04 mmol/mol and relative standard deviation (RSD) = 1.4%). The average relative precision of Mg/Ca for 16 replicate samples that were cleaned and analyzed at different sessions is 9%. Seventeen samples (~6% of the entire analyzed samples) with high Al/Ca, Fe/Ca, Mn/Ca (>average + 2$\sigma$) and 2 samples with exceptionally high Mg/Ca values were discarded from the record (Table 1). Eight samples with high Mn/Ca (>average + 2$\sigma$) from the interval 930–965 cm down-core and correlating with the mid Eemian gave consistent Mg/Ca values with samples having relatively lower Mn/Ca from the same interval. These were thus included in the study.

For the second set of minor/trace element analyses performed on *N. pachyderma* (s), 60–160 specimens (size fraction 150 to 250 µm) were gently crushed, weighed, cleaned following the full cleaning procedure of Martin and Lea (2002) with some slight modifications mainly from Pena et al. (2005). These modifications include the number of water rinses after the reduction and DTPA steps. Also, the samples were rinsed with $NH_4OH$ (Lea and Boyle, 1993) after the treatment with the DTPA solution instead of using 0.01N NaOH (Martin and Lea 2002). The samples were then analyzed by iCAPQ Inductively-Coupled Plasma Mass Spectrometry (ICP-MS) at Lamont Doherty Earth Observatory (LDEO) of Columbia University. Based on repeated measurements of in-house standard solutions, the intra-run precision is <1.4%, 1.9% and 1.4% for Mg/Ca, B/Ca and Li/Ca, respectively. The analyses of five replicate samples, picked and cleaned separately, showed

an average relative precision of 4.3%, 2.7% and 1.5% for Mg/Ca, B/Ca and Li/Ca, respectively. All cleaning and dissolution steps for the second set of analyses were done in boron-free filtered laminar flow benches and all used water was boron-free Milli-Q water. Four samples were omitted due to very high Al/Ca (Table 1). Sample weights were determined on a Mettler XP6 microbalance, and average shell weights were calculated using the number of tests in each sample. To evaluate potential instrumental bias between our ICP-MS and ICP-OES analyses, a suite of standards (ECRM 752-1, BAM RS3, and CMSI 1767) (Greaves et al., 2008) were measured by both laboratories. The inter-laboratory accuracy for Mg/Ca is 2.6%, 0.2% and 1.4% for ECRM 752-1, BAM RS3, and CMSI 1767, respectively. For both sets of analyses, blank samples were performed within every batch of samples in order to monitor potential contamination from reagents and vials.

### 2.2. Minor/trace element and $\delta^{18}O$ analyses for *M. barleeanus*

Core depth 910–1065 cm spans the Eemian interglacial and the latest part of Marine Isotope Stage (MIS) 6. From this interval, 18 to 60 specimens of *M. barleeanus* were picked from size fraction 150 to 315 µm for minor/trace element analyses. The foraminiferal tests were gently crushed and cleaned following the standard foraminiferal Mg/Ca cleaning protocol (Barker et al., 2003), then analyzed by ICP-OES at MARUM Bremen. Four samples were replicated by ICP-MS at LDEO, but cleaned following the 'Cd cleaning' procedure (Pena et al., 2005). The Mg/Ca values were converted to BWT using species-specific calibration equation ($Mg/Ca = 0.757 \pm 0.09 * \exp(0.119 \pm 0.014 * T)$), (Kristjánsdóttir et al., 2007).

About 15 specimens of *M. barleeanus* (size fraction 150 to 315 µm) were picked for stable isotope analysis. The analyses were performed using a Finnigan MAT 251 mass spectrometer with an automated carbonate preparation device at the Department of

Geosciences, University of Bremen. The external standard error of the oxygen isotope analyses is 0.07‰. Values are reported relative to the Vienna Pee Dee Belemnite, calibrated by using the National Bureau of Standards NBS18, 19, and 20.

### 2.3. Planktic foraminiferal assemblages

Core depth 50–255 cm spans the Last Glacial Maximum (LGM) to the mid Holocene (21 to 6 kyr BP; see section 3 below). From this interval at least 300 planktic foraminiferal specimens from the size fraction >100 µm were counted and identified to species level. Kandiano and Bauch (2002) pointed out that in cold polar areas more reliable temperature estimates can be obtained by using counts from planktic foraminiferal assemblages with mesh sizes <125 µm. Larger mesh-sizes tend to loose important small-sized subpolar species *Turborotalia quinqueloba* and *Globigerinita uvula*.

## 3. Age Model and Stratigraphy

We use the age model from Ezat et al. (second manuscript). Briefly, a total of ten tephra layers were identified in JM11-FI-19PC by vision, counting, correlation with nearby sediment cores and/or elemental chemistry (Ezat et al., 2014; Wastegård and Rasmussen, 2014; Ezat et al., second manuscript) (Figure 2). Five of those tephra layers are recorded in the Greenland ice cores (Davies et al., 2008; 2010 and references therein) and thus provide marine-ice tie points. With firm constraints from the identified tephra layers, the age model was subsequently refined by tying the start of DO interstadials as seen in the $\delta^{18}O$ record of the NGRIP ice core with the sharp transitions in magnetic susceptibility and K/Ti measured by XRF scanning (Ezat et al., 2014; Ezat et al., second manuscript). The correlation between magnetic susceptibility and planktic $\delta^{18}O$ records of JM11-FI-19PC to nearby sediment cores

ENAM93-21 and MD95-2009 (62°44'N, 03°52'W; 1020 m water depth) and to the $\delta^{18}O$ records of Greenland ice cores is very close (Figure 2).

JM11-FI-19PC spans the past 135,000 years, and includes the Holocene interglacial, the last glacial cycle with its characteristic DO events and the Eemian interglacial. A typical DO event in Greenland ice core records is characterized by three phases: the event begins with an abrupt warming of 8–16°C from stadial to interstadial conditions, followed by gradual cooling and finally a sudden cooling to stadial conditions (Dansgaard et al., 1993; Huber et al., 2006). In North Atlantic sediments, DO events are associated with the occurrence of Ice Rafted Debris (IRD). In addition, 11 layers rich in detrital carbonate were recorded in the North Atlantic dating from MIS 6–MIS 2. These events are called Heinrich events and are thought to be correlated with the coldest periods of the longest lasting stadials in the ice cores (Heinrich 1988; Bond et al., 1993; Broecker et al., 1994; Rasmussen et al., 2003b; Hemming et al., 2004). In this study we refer to the entire stadial periods during which a Heinrich event is recorded as Heinrich stadials (HS) (cf., Barker et al., 2009). Core JM11-FI-19PC recovered the latest part of MIS 6 representing the millennial scale event (HS11) deposited at transition into the full interglacial conditions of MIS 5e (the Eemian). During the Eemian, the summer temperatures at the northern hemisphere were higher than in the Holocene epoch (CAPE-Last Interglacial Project Members, 2006).

## 4. Results and discussion of cleaning methods

### 4.1. Comparison of *N. pachyderma* (s) Mg/Ca from 'Mg cleaning' and 'full cleaning' methods

The Mg/Ca results from the 'Mg cleaning' and 'full cleaning' methods are compared in Figure (3), along with Al/Ca, Fe/Ca and Mn/Ca as monitors for contamination by clay

minerals and/or Mn-oxyhydroxides/carbonates (Boyle, 1983; Barker et al., 2003). Holocene samples cleaned with either method gave indistinguishable Mg/Ca values, while significant and non-systematic offsets are observed down-core (Figure 3E). In general, the glacial and Eemian samples that were cleaned by the 'full cleaning' method yielded lower Mg/Ca by 10 to 50% than when the 'Mg cleaning' was applied. This decrease in the Mg/Ca is consistent with a decrease in both the Mn/Ca and Fe/Ca (Figure 3). If the decrease in our down-core Mg/Ca was caused by dissolution as a side effect from the extra cleaning (e.g., Barker et al., 2003; Yu et al., 2007b), we would expect this decrease to predominate in samples where the preservation of *N. pachyderma* (s) is lower and sample loss during the cleaning process is higher. However, we observe the opposite; samples with lowest shell weights and largest sample loss during cleaning yield almost identical Mg/Ca values from both cleaning methods (e.g., Holocene and interstadial 8), while most of the significant differences in Mg/Ca values occur at intervals with highest shell weights and smallest sample loss during the cleaning process (e.g., Last Glacial Maximum (LGM) and HS4) (Figure 3). To directly assess on the effect of additional steps in the 'full cleaning' method relative to the 'Mg cleaning' method, weight loss% should be compared between the two methods. Unfortunately, we lack information about the weight loss % from the samples cleaned by the 'Mg cleaning' method for the minor/trace element analyses, but we have a very low resolution weight loss % from samples cleaned by 'Mg Cleaning' method for boron isotope analyses on the same sediment core (Ezat et al., second manuscript). The difference in weight loss% between the 'full cleaning' and 'Mg cleaning' methods (Δ weight loss %), when available, almost varies the same way as the weight loss % from the 'full cleaning' method (Figure 3H) and in antiphase with Δ Mg/Ca (Figure 3F). Thus, it is unlikely that the Δ Mg/Ca is caused due to partial dissolution as a side effect from the extra cleaning. These results support the distinction highlighted by Brian and Martin (2010) between natural dissolution and laboratory-induced

dissolution influences on Mg/Ca, while the effects of the natural dissolution in water column or at sea floor are known to preferentially remove the Mg-rich layers from the foraminiferal shells and lowers the initially incorporated Mg/Ca signal (e.g., Dekens et al., 2002; Regenberg et al., 2006), our results do not show the same effect from the laboratory-induced dissolution (Figure 3F&H).

Sixteen samples, selected from different intervals were re-picked, and duplicated by the 'Mg cleaning' method. Regardless of their apparent noise in Fe/Ca and Al/Ca, their Mg/Ca and Mn/Ca show the same trend and consistent values (Figure 4). When the 'full cleaning' method was applied to samples from the same depths, considerable decreases in Mg/Ca only occurred in samples with high Mn/Ca from the 'Mg cleaning' method (Figure 4). Hence, the differences are not dependent on the preservation state of the samples as inferred from shell weights of the analyzed samples and the mass loss during the cleaning (Figure 4). This confirms that the difference between down-core Mg/Ca between the two sets of analyses is mainly due to more efficient removal of Mn-contaminated coatings, when the 'full cleaning method' was applied.

It is notable that our Mg/Ca results from the 'Mg cleaning' method during HS4 show an increase in Mg/Ca coincident with a decrease in $\delta^{18}O$ values of *N. pachyderma* (s) (Figure 3). This result is similar in both trend and absolute values to those obtained by Jonkers et al. (2010) in samples from the Irminger Sea. However, this increase in Mg/Ca disappears in our samples, when the 'full cleaning' method is used. Again the decrease in Mg/Ca from this interval occurred in samples with the highest shell weights and lowest weight loss% and is consistent with a decrease in Mn/Ca (Figure 3).

The relation between the differences in Mg/Ca and Mn/Ca due to variant cleaning methods is not linear (Figure 5). This may be a cause of presence of different Mn-contaminant phases and/or variation in the Mg enrichment in these coatings. It also seems that Mn-coatings

on Eemian samples contain much less Mg than in glacial samples. In addition, the 'full cleaning' method might have removed contaminating phases other than Mn-oxide/carbonate coatings that might have been trapped by such coating and were only released by its removal (Barker et al., 2005). We therefore limit our later discussions on *N. pachyderma* (s) Mg/Ca to the minor/trace element results from the 'full cleaning' method although these results are of much lower resolution than the results from the 'Mg cleaning' method.

### 4.2. Benthic Mg/Ca

Mg/Ca, Mn/Ca, Fe/Ca and Al/Ca measured in the benthic species *M. barleeanus* cleaned by the 'Mg cleaning' method indicate no correlation between Mg/Ca and Al/Ca and Fe/Ca (Figure 6). A correlation with Mn/Ca is only observed for the mid/late Eemian. Four samples cleaned by the 'Cd cleaning' method (Pena et al., 2005) show a good general agreement with the samples cleaned by the 'Mg/Ca cleaning' method. Mn/Ca values are relatively low in the early Eemian interval and even lower in the HS11 event. This may suggest that the large increase in Mg/Ca recorded for HS11 relative to the early Eemian is not an artifact of contamination from Mn-rich coatings. Unfortunately, there was not sufficient material in the HS11 interval to repeat analyses using the 'Cd cleaning' method. The Mn/Ca values are exceptionally high in samples from the mid/late Eemian interval, but two reductively cleaned samples gave Mg/Ca values lower by 0 to 0.2 mmol/mol (equivalent to ~ 0 to 2 °C) (Figure 6). Altogether, the general trend in Mg/Ca from MIS 6 to MIS 5d does not look to be significantly affected by Mn-contaminant phases. However, the temperature reconstructions based on these Mg/Ca data for the mid/late Eemian may be overestimated because of the high Mn/Ca here (Figure 6) and we will thus avoid discussing this interval in terms of bottom water temperature.

## 5. Results and discussion of past hydrographic changes

### 5.1. Estimating calcification temperatures of *N. pachyderma* s

*N. pachyderma* (s) is the most dominant planktic species in the polar and subpolar areas (Bé and Tolderlund, 1971) and therefore most often used in paleoceanographic reconstructions in records from high latitudes. However, identifying which water mass *N. pachyderma* (s) records remains a challenge. Several studies from the Nordic seas show a wide, but region-specific range of calcification depth of *N. pachyderma* (s). For example, Simstich et al. (2003) suggested a calcification depth for *N. pachyderma* (s) between 70 and 250 m off Norway, between 70 and 130 m in the region of the East Greenland Current, and between 20 and 50 m in the Arctic water domain of the central Nordic seas. In the central Irminger Sea, a recent study suggested a shallow (~50 m) calcification depth for *N. pachyderma* (s) based on comparison of the seasonal variability of $\delta^{18}O$ and Mg/Ca in *N. pachyderma* (s) and *Globigerina bulloides* from sediment trap samples (Jonkers et al., 2013). In general, the signal recorded by *N. pachyderma* (s) seems likely to reflect a thick part of the water column (i.e., not overprinted much by regional or seasonal surface variability) which makes it a good tracer for water masses (Bauch et al., 1997), but not ideal for inferring environmental conditions at the sea surface.

Core-top and sediment trap studies show an exponential Mg/Ca sensitivity of ~ 9–10% per 1°C in several planktic foraminiferal species based on calibration of the foraminiferal Mg/Ca to $\delta^{18}O_{foram}$-derived temperatures (Elderfield and Ganssen, 2000; Anand et al., 2003). The absence of such a clear relationship between *N. pachyderma* (s) Mg/Ca and $\delta^{18}O$-derived temperatures in core-top and sediment trap data (Meland et al., 2006; Nyland et al., 2006; Jonkers et al., 2013) suggests other factors affected the incorporation of Mg in shells of the species (e.g., seawater carbonate chemistry and salinity), variable degrees of encrustation

(Kozdon et al., 2009), and/or undetermined species-specific mechanisms of bio-mineralization. Consequently, Mg/Ca measured in *N. pachyderma* (s) should be treated carefully and not directly interpreted in terms of calcification temperature (Hendry et al., 2009; Jonkers et al., 2013).

Culture studies show that Mg/Ca in planktic foraminifera decrease with increasing seawater pH and carbonate ion concentration, but the sensitivity is species specific. pH-sensitivity ranges from ~7 to 16% per 0.1 unit change in pH for *O. universa* and *G. bulloides*, respectively (e.g., Russell et al., 2004). Importantly, it was noted that the effect of pH on foraminiferal Mg/Ca is insignificant above modern pH values (Russell et al., 2004). However, based on sediment trap samples off the West Antarctic peninsula, Hendry et al. (2009) found an increase in Mg/Ca in *N. pachyderma* (s) by ~10–20% per 10 µmol $kg^{-1}$ increase in carbonate ion concentration, in clear conflict with the culture experiments that were performed on other planktic species. The carbonate ion concentration data in Hendry et al. (2009) are mainly derived from B/Ca measured in *N. pachyderma* (s) using a calibration based on measurements in *Globorotalia inflata* (Yu et al., 2007). Although, B/Ca in planktic foraminifera is shown to co-vary with seawater carbonate chemistry (Yu et al., 2007a; Allen et al., 2012), a quantitative assessment is complicated (Allen et al., 2012). As this study was performed on the same species and under oceanographic conditions likely not very different from the glacial and deglacial situation at our site, we attempted to correct for carbonate ion concentration influence on Mg/Ca assuming a 10% increase in Mg/Ca per 10 µmol $kg^{-1}$ increase in carbonate ion concentration. For this, we used our B/Ca to calculate the carbonate ion concentration using calibration from (Yu et al., 2007a) as in Hendry et al. (2009) (Figure 7). Here, we are more assuming that the same environmental parameters affect the B/Ca in *N. pachyderma* (s) the same way in our area and in Hendry's et al. (2009) area rather than assuming B/Ca as a proxy for carbonate ion concentration. Bryan and Marchitto (2008)

suggested that Li/Ca can be used to correct for the influence of carbonate ion concentration on Mg/Ca in benthic foraminifers. Investigating this hypothesis on four benthic foraminiferal species from core-top samples from the Florida Straits, they concluded that Mg/Li might serve as a more reliable proxy for calcification temperature. The good match between the carbonate ion concentration-corrected Mg/Ca and Mg/Li in our study derived from the B/Ca (Figure 7) is not surprising given the significant correlation between Li/Ca and B/Ca ($R^2$=0.8). Further empirical studies are needed to evaluate the use of Mg/Li in *N. pachyderma* (sinistral) as a temperature proxy. Also, it might be possible that the sensitivity of Mg/Ca to changes in carbonate chemistry is different, or even has opposite responses, at different temperatures and/or saturation states as observed in benthic foraminifera (Elderfield et al., 2006; Hintz et al., 2006; see also discussion in Bryan and Marchitto, 2008). A sensitivity of 4–8% in Mg/Ca per salinity unit was recorded in other planktic foraminiferal species (for details see Hönisch et al., 2013), but no empirical attempts have been done to test the salinity influence on Mg/Ca in shells of *N. pachyderma* (s).

The Mg/Ca values were used to reconstruct the calcification temperatures based on a Mg/Ca-temperature calibration: Mg/Ca=Pre-exponential constant * exp (0.1T) (Elderfield and Ganssen, 2000), where the pre-exponential constant is calibrated to our core-top samples yielding a value of 0.4 and T is the temperature. We then calculated $\delta^{18}O_{SW}$ by removing the temperature effect from *N. pachyderma* (s) $\delta^{18}O$ using the equation from Shackleton (1974). We used the global eustatic sea level record of Grant et al. (2012) to correct for the temporal changes in ice volume, assuming a 1‰ increase in $\delta^{18}O$ due to 120 m sea level drop (Adkins et al., 2002). We estimated the temperature and $\delta^{18}O_{SW}$ based on both crude Mg/Ca and carbonate ion concentration- corrected Mg/Ca as described above (Figure 7). Note that the main difference in temperature when correcting the Mg/Ca for carbonate ion concentration influence according to Hendry et al. (2009) is a decrease by ~2.5 °C during the LGM.

### 5.2. Reconstructions for the last deglaciation

During the late LGM (21–19 kyr BP), the *N. pachyderma* (s)- based temperature and $\delta^{18}O_{SW}$ are ~2.5 °C and ~0.4‰ or ~4.5 °C and ~0.9‰ when using the raw Mg/Ca (see section 4.3) (Figure 8). During HS1, the temperature increased to ~6 °C and the $\delta^{18}O_{SW}$ decreased to -0.4‰ (Figure 8).

At the onset of the Bølling-Allerød (BA) interstadials (~14.6 kyr BP), $\delta^{18}O_{SW}$ and temperature increased to 1‰ and 7 °C (Figure 8). Due to the relatively large sample size required for the full cleaning method and the low abundance of well-preserved specimens of *N. pachyderma* (s) from the Younger Dryas (YD), this period is poorly resolved in the Mg/Ca record. The ice-volume corrected $\delta^{18}O$ values show a decrease of about 0.75‰ during the YD as previously recorded in the southeastern Nordic seas (Rasmussen et al., 1996; Meland et al., 2008). After the end of YD, the temperature and $\delta^{18}O_{SW}$ had values similar to those recorded during the early part of the BA interstadials. An average temperature of 6 °C and $\delta^{18}O_{SW}$ of 0.35 ‰ are recorded for the past 9 kyr (Figure 7).

Previous studies obtained conflicting temperature reconstructions for the LGM in the Nordic seas of Mg/Ca in *N. pachyderma* (s) compared to estimates based on planktic foraminiferal assemblage studies (e.g., Meland et al., 2005; see for review de Vernal et al., 2006). The temperature estimates based on the corrected Mg/Ca (see section 4.3) shows a better match with the foraminiferal assemblages suggesting a decreased temperature by ~3 °C during the LGM relative to the Holocene (Figure 8). In general, there is an agreement between the % *N. pachyderma* (s) (which decreases with increasing northward advection of warm Atlantic water masses), and the Mg/Ca-based temperatures during both the LGM and the BA interstadial, while there is a large discrepancy between the two temperature proxies for HS1. This correlates with low $\delta^{18}O_{SW}$ values and can be explained by fresh water-induced stratification of the upper ocean and development of a halocline, at least during the

calcification seasons of *N. pachyderma* (s) (Figure 8). It has been suggested that subsurface inflow of relatively warm subtropical water into the Nordic seas occurred during the DO stadials (e.g., Rasmussen et al., 1996; Rasmussen and Thomsen, 2004; Ezat et al., 2014), which at the end of the stadial events destabilized the water column and resulted in the resumption of the open ocean convection in the Nordic seas. Such recurrent development and rapid erosion of a halocline in the subpolar North Atlantic was hypothesized to have significantly contributed to the abrupt onset of the regional warmings (Rasmussen and Thomsen 2004). Interestingly, the lowest reconstructed temperature in our record (between 20–18 kyr BP) agrees with the hypothesized perennial sea ice cover at the western margin of Svalbard based on sea ice proxies ($IP_{25}$ and brassicasterol) (Müller and Stein, 2014). An abrupt change to ice free summers in the eastern Fram Strait occurred at 17.6 kyr BP (Müller and Stein, 2014) coincident with the subsurface temperature increase at our site. Within the uncertainties in the age models, it is difficult to say if the inflow of subsurface warm water has contributed to sea ice melting in the eastern Fram Strait or the latter has contributed to the stratification of the upper water column. Melting of sea ice in the eastern Fram Strait can significantly increase surface buoyancy in the southern Nordic seas via the direct release of freshwater, but also through opening of the Fram Strait gateways and increase in the East Greenland Current allowing meltwater to reach south to the Nordic seas and into the North Atlantic.

Our results show that the increase in temperature can explain up to ~1‰ of the large decrease in *N. pachyderma* (s) $\delta^{18}O$ values during the late part of HS1, leaving ~1‰ still to be explained (Figure 8). Addition of low $\delta^{18}O$ water from melt- and meteoric water could have been responsible for the ~1‰ decrease through a direct recording of the signal (e.g., Bond et al., 1993; Fronval et al., 1995; Rasmussen et al., 1996) or by transfer of the signal via brines deeper in the upper water column (Hillaire-Marcel and de Vernal, 2008) where *N.*

*pachyderma* (s) may have precipitated most of its calcite as suggested by some studies (Kozdon et al., 2009).

It is also noteworthy that the applied correction for ice volume changes, using an eustatic sea level record, does not account for the spatiotemporal propagation of the $\delta^{18}O$ signal, due to growth/collapse of ice sheets, into the global surface/deep ocean especially during periods of a reduced ocean meridional circulation (e.g., Friedrich and Timmermann, 2012) and given the close location of our site to the glacial ice sheets. A correction for the effect of carbonate chemistry changes on the $\delta^{18}O$ based on the pH reconstructions from the same core record (Ezat et al., second manuscript), and assuming a decrease of 0.22‰ in $\delta^{18}O$ per 0.2 units increase in pH (Zeebe, 1999), would decrease the $\delta^{18}O_{SW}$ for the LGM by only 0.22. The impact of pH change elsewhere in the record is almost negligible.

Similar decreases in the $\delta^{18}O_{SW}$ at the calcification depth and seasons of *N. pachyderma* (s) of about 0.9‰ and 1.5‰ are also recorded for HS4 and HS6, respectively (Figure 7). The $\delta^{18}O_{SW}$ decreases during HS4 and HS6 can be explained similarly as for late HS1.

### 5.3. Reconstructions of Termination II, Eemian and last glacial inception

During the latest part of Termination II (=HS11), both *N. pachyderma* (s) and the benthic foraminiferal records show similar $\delta^{18}O$ values (= 2.7‰) (Figure 9). At the beginning of the Eemian interglacial, the two records diverge significantly from each other. The $\delta^{18}O$ values of *N. pachyderma* (s) increase slightly to 3‰, while the benthic $\delta^{18}O$ values increase abruptly to 4‰. This is similar to previous studies from the southern Norwegian Sea (Balbon 2000; Rasmussen et al., 2003) as well as in the central and northern parts of the Norwegian Sea (Fronval et al., 1998). The bottom water temperatures based on Mg/Ca measured in *M. barleeanus* decrease from ~5 °C during late HS11 to ~0 °C during the early Eemian (Figure

9). At the same time the calcification temperature of *N. pachyderma* (s) decreased by ~1.5 °C. These results show that the benthic and planktic $\delta^{18}O$ variability at the MIS 6–5 transition is primarily due to temperature changes, at least in the southern Norwegian Sea. The high deposition of IRD in the area (Rasmussen et al., 2003a) and the low $\delta^{18}O_{SW}$ during late HS11 (Figure 9) indicate presence of icebergs and meltwater at the surface (see section 5.2 for discussing the low $\delta^{18}O_{SW}$ recorded by *N. pachyderma* (s)). Thus, the relatively high temperatures based on Mg/Ca in *N. pachyderma* (s) (~6.5 °C) and very high BWT (~4 °C higher than today and early Eemian) most likely indicate the presence of a strong halocline and thickening of the warm Atlantic waters to at least 1200 m water depth during HS11 (see also Ezat et al., 2014). The subsurface inflow of the Atlantic water into the Nordic seas and thickening to deeper than 1000 m during HS11 was previously suggested based on the disappearance of the gradient in the benthic foraminiferal composition between the north and south Iceland-Scotland ridge (Rasmussen et al., 2003a).

The evolution in near-surface temperature during the Eemian based on our Mg/Ca measured in *N. pachyderma* (s) is in a good agreement with previous estimates based on planktic foraminiferal assemblages and dinoflagellate cysts (Rasmussen et al., 2003a; van Nieuwenhove et al., 2011) documenting a delay in the Eemian peak warmth and a late Eemian warming in the southeastern Nordic seas (see also Capron et al., 2014). The *N. pachyderma* (s)-based temperature gradually increased from 5 °C during the early Eemian (130–125 kyr BP) reaching its maximum ~8 °C during the late Eemian and early part of the glacial inception (120–116 kyr BP) (Figure 9). The temperature gradually decreased at 115 kyr BP to ~5 °C at 111 kyr BP at the inception of the Weichselian glacial (Figure 9). Though the IRD significantly decreased at the onset of the Eemian (~126 kyr BP), there is almost no change in the % *N. pachyderma* (s) (>90%) from HS11 into the early Eemian until ~126 kyr BP indicating continued presence of polar water at the surface (Fronval and Jansen 1997; Fronval

et al., 1998; Rasmussen et al., 2003). The $\delta^{18}O_{SW}$ at the calcification depth and seasons of *N. pachyderma* (s) (=~0.6‰) was about 0.25‰ higher than the average values for the mid/late Eemian and the Holocene. Assuming that the $\delta^{18}O_{SW}$ composition of the freshwater sources and their relative contribution in our area did not change much through the Eemian and the Holocene, this may indicate presence of near surface Atlantic water below a thin layer of polar waters, as the polar water signature is not recorded by the relatively deeper dwelling *N. pachyderma* (s). The BWT was ~0.5 °C during this period, which is comparable to the late Holocene values (Figure 9). This supports that the deep outflow from this area into the North Atlantic was active at that time as also indicated by the dominance of modern-like benthic foraminifera (Rasmussen et al., 1999; Rasmussen et al., 2003a).

The late Eemian warming in the eastern Nordic seas, which extended to the time of summer insolation minimum at 60°N (e.g., Figure 8) has been explained by weakening of the subpolar gyre (e.g., Born et al., 2011). Records show cooling at that time in the western Iceland Sea, which gives further evidence for the hypothesis of weakening of the subpolar gyre (Van Nieuwenhove et al., 2013).

Both planktic (*N. pachyderma* (s)) and benthic $\delta^{18}O$ values reached their maximum and similar values during the glacial inception (110 kyr BP; ~4.5‰). It is noteworthy that during late HS11, both planktic and benthic $\delta^{18}O$ had also similar values, but to minima. The Mg/Ca results indicate very different situations. In late HS11 the modern-like stratification of the water column between the calcification depth of *N. pachyderma* (s) and >1 km had almost disappeared, where it clearly persisted during the glacial inception. Hence, caution is needed when using the difference between planktic and benthic $\delta^{18}O$ values for inferences about the thermal structure and stratification of the water column. The increase in the *N. pachyderma* (s)- based $\delta^{18}O_{SW}$ during the glacial inception (Figure 8) may be due to the enhanced storage of freshwater in the ice sheets and reduced precipitation.

## 6. Conclusions

We combined measurements of Mg/Ca and $\delta^{18}O$ in shells of the planktic foraminiferal species *Neogloboquadrina pachyderma* (sinistral) to reconstruct the subsurface hydrography during the last interglacial-glacial cycle. First, we reported the downcore Mg/Ca, Al/Ca, Mn/Ca, Fe/Ca results from two different cleaning methods ('Mg cleaning' and 'full cleaning'), along with the shell weights of *N. pachyderma* (s) and weight loss % during the cleaning. We concluded that the 'Mg cleaning' method was not sufficiently effective in removing different contaminants. This may also apply to areas with similar depositional settings and thus we recommend, similar to previous studies (e.g., Barker et al., 2005), that a screening test for different cleaning protocols should be applied before deciding which cleaning protocol to use.

Low seawater $\delta^{18}O$, relatively high temperature and dominance of *N. pachyderma* (s) (>80%) are recorded during Heinrich Stadial (HS)1, which suggests a strong stratification in the upper water column and likely a subsurface inflow of Atlantic water below a well-developed halocline. This adds to a growing evidence for a subsurface inflow of relatively warm Atlantic water into the Nordic seas, when the latter was covered by freshwater and sea ice at the surface. Similar hydrographic features were also observed during HS11 in Termination II. Mostly, our Mg/Ca record based on the full cleaning method is discontinuous and in certain intervals of low resolution and was not capable of resolving all glacial millennial scale climatic events. However, low $\delta^{18}O_{SW}$ values were recorded for HS4, HS3 and HS6, similar to HS1 and HS11.

The evolution in the Mg/Ca-based subsurface temperatures during the Eemian generally agrees with previous estimates based on planktic foraminiferal assemblages and dinoflagellate cysts documenting an early cooling and late warming during the Eemian in the

eastern Nordic seas relative to the North Atlantic. However, our high values of $\delta^{18}O_{SW}$ during the early Eemian may refer to a subsurface inflow of Atlantic water below a thin layer of polar water. Furthermore, the results of bottom water temperatures suggest an active outflow of intermediate/deep water from our area during the early Eemian, similar to the modern situation.

**Acknowledgements**

We sincerely thank J. Ruprecht, P. DeMenocal, K. Esswein, M. Forwick, U. Hoff, J. Farmer, L. Pena, K. Allen, T. Dahl, E. Ellingsen, I. Hald, N. L. Rasmussen, M. Segl and S. Pape for valuable support in the laboratory. This research is funded by UiT, Arctic University of Norway, the Mohn Foundation and supported by the Research Council of Norway through its Centres of Excellence funding scheme, project number 223259.

**Figure Captions**

**Figure 1:** Map showing the major surface and bottom water currents in the northern North Atlantic and the Nordic seas (Hansen and Østerhus, 2000; Mork and Blindheim, 2000; Orvik and Niiler, 2002; Jakobsen et al., 2003). The location of core JM11-FI-19PC is also indicated.

**Figure 2:** Correlation of magnetic susceptibility and planktic $\delta^{18}O$ in JM-FI-19PC to nearby sediment cores ENAM93-21 and MD95-2009 (Rasmussen et al., 1996, 1999, 2003) and to $\delta^{18}O$ values from Greenland ice cores (Seierstad et al., 2014; Rasmussen et al., 2014 and references therein). Solid black horizontal lines mark tephra layers identified in both marine and ice cores (Davies et al., 2008, 2010). Tephra layers not yet confirmed in the ice cores and their potential location in ice records are shown by dashed black lines. Interstadial (black) and Heinrich event numbers (brown) are indicated.

**Figure 3:** Comparison of downcore minor/trace element results for planktic foraminiferal species *Neogloboquadrina pachyderma* (sinistral) from the 'Mg cleaning' (Red) and 'full cleaning' (Blue) methods. (a) Oxygen isotopes measured in *N. pachyderma* (s). (b) Al/Ca in µmol/mol. (c) Fe/Ca in µmol/mol. (d) Mn/Ca in µmol/mol. (e) Mg/Ca in mmol/mol. (f) Difference in Mg/Ca (ΔMg/Ca) between the two cleaning methods calculated by subtracting the Mg/Ca values from the 'full cleaning' method from the Mg/Ca values from the 'Mg cleaning method' (g) shell weight of *N. pachyderma* (s) in µgram. Closed circles represent the shell weights based on samples used for minor/trace element analyses using the 'full cleaning' method (where number of specimens = 60–160) and open diamonds represent shell weights based on samples used for boron isotope analyses (where number of specimens = 200–450). (h) black line-scatter plot refers to weight loss% from samples cleaned by the full cleaning method, while green circles refer to weight loss% from the 'full cleaning' minus the weight loss% from 'Mg cleaning methods' (Δ weight loss%). Light blue bars refer to intervals with significant differences between the two cleaning methods and grey bars refer to intervals with almost no differences between the two cleaning methods. Abbreviations: HS; Heinrich Stadials, LGM; Last Glacial Maximum, IS; Interstadial.

**Figure 4:** Al/Ca (a), Fe/Ca (b), Mn/Ca (c) and Mg/Ca (d) for *N. pachyderma* (sinistral) cleaned twice by the 'Mg cleaning' method (open and closed black circles) and once using the 'full cleaning' method (green circles) (see text for explanation). (e) Shell weights based on samples cleaned by the 'full cleaning' method. Note the break in the y-axis of Fe/Ca plot.

**Figure 5:** Relationship between the corresponding differences in Mg/Ca and Mn/Ca for *N. pachyderma* (sinistral) from the 'Mg cleaning' and 'full cleaning' methods. ΔMg/Ca

(ΔMn/Ca) is calculated by subtracting the Mg/Ca (Mn/Ca) from the 'Mg cleaning' from the Mg/Ca (Mn/Ca) from the 'full cleaning' method.

**Figure 6:** Al/Ca (a), Fe/Ca (b), Mn/Ca (c), Mg/Ca (d) for *M. barleeanus* cleaned by the 'Mg cleaning' method (black circles) and the 'Cd cleaning' method (open blue circles). Abbreviations: HS; Heinrich stadial.

**Figure 7:** Downcore reconstructions of temperature and seawater $\delta^{18}O$ at calcification depth and season of *N. pachyderma* (s). (a) $\delta^{18}O_{calcite}$. (b) Mg/Ca in mmol/mol. (c) B/Ca in µmol/mol. (d) Li/Ca in µmol/mol. (e) Corrected Mg/Ca based on B/Ca (see text for explanation). (f) Mg/Li, calculated by dividing Mg/Ca by Li/Ca. (g) Temperature based on raw Mg/Ca data (red circles) and Mg/Ca values corrected for carbonate ion concentration Mg/Ca (black circles). Red and black lines represent 3-point moving averages based on raw Mg/Ca and corrected Mg/Ca, respectively. (h) seawater $\delta^{18}O$, calculated using raw Mg/Ca-based temperatures (red circles) and using corrected Mg/Ca-based temperatures (black circles). Solid lines represent 3-point moving averages. Abbreviations: HS; Heinrich Stadial.

**Figure 8:** Near surface hydrographic details of the last deglaciation. (a) $\delta^{18}O$ values measured on *N. pachyderma* (s). (b) Temperature based on Mg/Ca measured on *N. pachyderma* (s). (c) Seawater $\delta^{18}O$ based on Mg/Ca and $\delta^{18}O$ values measured on *N. pachyderma* (s). Ssolid and dashed lines in (b) and (c) are 3-point moving averages based on corrected (Figure 6) and raw Mg/Ca, respectively. (d) Percentages of planktic foraminiferal species: % *Nps* in black, % *Turborotalia quinqueloba* (*T. q*) in red and % *Globigerinita uvula* in green. Abbreviations: HS; Heinrich Stadial, BA; Bølling-Allerød interstadials, YD; Younger Dryas, *Nps*; *N. pachyderma* (sinistral).

**Figure 9:** Climate records for the last interglacial. (a) seawater $\delta^{18}O$ based on Mg/Ca and $\delta^{18}O$ values measured on *N. pachyderma* (sinistral). (b) Temperature based on Mg/Ca measured on *N. pachyderma* (s). Solid and dashed lines in (a) and (b) are 3-point moving averages based on corrected (Figure 6) and raw Mg/Ca respectively. (c) Bottom Water Temperature (BWT) based on Mg/Ca measured on *M. barleeanus* using the 'Mg cleaning' procedure. Open black circles represent four samples cleaned by the 'Cd cleaning' method. The blue circle at the y-axis represents the average BWT of the late Holocene based on Mg/Ca measured in *M. barleeanus* using the 'Mg cleaning' procedure (Ezat et al., 2014). (d) Summer solar insolation at 60°N (Berger et al., 1978). (e) Foraminiferal $\delta^{18}O$ values measured in *M. barleeanus* (blue), *N. pachyderma* (s) (black). Yellow curve is a glacio-eustatic sea level record from Grant et al. (2012). Abbreviations: HS; Heinrich Stadial.

**Table 1:** Excluded samples due to high Al/Ca, Mn/Ca and/or Fe/Ca (in red).

## References


Adkins, J. F., McIntyre, K., & Schrag, D. P. (2002). The Salinity, Temperature, and $\delta^{18}O$ of the Glacial Deep Ocean. *Science, 298*(5599), 1769-1773.

Allen, K. A., & Hönisch, B. (2012). The planktic foraminiferal B/Ca proxy for seawater carbonate chemistry: A critical evaluation. *Earth and Planetary Science Letters, 345–348*(0), 203-211

Anand, P., Elderfield, H., & Conte, M. H. (2003). Calibration of Mg/Ca thermometry in planktonic foraminifera from a sediment trap time series. *Paleoceanography, 18*(2). doi: 10.1029/2002PA000846

Bahr, A., et al. (2013). Comparison of Ba/Ca and as freshwater proxies: A multi-species core-top study on planktonic foraminifera from the vicinity of the Orinoco River mouth. *Earth and Planetary Science Letters, 383*(0), 45-57.

Balbon, E., (2000). Variabilite climatique et circulation thermohaline dans l'Ocean Atlantique nord eten Mer de Norve`ge au cours du Quaternaire Superieur, PhD dissertation, Univ. of Paris, Paris.

Barker, S., Cacho, I., Benway, H., & Tachikawa, K. (2005). Planktonic foraminiferal Mg/Ca as a proxy for past oceanic temperatures: a methodological overview and data compilation for the Last Glacial Maximum. *Quaternary Science Reviews, 24*(7–9), 821-834.

Barker, S., Greaves, M., & Elderfield, H. (2003). A study of cleaning procedures used for foraminiferal Mg/Ca paleothermometry. *Geochemistry, Geophysics, Geosystems, 4*(9). doi: 10.1029/2003GC000559

Barker, S., et al. (2011). 800,000 Years of Abrupt Climate Variability. *Science, 334*(6054), 347-351.

Bauch, D., Carstens, J., & Wefer, G. (1997). Oxygen isotope composition of living *Neogloboquadrina pachyderma* (sin.) in the Arctic Ocean. *Earth and Planetary Science Letters, 146*(1–2), 47-58.

Berger, A. (1978). Long-term variations of caloric insolation resulting from the earth's orbital elements. *Quaternary Research, 9*(2), 139-167.

Bé, A. W. H., Tolderlund, D. S. (1971). Distribution and ecology of living planktonic foraminifera in surface waters of the Atlantic and Indian Oceans. In: Funnel BM, Riedel WR (eds) The micropaleontology of the oceans. Cambridge University Press, London, 105–149

Bian, N., & Martin, P. A. (2010). Investigating the fidelity of Mg/Ca and other elemental data from reductively cleaned planktonic foraminifera. *Paleoceanography, 25*(2). doi: 10.1029/2009PA001796

Bond, G., et al. (1993). Correlations between climate records from North Atlantic sediments and Greenland ice. *Nature, 365*(6442), 143-147

Born, A., Nisancioglu, K. H., & Risebrobakken, B. (2011). Late Eemian warming in the Nordic Seas as seen in proxy data and climate models. *Paleoceanography, 26*(2). doi: 10.1029/2010PA002027

Boyle, E. A. (1981). Cadmium, zinc, copper, and barium in foraminifera tests. *Earth and Planetary Science Letters, 53*(1), 11-35.

Boyle, E. A., & Keigwin, L. D. (1985). Comparison of Atlantic and Pacific paleochemical records for the last 215,000 years: changes in deep ocean circulation and chemical inventories. *Earth and Planetary Science Letters, 76*(1–2), 135-150.

Broecker, W. S. (1994). Massive iceberg discharges as triggers for global climate change. *Nature, 372*(6505), 421-424.

Broecker, W. S. (1998). Paleocean circulation during the Last Deglaciation: A bipolar seesaw? *Paleoceanography, 13*(2), 119-121.

Bryan, S. P., & Marchitto, T. M. (2008). Mg/Ca–temperature proxy in benthic foraminifera: New calibrations from the Florida Straits and a hypothesis regarding Mg/Li. *Paleoceanography, 23*(2). doi: 10.1029/2007PA001553

CAPE-Last Interglacial Project Members (2006). Last Interglacial Arctic warmth confirms polar amplification of climate change. *Quaternary Science Reviews, 25*(13–14), 1383-1400.

Capron, E., et al. (2014). Temporal and spatial structure of multi-millennial temperature changes at high latitudes during the Last Interglacial. *Quaternary Science Reviews, 103*(0), 116-133.

Craig, H. (1961). Isotopic Variations in Meteoric Waters. *Science, 133*(3465), 1702-1703.

Dansgaard, W. (1964). Stable isotopes in precipitation. *Tellus, 16*(4), 436-468.

Dansgaard, W., et al. (1993). Evidence for general instability of past climate from a 250-kyr ice-core record. *Nature, 364*(6434), 218-220.

Davies, S. M., et al. (2008). Identification of the Fugloyarbanki tephra in the NGRIP ice core: a key tie-point for marine and ice-core sequences during the last glacial period. *Journal of Quaternary Science, 23*(5), 409-414.

Davies, S. M., et al. (2010). Tracing volcanic events in the NGRIP ice-core and synchronising North Atlantic marine records during the last glacial period. *Earth and Planetary Science Letters, 294*(1–2), 69-79.

de Vernal, A., et al. (2006). Comparing proxies for the reconstruction of LGM sea-surface conditions in the northern North Atlantic. *Quaternary Science Reviews, 25*(21–22), 2820-2834.

Dekens, P. S., Lea, D. W., Pak, D. K., & Spero, H. J. (2002). Core top calibration of Mg/Ca in tropical foraminifera: Refining paleotemperature estimation. *Geochemistry, Geophysics, Geosystems, 3*(4), 1-29.

Elderfield, H., & Ganssen, G. (2000). Past temperature and $\delta^{18}O$ of surface ocean waters inferred from foraminiferal Mg/Ca ratios. *Nature, 405*(6785), 442-445.

Elderfield, H., Yu, J., Anand, P., Kiefer, T., & Nyland, B. (2006). Calibrations for benthic foraminiferal Mg/Ca paleothermometry and the carbonate ion hypothesis. *Earth and Planetary Science Letters, 250*(3–4), 633-649.

Emiliani, C. (1955). Pleistocene Temperatures. *The Journal of Geology, 63*(6), 538-578.

Ezat, M. M., Rasmussen, T. L., & Groeneveld, J. (2014). Persistent intermediate water warming during cold stadials in the southeastern Nordic seas during the past 65 k.y. *Geology*. *42*(8), 663-666.

Ezat, M. M., et al. A 135 kyr record of subsurface $pCO_2$, nutrient levels and ventilation in the Norwegian Sea. In preparation for submission to *Nature Geoscience*.

Friedrich, T., & Timmermann, A. (2012). Millennial-scale glacial meltwater pulses and their effect on the spatiotemporal benthicδ18O variability. *Paleoceanography, 27*(3). doi: 10.1029/2012PA002330

Fronval, T., Jansen, E., Bloemendal, J., & Johnsen, S. (1995). Oceanic evidence for coherent fluctuations in Fennoscandian and Laurentide ice sheets on millennium timescales. *Nature, 374*(6521), 443-446.

Fronval, T., & Jansen, E. (1997). Eemian and Early Weichselian (140–60 ka) Paleoceanography and paleoclimate in the Nordic Seas with comparisons to Holocene conditions. *Paleoceanography, 12*(3), 443-462.

Fronval, T., Jansen, E., Haflidason, H., & Sejrup, H. P. (1998). Variability in surface and deep water conditions in the nordic seas during the last interglacial period. *Quaternary Science Reviews, 17*(9–10), 963-985.

Grant, K. M., et al. (2012). Rapid coupling between ice volume and polar temperature over the past 150,000 years. *Nature, 491*(7426), 744-747.

Greaves, M., et al. (2008). Interlaboratory comparison study of calibration standards for foraminiferal Mg/Ca thermometry. *Geochemistry, Geophysics, Geosystems, 9*(8). doi: 10.1029/2008GC001974

Hansen, B., & Østerhus, S. (2000). North Atlantic–Nordic Seas exchanges. *Progress in Oceanography, 45*(2), 109-208.

Heinrich, H. (1988). Origin and consequences of cyclic ice rafting in the Northeast Atlantic Ocean during the past 130,000 years. *Quaternary Research, 29*(2), 142-152.

Hemming, S. R. (2004). Heinrich events: Massive late Pleistocene detritus layers of the North Atlantic and their global climate imprint. *Reviews of Geophysics, 42*(1). doi: 10.1029/2003RG000128

Hendry, K. R., Rickaby, R. E. M., Meredith, M. P., & Elderfield, H. (2009). Controls on stable isotope and trace metal uptake in Neogloboquadrina pachyderma (sinistral) from an Antarctic sea-ice environment. *Earth and Planetary Science Letters, 278*(1–2), 67-77.

Hillaire-Marcel, C., & de Vernal, A. (2008). Stable isotope clue to episodic sea ice formation in the glacial North Atlantic. *Earth and Planetary Science Letters, 268*(1–2), 143-150.

Hintz, C. J., et al. (2006). Calcite saturation state effects on cultured benthic foraminiferal trace-element distribution coefficients, Eos Trans. AGU, *87*(52), Fall Meet. Suppl., Abstract B13B1080

Huber, C., et al. (2006). Isotope calibrated Greenland temperature record over Marine Isotope Stage 3 and its relation to CH4. *Earth and Planetary Science Letters, 243*(3–4), 504-519.

Hönisch, B., et al. (2011). Planktic foraminifers as recorders of seawater Ba/Ca. *Marine Micropaleontology, 79*(1–2), 52-57.

Hönisch, B., et al. (2013). The influence of salinity on Mg/Ca in planktic foraminifers – Evidence from cultures, core-top sediments and complementary $\delta^{18}O$. *Geochimica et Cosmochimica Acta, 121*(0), 196-213.

Jakobsen, P. K., Ribergaard, M. H., Quadfasel, D., Schmith, T., & Hughes, C. W. (2003). Near-surface circulation in the northern North Atlantic as inferred from Lagrangian drifters: Variability from the mesoscale to interannual. *Journal of Geophysical Research: Oceans, 108*(C8), 3251. doi: 10.1029/2002JC001554

Jonkers, L., et al. (2010). A reconstruction of sea surface warming in the northern North Atlantic during MIS 3 ice-rafting events. *Quaternary Science Reviews, 29*(15–16), 1791-1800.

Jonkers, L., Jiménez-Amat, P., Mortyn, P. G., & Brummer, G.-J. A. (2013). Seasonal Mg/Ca variability of N. pachyderma (s) and G. bulloides: Implications for seawater temperature reconstruction. *Earth and Planetary Science Letters, 376*(0), 137-144.

Kandiano, E. S., & Bauch, H. A. (2002). Implications of planktic foraminiferal size fractions for the glacial-interglacial paleoceanography of the polar North Atlantic, J. Foraminiferal Research, *32*, 245– 251

Kozdon, R., Ushikubo, T., Kita, N. T., Spicuzza, M., & Valley, J. W. (2009). Intratest oxygen isotope variability in the planktonic foraminifer N. pachyderma: Real vs. apparent vital effects by ion microprobe. *Chemical Geology, 258*(3–4), 327-337.

Kristjánsdóttir, G. B., Lea, D. W., Jennings, A. E., Pak, D. K., & Belanger, C. (2007). New spatial Mg/Ca-temperature calibrations for three Arctic, benthic foraminifera and reconstruction of north Iceland shelf temperature for the past 4000 years. *Geochemistry, Geophysics, Geosystems, 8*(3). doi: 10.1029/2006GC001425

Lea, D. W., & Boyle, E. A. (1991). Barium in planktonic foraminifera. *Geochimica et Cosmochimica Acta, 55*(11), 3321-3331.

Martin, P. A., & Lea, D. W. (2002). A simple evaluation of cleaning procedures on fossil benthic foraminiferal Mg/Ca. *Geochemistry, Geophysics, Geosystems, 3*(10), 1-8.

Meland, M. Y., et al. (2006). Mg/Ca ratios in the planktonic foraminifer *Neogloboquadrina pachyderma* (sinistral) in the northern North Atlantic/Nordic Seas. *Geochemistry, Geophysics, Geosystems, 7*(6). doi: 10.1029/2005GC001078

Meland, M. Y., Dokken, T. M., Jansen, E., & Hevrøy, K. (2008). Water mass properties and exchange between the Nordic seas and the northern North Atlantic during the period 23–6 ka: Benthic oxygen isotopic evidence. *Paleoceanography, 23*(1). doi: 10.1029/2007PA001416

Mork, K. A., & Blindheim, J. (2000). Variations in the Atlantic inflow to the Nordic Seas, 1955–1996. *Deep Sea Research Part I: Oceanographic Research Papers, 47*(6), 1035-1057.

Müller, J., & Stein, R. (2014). High-resolution record of late glacial and deglacial sea ice changes in Fram Strait corroborates ice–ocean interactions during abrupt climate shifts. *Earth and Planetary Science Letters, 403*(0), 446-455.

Nürnberg, D., Bijma, J., & Hemleben, C. (1996). Assessing the reliability of magnesium in foraminiferal calcite as a proxy for water mass temperatures. *Geochimica et Cosmochimica Acta, 60*(5), 803-814.

Nyland, B. F., Jansen, E., Elderfield, H., & Andersson, C. (2006). Neogloboquadrina pachyderma (dex. and sin.) Mg/Ca and $\delta^{18}O$ records from the Norwegian Sea. *Geochemistry, Geophysics, Geosystems, 7*(10). doi: 10.1029/2005GC001055

Orvik, K. A., & Niiler, P. (2002). Major pathways of Atlantic water in the northern North Atlantic and Nordic Seas toward Arctic. *Geophysical Research Letters, 29*(19). doi: 10.1029/2002GL015002

Pena, L. D., Calvo, E., Cacho, I., Eggins, S., & Pelejero, C. (2005). Identification and removal of Mn-Mg-rich contaminant phases on foraminiferal tests: Implications for Mg/Ca past temperature reconstructions. *Geochemistry, Geophysics, Geosystems, 6*(9). doi: 10.1029/2005GC000930

Raitzsch, M., Kuhnert, H., Groeneveld, J., & Bickert, T. (2008). Benthic foraminifer Mg/Ca anomalies in South Atlantic core top sediments and their implications for paleothermometry. *Geochemistry, Geophysics, Geosystems, 9*(5). doi: 10.1029/2007GC001788

Rasmussen, S. O., et al. (2014). A stratigraphic framework for abrupt climatic changes during the Last Glacial period based on three synchronized Greenland ice-core records: refining and extending the INTIMATE event stratigraphy. *Quaternary Science Reviews, 106*(0), 14-28.

Rasmussen, T. L., Thomsen, E., Labeyrie, L., & van Weering, T. C. E. (1996). Circulation changes in the Faeroe-Shetland Channel correlating with cold events during the last glacial period (58–10 ka). *Geology, 24*(10), 937-940.

Rasmussen, T. L., Balbon, E., Thomsen, E., Labeyrie, L., & Van Weering, T. C. E. (1999). Climate records and changes in deep outflow from the Norwegian Sea ~150–55 ka. *Terra Nova, 11*(2-3), 61-66.

Rasmussen, T. L., Thomsen, E., Kuijpers, A., & Wastegård, S. (2003a). Late warming and early cooling of the sea surface in the Nordic seas during MIS 5e (Eemian Interglacial). *Quaternary Science Reviews, 22*(8–9), 809-821.

Rasmussen, T. L., Oppo, D. W., Thomsen, E., & Lehman, S. J. (2003b). Deep sea records from the southeast Labrador Sea: Ocean circulation changes and ice-rafting events during the last 160,000 years. *Paleoceanography, 18*(1). doi: 10.1029/2001PA000736

Rasmussen, T. L., & Thomsen, E. (2004). The role of the North Atlantic Drift in the millennial timescale glacial climate fluctuations. *Palaeogeography, Palaeoclimatology, Palaeoecology, 210*(1), 101-116.

Regenberg, M., et al. (2006). Assessing the effect of dissolution on planktonic foraminiferal Mg/Ca ratios: Evidence from Caribbean core tops. *Geochemistry, Geophysics, Geosystems, 7*(7). doi: 10.1029/2005GC001019

Rosenthal, Y., et al. (2004). Interlaboratory comparison study of Mg/Ca and Sr/Ca measurements in planktonic foraminifera for paleoceanographic research. *Geochemistry, Geophysics, Geosystems, 5*(4). doi: 10.1029/2003GC000650

Russell, A. D., Hönisch, B., Spero, H. J., & Lea, D. W. (2004). Effects of seawater carbonate ion concentration and temperature on shell U, Mg, and Sr in cultured planktonic foraminifera. *Geochimica et Cosmochimica Acta, 68*(21), 4347-4361.

Seierstad, I. K., et al. (2014). Consistently dated records from the Greenland GRIP, GISP2 and NGRIP ice cores for the past 104 ka reveal regional millennial-scale $\delta^{18}O$ gradients with possible Heinrich event imprint. *Quaternary Science Reviews, 106*(0), 29-46.

Shackleton, N. (1967). Oxygen Isotope Analyses and Pleistocene Temperatures Re-assessed. *Nature, 215*(5096), 15-17.

Shackleton, N. J. (1974). Attainment of isotopic equilibrium between ocean water and the benthic foraminifera genus Uvigerina: Isotopic changes in the ocean during the last glacial. In: J. Labeyrie (Ed.), Me´thodes quantitatives d'e´tude des variations du climat au cours du Ple´istoce`ne (pp. 203–209). France: Editions du C.N.R.S.

Sigman, D. M., & Boyle, E. A. (2000). Glacial/interglacial variations in atmospheric carbon dioxide. *Nature, 407*(6806), 859-869.

Simstich, J., Sarnthein, M., & Erlenkeuser, H. (2003). Paired $\delta^{18}O$ signals of *Neogloboquadrina pachyderma* (s) and *Turborotalita quinqueloba* show thermal stratification structure in Nordic Seas. *Marine Micropaleontology, 48*(1–2), 107-125.

Skinner, L. C., Shackleton, N. J., & Elderfield, H. (2003). Millennial-scale variability of deep-water temperature and $\delta^{18}O_{dw}$ indicating deep-water source variations in the Northeast Atlantic, 0–34 cal. ka BP. *Geochemistry, Geophysics, Geosystems, 4*(12). doi: 10.1029/2003GC000585

Spero, H. J., Bijma, J., Lea, D. W., & Bemis, B. E. (1997). Effect of seawater carbonate concentration on foraminiferal carbon and oxygen isotopes. *Nature, 390*(6659), 497-500.

Spero, H. J., et al. (2015). Timing and mechanism for intratest Mg/Ca variability in a living planktic foraminifer. *Earth and Planetary Science Letters, 409*(0), 32-42.

Thornalley, D. J. R., Elderfield, H., & McCave, I. N. (2009). Holocene oscillations in temperature and salinity of the surface subpolar North Atlantic. *Nature, 457*(7230), 711-714.

Van Nieuwenhove, N., Bauch, H. A., & Andruleit, H. (2013). Multiproxy fossil comparison reveals contrasting surface ocean conditions in the western Iceland Sea for the last two interglacials. *Palaeogeography, Palaeoclimatology, Palaeoecology, 370*(0), 247-259.

Van Nieuwenhove, N., et al. (2011). Evidence for delayed poleward expansion of North Atlantic surface waters during the last interglacial (MIS 5e). *Quaternary Science Reviews, 30*(7–8), 934-946.

Waelbroeck, C., et al. (2011). The timing of deglacial circulation changes in the Atlantic. *Paleoceanography, 26*(3). doi: 10.1029/2010PA002007

Wastegård, S., & Rasmussen, T. L. (2014). Faroe Marine Ash Zone IV: a new MIS 3 ash zone on the Faroe Islands margin. *Geological Society, London, Special Publications, 398*(1), 81-93.

Wit, J. C., de Nooijer, L. J., Wolthers, M., & Reichart, G. J. (2013). A novel salinity proxy based on Na incorporation into foraminiferal calcite. *Biogeosciences, 10*(10), 6375-6387.

Wunsch, C. (2006). Abrupt climate change: An alternative view. *Quaternary Research, 65*(2), 191-203.

Yu, J., & Elderfield, H. (2007). Benthic foraminiferal B/Ca ratios reflect deep water carbonate saturation state. *Earth and Planetary Science Letters, 258*(1–2), 73-86.

Yu, J., Elderfield, H., & Hönisch, B. (2007a). B/Ca in planktonic foraminifera as a proxy for surface seawater pH. *Paleoceanography, 22*(2). doi: 10.1029/2006PA001347

Yu, J., Elderfield, H., Greaves, M., & Day, J. (2007b). Preferential dissolution of benthic foraminiferal calcite during laboratory reductive cleaning. *Geochemistry, Geophysics, Geosystems, 8*(6). doi: 10.1029/2006GC001571

Zeebe, R. E. (1999). An explanation of the effect of seawater carbonate concentration on foraminiferal oxygen isotopes. *Geochimica et Cosmochimica Acta, 63*(13–14), 2001-2007.

**Figure 1**

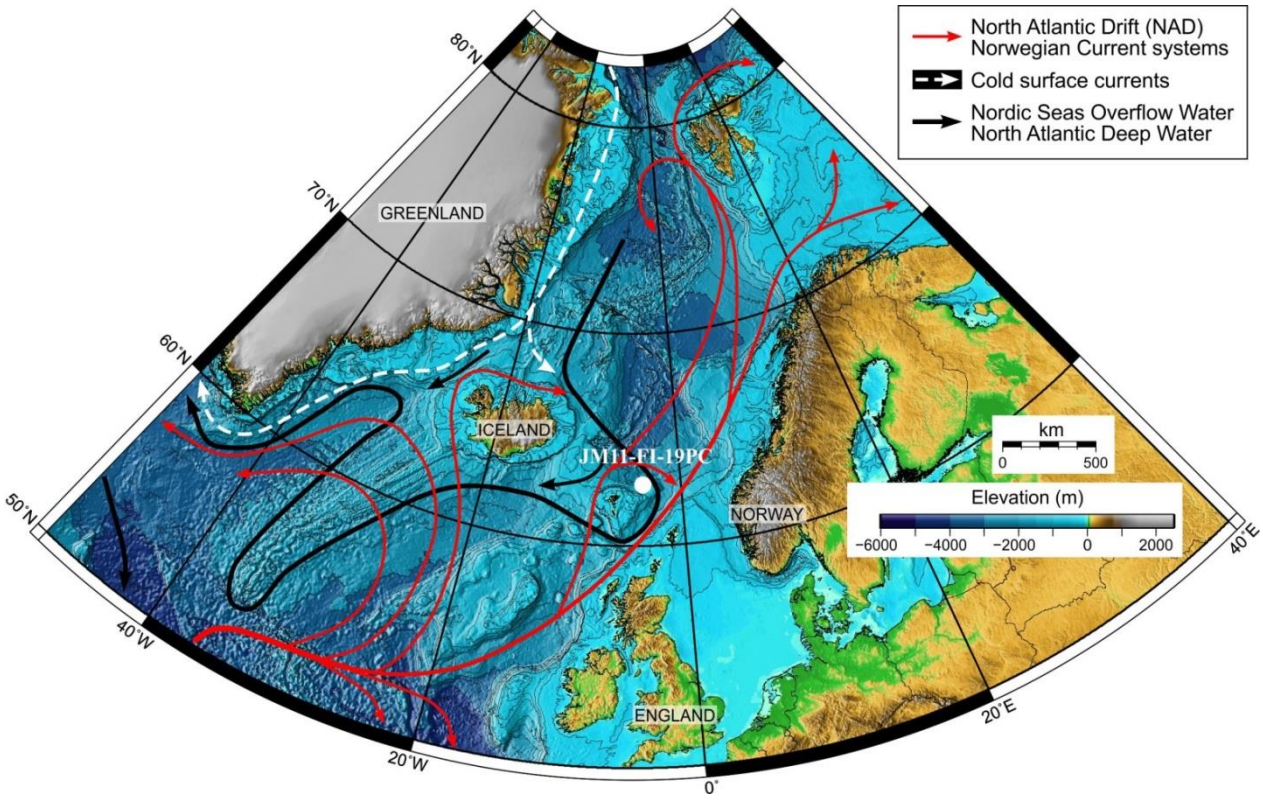
North Atlantic Drift (NAD)
Norwegian Current systems
Cold surface currents
Nordic Seas Overflow Water
North Atlantic Deep Water
80°N
70°N
60°N
50°N
40°W
20°W
0°
20°E
40°E
GREENLAND
ICELAND
JM11-FI-19PC
NORWAY
ENGLAND
km
0
500
Elevation (m)
−6000
−4000
−2000
0
2000

**Figure 2**

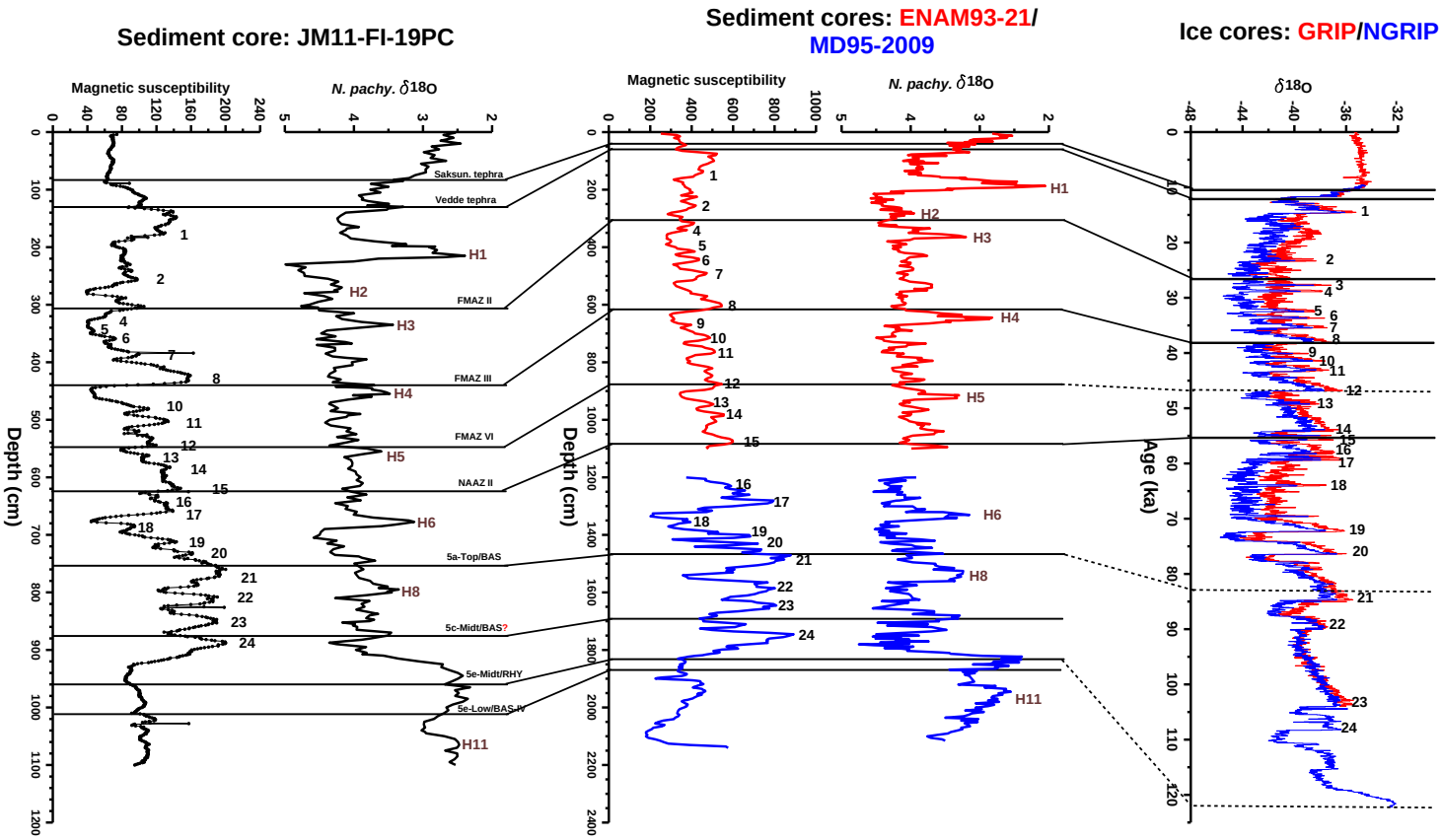
Sediment core: JM11-FI-19PC
Magnetic susceptibility
N. pachy. δ18O
Saksun. tephra
Vedde tephra
FMAZ II
FMAZ III
FMAZ VI
NAAZ II
5a-Top/BAS
5c-Midt/BAS?
5e-Midt/RHY
5e-Low/BAS-IV
H1
H2
H3
H4
H5
H6
H8
H11
Depth (cm)
Sediment cores: ENAM93-21/ MD95-2009
Magnetic susceptibility
N. pachy. δ18O
Depth (cm)
Ice cores: GRIP/NGRIP
δ18O
Age (ka)

**Figure 3**

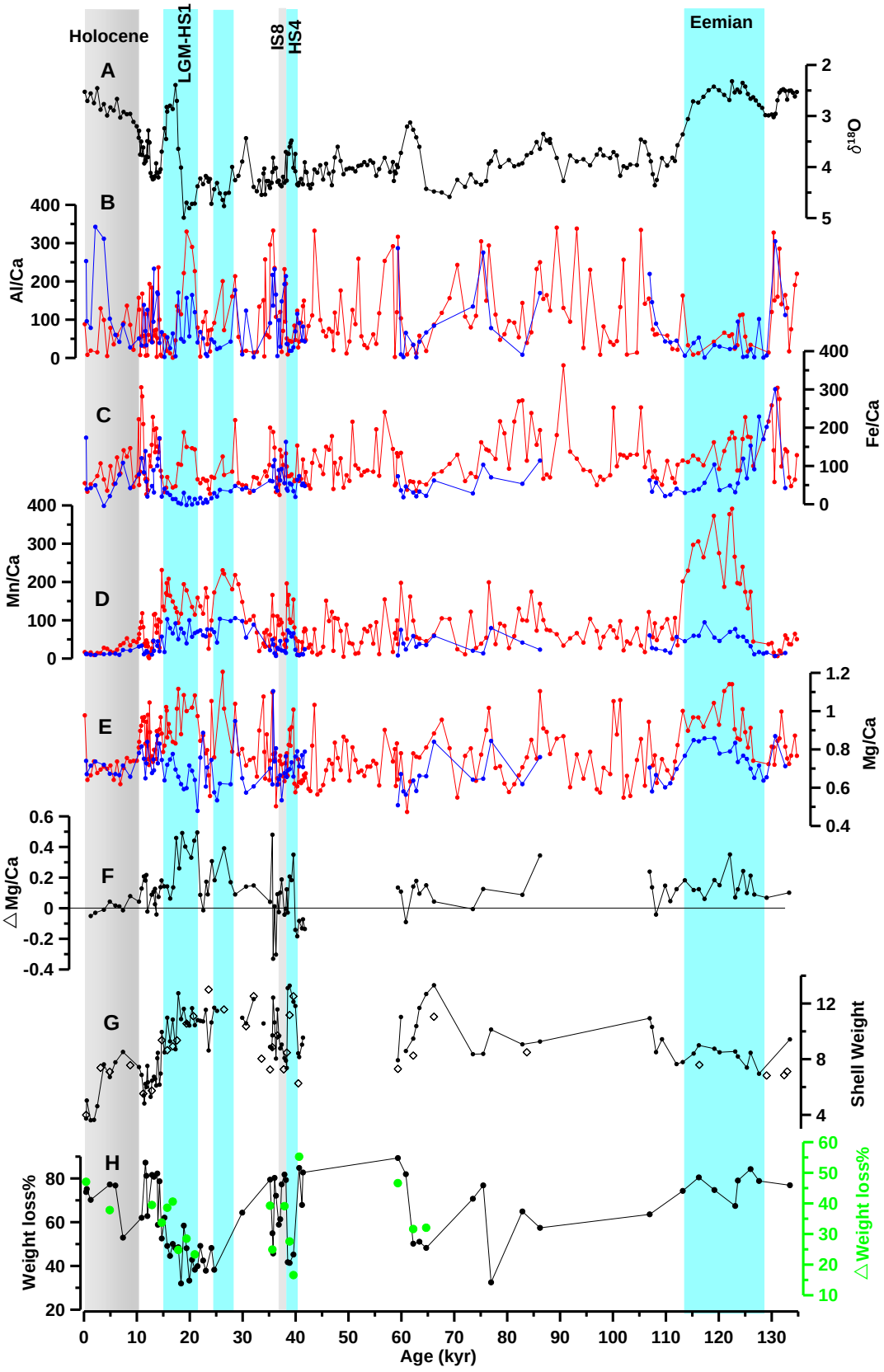
Holocene
LGM-HS1
IS8
HS4
Eemian
A
B
C
D
E
F
G
H
δ18O
Al/Ca
Fe/Ca
Mn/Ca
Mg/Ca
△Mg/Ca
Shell Weight
Weight loss%
△Weight loss%
Age (kyr)

**Figure 4**

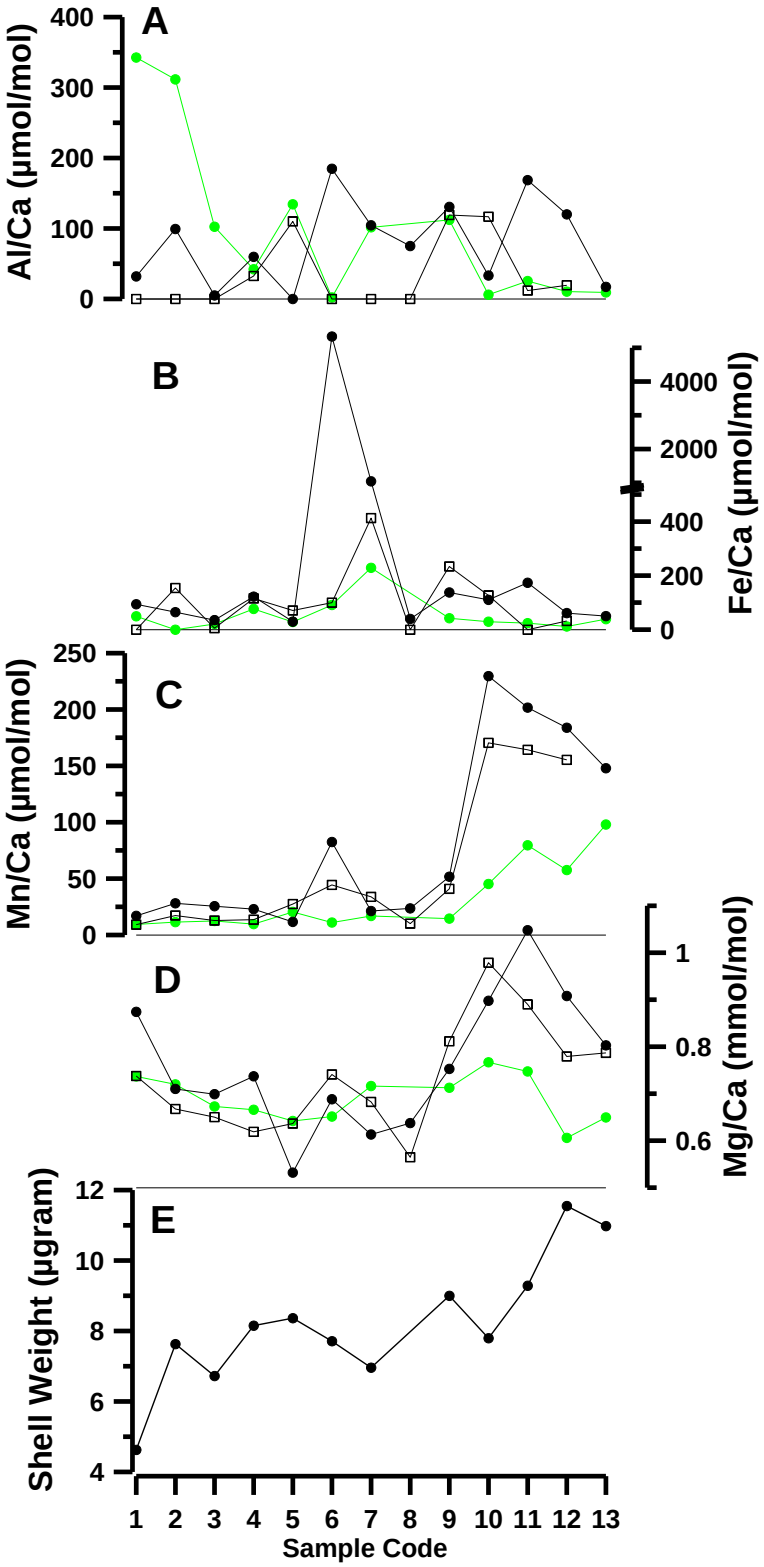
A
Al/Ca (µmol/mol)
400
300
200
100
0
B
Fe/Ca (µmol/mol)
4000
2000
400
200
0
C
Mn/Ca (µmol/mol)
250
200
150
100
50
0
D
Mg/Ca (mmol/mol)
1
0.8
0.6
E
Shell Weight (µgram)
12
10
8
6
4
1 2 3 4 5 6 7 8 9 10 11 12 13
Sample Code

**Figure 5**

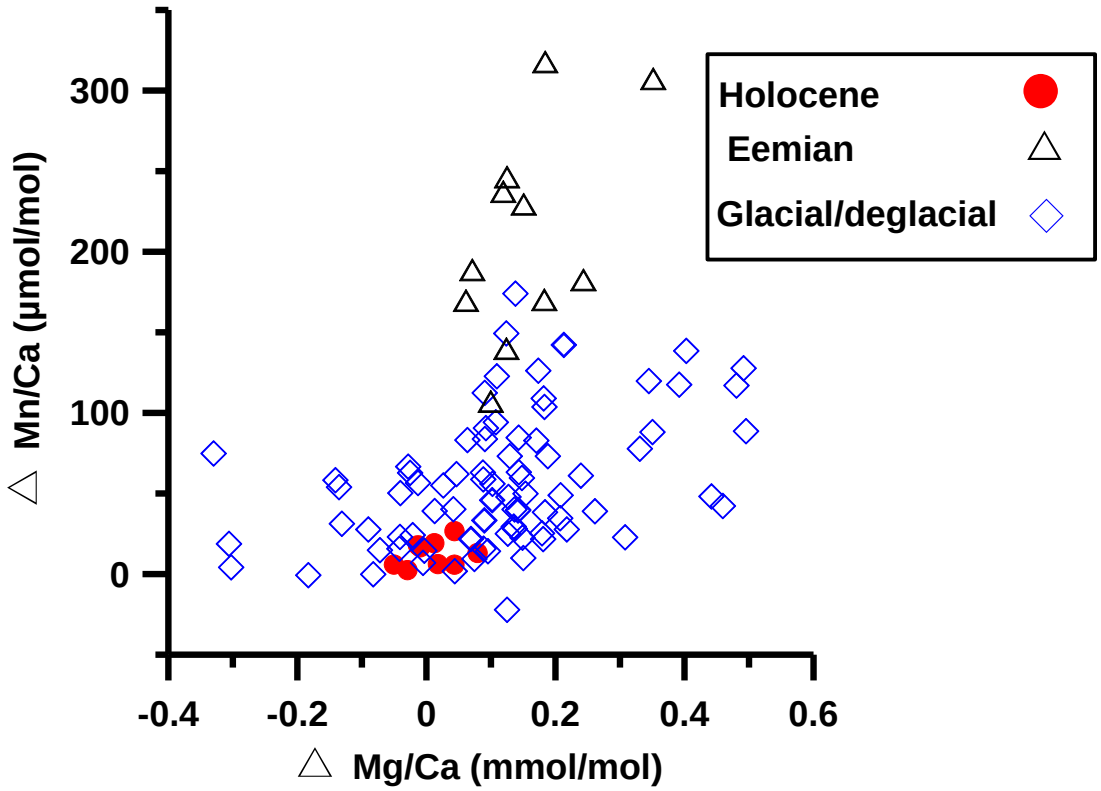
Holocene
Eemian
Glacial/deglacial
Mn/Ca (µmol/mol)
Mg/Ca (mmol/mol)
300
200
100
0
-0.4
-0.2
0
0.2
0.4
0.6

**Figure 6**

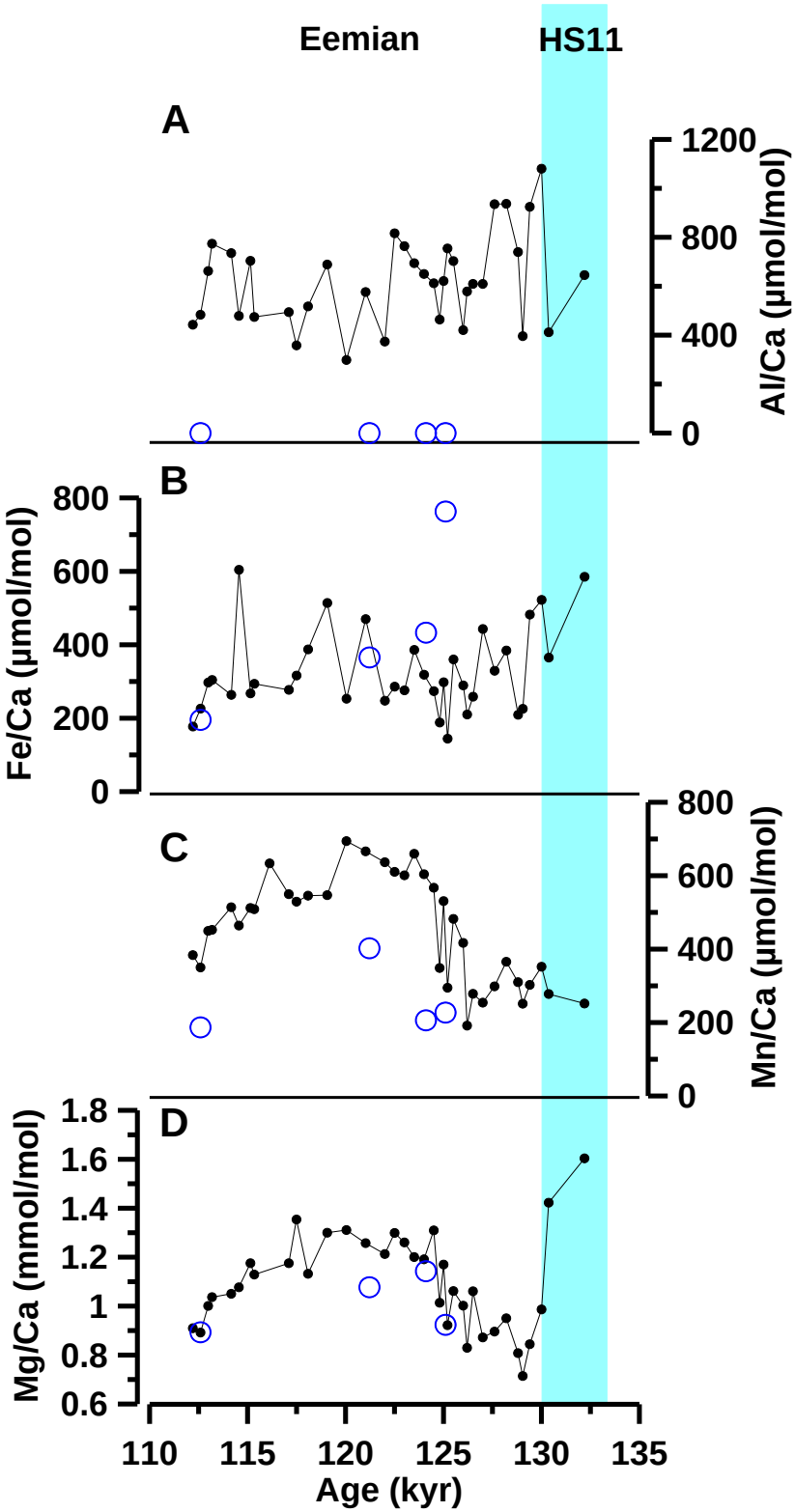
Eemian
HS11
A
1200
800
400
0
Al/Ca (µmol/mol)
B
800
600
400
200
0
Fe/Ca (µmol/mol)
C
800
600
400
200
0
Mn/Ca (µmol/mol)
D
1.8
1.6
1.4
1.2
1
0.8
0.6
Mg/Ca (mmol/mol)
110
115
120
125
130
135
Age (kyr)

**Figure 7**

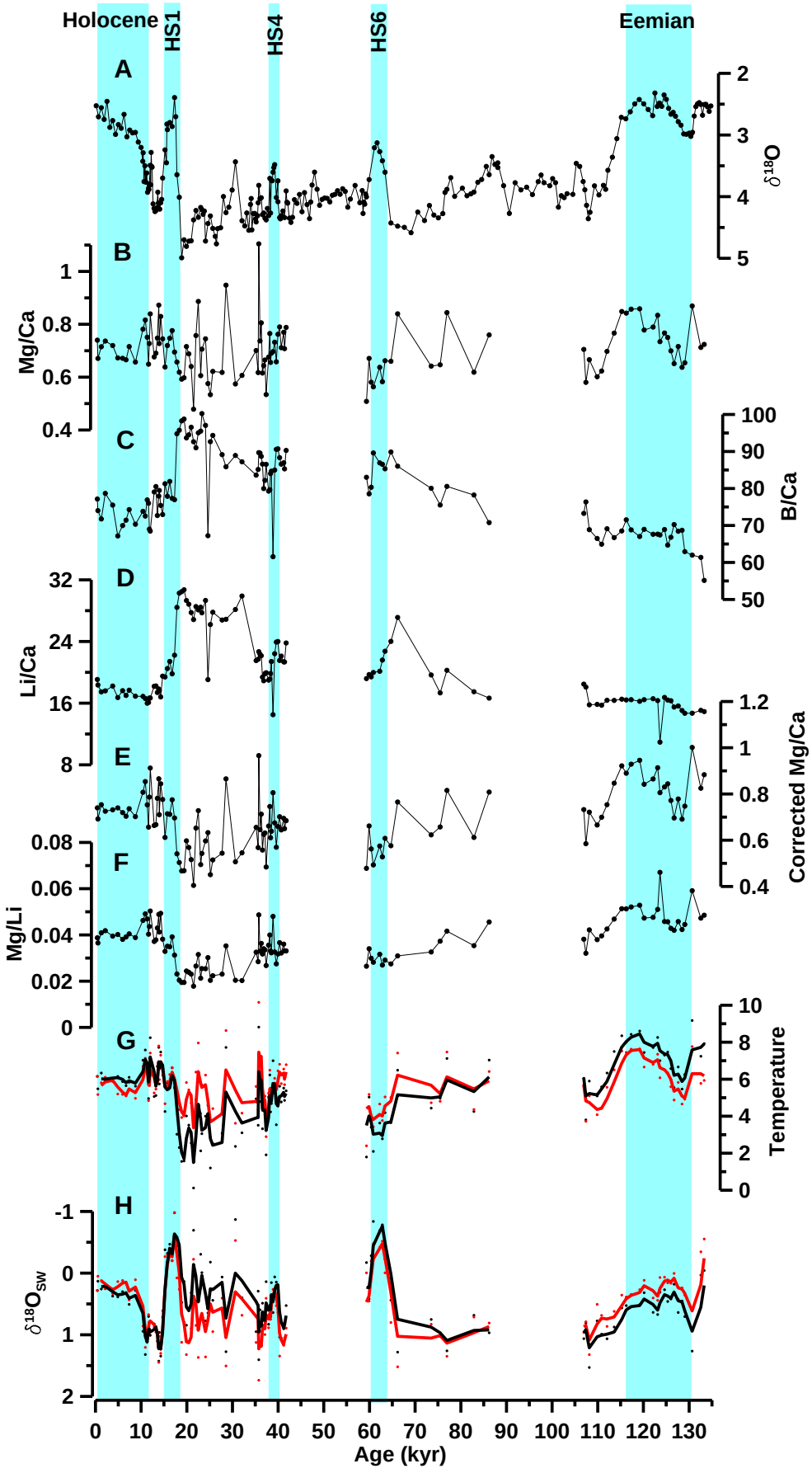
Holocene
HS1
HS4
HS6
Eemian
A
B
C
D
E
F
G
H
δ18O
Mg/Ca
B/Ca
Li/Ca
Corrected Mg/Ca
Mg/Li
Temperature
δ18OSW
Age (kyr)

**Figure 8**

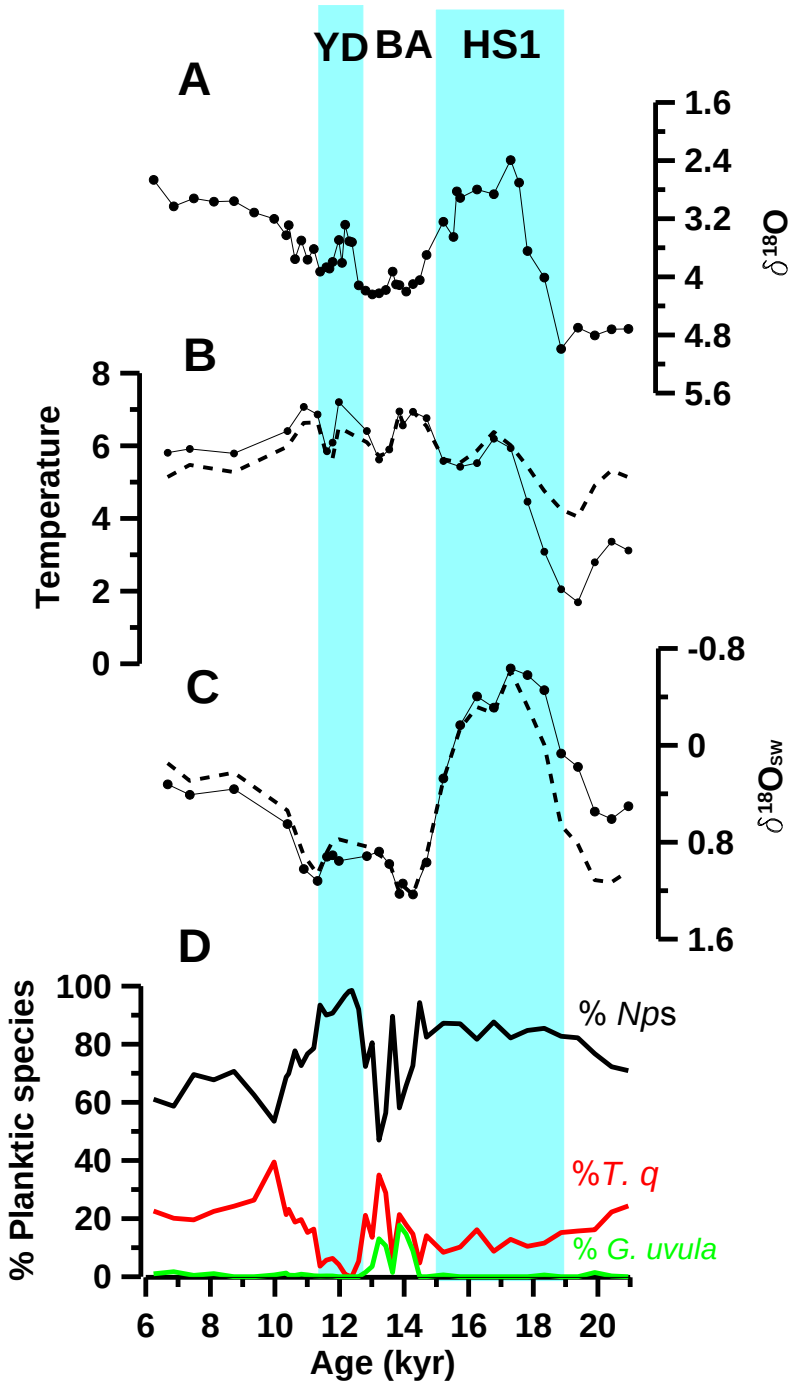
YD
BA
HS1
A
1.6
2.4
3.2
4
4.8
5.6
δ18O
B
Temperature
8
6
4
2
0
C
-0.8
0
0.8
1.6
δ18Osw
D
% Planktic species
100
80
60
40
20
0
% Nps
%T. q
% G. uvula
6
8
10
12
14
16
18
20
Age (kyr)

**Figure 9**

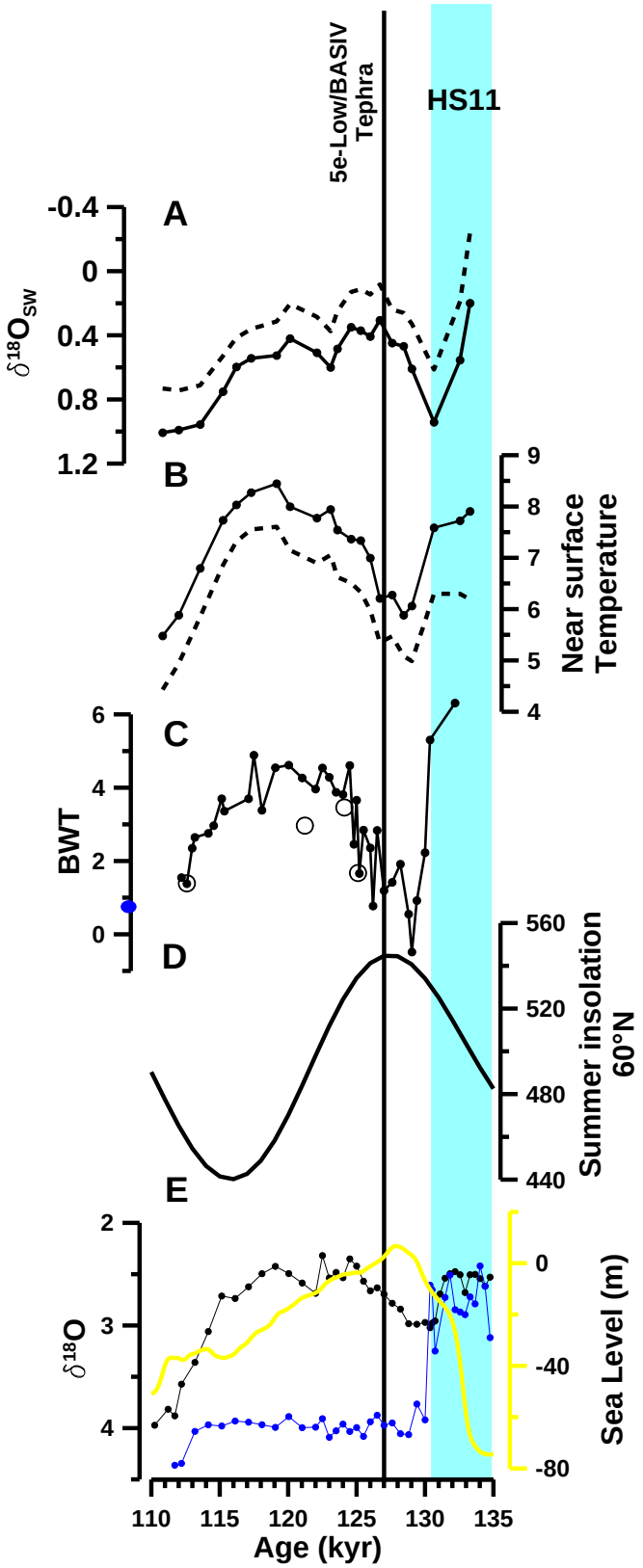
5e-Low/BASIV Tephra
HS11
A
B
C
D
E
$\delta^{18}O_{SW}$
-0.4
0
0.4
0.8
1.2
Near surface Temperature
9
8
7
6
5
4
BWT
6
4
2
0
Summer insolation 60°N
560
520
480
440
$\delta^{18}O$
2
3
4
Sea Level (m)
0
-40
-80
110
115
120
125
130
135
Age (kyr)

**Table 1**

| Depth | Mg/Ca | Al/Ca | Mn/Ca | Fe/Ca | |
|---|---|---|---|---|---|
| Cm | mmol/mol | umol/mol | umol/mol | umol/mol | Method |
| 128 | 1,38 | 599 | 13 | 205 | Full cleaning |
| 240 | 1,19 | 393 | 164 | 159 | Mg Cleaning |
| 290 | 1,00 | 153 | 273 | 76 | Mg Cleaning |
| 305 | 0,86 | 110 | 289 | 125 | Mg Cleaning |
| 310 | 1,01 | 140 | 349 | 112 | Mg Cleaning |
| 360 | 0,81 | 635 | 33 | 133 | Mg Cleaning |
| 360 | 1,12 | 613 | 11 | 162 | Full cleaning |
| 365 | 1,12 | 374 | 17 | 47 | Full cleaning |
| 380 | 0,97 | 520 | 28 | 341 | Mg Cleaning |
| 390 | 0,82 | 453 | 16 | 133 | Mg Cleaning |
| 390 | 0,55 | 433 | 9 | 63 | Full cleaning |
| 495 | 0,59 | 564 | 17 | 80 | Mg Cleaning |
| 635 | 0,66 | 555 | 27 | 1683 | Mg Cleaning |
| 645 | 0,85 | 399 | 19 | 108 | Mg Cleaning |
| 1010 | 0,68 | 35 | 34 | 413 | Mg Cleaning |
| 1015 | 0,67 | 33 | 39 | 564 | Mg Cleaning |
| 1020 | 0,85 | 8 | 77 | 597 | Mg Cleaning |
| 1045 | 1,05 | 523 | 20 | 271 | Mg Cleaning |
| 1065 | 1,60 | 476 | 26 | 399 | Mg Cleaning |
| 1090 | 0,89 | 385 | 45 | 193 | Mg Cleaning |
| 1105 | 1,30 | 787 | 63 | 261 | Mg Cleaning |